Tetrazoles are potent anion recognition elements in a variety of structural contexts

by

Thomas Pinter
BSc, Simon Fraser University, 2009

A Dissertation Submitted in Partial Fulfillment
of the Requirements for the Degree of

DOCTOR OF PHILOSOPHY

in the Department of Chemistry

© Thomas Pinter, 2015
University of Victoria

All rights reserved. This dissertation may not be reproduced in whole or in part, by photocopy or other means, without the permission of the author.

Supervisory Committee

Tetrazoles are potent anion recognition elements in a variety of structural contexts

by

Thomas Pinter
BSc, Simon Fraser University, 2009

Supervisory Committee

Dr. Fraser Hof, Department of Chemistry
Supervisor

Dr. Jeremy Wulff, Department of Chemistry
Departmental Member

Dr. Scott McIndoe, Department of Chemistry
Departmental Member

Dr. Brian Christie, Division of Medical Sciences
Outside Member

Abstract

Supervisory Committee
Dr. Fraser Hof, Department of Chemistry
Supervisor
Dr. Jeremy Wulff, Department of Chemistry
Departmental Member
Dr. Scott McIndoe, Department of Chemistry
Departmental Member
Dr. Brian Christie, Division of Medical Sciences
Outside Member

In efforts to expand the limited amount of functional groups available for anion recognition, a series of highly acidic, strongly hydrogen bond-donating groups were envisaged as suitable candidates. These included the thoroughly studied *N*-aryl sulfonamides along with the less utilized *N*-acyl sulfonamides and tetrazoles. These groups were affixed to a well-understood supramolecular platform in calix[4]arene and their binding affinities for various halides and oxyanions probed. It was found that although in its least energetically favourable conformation that is orthogonal to the aryl group to which it was bound, the tetrazole proved a superior anion-binding element.

Noting that tetrazoles prefer co-planarity with aryl neighbours, a series of pyrrolyl-tetrazole anion binding compounds were prepared, first a simple bidentate pyrrolyl-tetrazole which when tested for anion binding affinity demonstrated some of the strongest binding with anions for a bidentate compound ever observed, especially chloride.

It was then conceived to hybridize this new binding motif with the well-known amidopyrrole moiety and two new tetrazolyl-amidopyrroles were constructed. When compared to an ester-functionalized pyrrolyl-tetrazole, binding strength with halides was not much different, leading to the postulation that the amide N-H may just be a spectator in the binding event, and the electron-withdrawing nature of the adjacent carbonyl was what led to the binding potency.

Nonetheless, a new class of diversifiable anion binders with superior strength to analogous amidopyrroles has been constructed and could perhaps be used in a variety of functional applications.

Table of Contents

List of Tables

List of Figures

List of Schemes

List of Abbreviations

Ac	Acetyl
AMP	Adenosine monophosphate
Assoc	Association
ATP	Adenosine triphosphate
Bu	Butyl
Bu^t	*tert*-butyl
Bz	Benzoyl
BzO^-	Benzoate
CSD	Cambridge Structural Database
Dba	Dibenzylideneacetone
DCC	*N,N'*-dicyclohexylcarbodiimide
DFT	Density Functional Theory
DMAP	4-dimethylaminopyridine
DMF	Dimethylformamide
DMSO	Dimethylsulfoxide
Dppf	1,1'-*bis*(diphenylphosphino)ferrocene
EDC	1-ethyl-3-(3-dimethylaminopropyl)carbodiimide
Et	Ethyl
HF	Hartree-Fock
HG	Host-Guest
HOBT	Hydroxybenzenetriazole
i-Pr	Isopropyl
Me	Methyl
NBS	*N*-bromosuccinimide
NMR	Nuclear Magnetic Resonance
Pyr	Pyridine
RNA	Ribonucleic acid
TsO^-	Tosylate
UV-vis	Ultraviolet-Visible

Acknowledgments

I would first and foremost like to acknowledge and whole heartedly thank my supervisor Dr. Fraser Hof. Throughout the years he has demonstrated patience and understanding and helpfulness like no other. He has become my mentor and a friend, and the appreciation I have for all he has done for me is beyond words. Thank you Fraser. I would, in the same vein like to thank my mother, her unconditional love and support have picked me up through a lot of rough patches and similarly, the words "I love you" don't even scratch the surface. During the coming years, I will sorely miss you while experiencing new adventures. You will always be in my mind and heart.

I would like to thank my graduate committee, Dr. Jeremy Wulff, Dr. Scott McIndoe and Dr. Brian Christie for taking the time to go through this manuscript and to sit down during my defense, I know you are all very busy and I appreciate you putting off your important work on account of me and my future.

I would also like to thank Dr. Peter Marrs who was an excellent senior lab coordinator and teaching supervisor. You made teaching a bit more bearable Dr. Marrs and I appreciate it. On that note I would also like to thank Dr. Marrs, along with Dr. Tom Fyles and again Dr. Hof for sending out so many reference letters I'm sure they have lost count. Without this, I would not have this opportunity that awaits me, thank you so much.

I cannot write this section without acknowledging the oil that keep the machine that is UVic chemistry running, the instrument gurus, technical and administrative staff. Chris Barr for his impeccable upkeep of the NMR facility, and Chris Greenwood his predecessor. Also Ori Granot for acquiring tricky accurate masses and making the mass spec walk-up instrument quite convenient. "That was easy!" The technical crew Andrew Macdonald for not hesitating to promptly fix any busted equipment when possible. Shuba Hosalli for not hesitating to promptly fix any computer problems when possible. Sean Adams for fixing broken glassware, I was down there far too often. And I cannot forget to mention the science stores crew Glenda Catalano, Derek Harrison, Rob Iuvale, Bev Scheurle and Kara White who always offered service with a smile. Finally, not to be outdone, the administrative staff Patricia Ormond, Rosemary Pulez, Fariba Ardestani and Sandra Baskett, thank you for all your hard work keeping this department running smoothly.

That said, an extra special thanks to Sandra Baskett and Dr. Robin Hicks along with, of course, Dr. Hof for taking time out of their busy schedules and going out of their way in efforts to expedite my defense so I can make it to my new post with the defense behind me. Your dedication and commitment is truly remarkable and greatly appreciated.

Finally, all the friends I've made in the department over the years, you guys are all awesome and I will never forget you. Hopefully one day we will all enjoy success and our paths will cross again. I will miss you all, thank you all for everything.

Cheers

Dedication

For Dad – Wish you were here

Chapter 1. Introduction

Portions of this chapter were previously published and reprinted with permission from Hof, F.; Pinter, T., Learning from Proteins and Drugs: Receptors That Mimic Biomedically Important Binding Motifs. In *Designing Receptors for the Next Generation of Biosensors*, Piletsky, S. A.; Whitcombe, M. J., Eds. Springer Berlin Heidelberg: 2013; Vol. 12, pp 33-51, with permission from Springer Science and Business Media.

1.1 Prologue

Since the discovery of crown ethers and cryptands in the 1960s study of supramolecular chemistry, broadly defined as "the chemistry of the non-covalent bond" has been a burgeoning field, with much early attention focused on cation recognition. Anion recognition chemistry, however, has received comparatively less attention until relatively recently.[1,2] The importance of anionic species to living systems is critical. Anions are ubiquitous in biological systems: careful regulation of intra- and extracellular charge gradients is necessary to maintain homeostasis, and the majority of enzyme substrates and cofactors carry a negative charge. DNA owes its helical shape to well-defined hydrogen bond networks between complementary base pairs, phosphates provide the energy source crucial to all biochemical processes, transport channels for small anions such as chloride and sulfate regulate the flow of nutrients and osmotic pressure in and out the cell.

Misregulation of certain chloride channels has been proven to cause various disease states. A seminal example is displayed in the malfunction of the cystic fibrosis transmembrane conductance regulator (CFTR). A known mutation in this gene product is the deletion of a phenylalanine residue which leads to decreased expression of said channel along with decreased Cl^- efflux capability resulting in the debilitating lung disease cystic fibrosis (CF).[3] It is conceivable that novel therapeutics that act to promote chloride efflux through these channels could effectively aid in CF treatment. Dent's disease, a degenerative renal ailment characterized by low molecular weight proteinuria (excess of serum proteins in the urine), hypercalciuria (excessive calcium excretion in the urine) and kidney stones is caused by malfunctioning ClC-5 chloride channels in the kidneys.[4] Similarly, the renal ailment Bartter's syndrome characterized by hypokalaemic alkalosis (low potassium concentration in the serum) with salt wasting along with hypercalciuria is caused by malfunctioning CLCNKB chloride channels. These channels play a crucial role in renal salt reabsorption and blood-pressure homeostasis.[5]

Anions also play important roles in the environment. Many pollutants, be it from agricultural runoff (lake eutrophication from excess phosphate) or nuclear wastes such as radioactive pertechnetate ($^{99}TcO_4^-$) discarded into the ocean are a cause of growing

environmental concern and are anionic in nature.[6,7]. ^{99m}Tc ($t_{1/2}$ ~ 6 h) generated from decaying ^{99}Mo and trapped as the sodium salt of $^{99m}TcO_4^-$ is widely used in medical radioimaging. Its short half-life subjects the patient to minimal radioactive exposure prior to excretion. Once excreted however, it decays to $^{99}TcO_4$ ($t_{1/2}$ ~ 200 000 years) causing lasting harmful environmental effects.[8]

It is not surprising then that much attention has been focused on creating potent receptors that are selective for anionic species of interest with the intention of constructing anion sensors, extractants and transmembrane transporters.[9-11] During the construction of such receptors, two key factors must be taken into account. The spatial orientation of the anion in question: anions represent a wide range of geometries (Figure 1.1)[9] and tunability of receptor design to allow for introduction of selectivity for the guest anion of interest. Size complementarity is also clearly a factor in host-guest chemistry. The guest must be within a reasonable distance from the binding element(s) of the host for an energetically favourable interaction to take place.

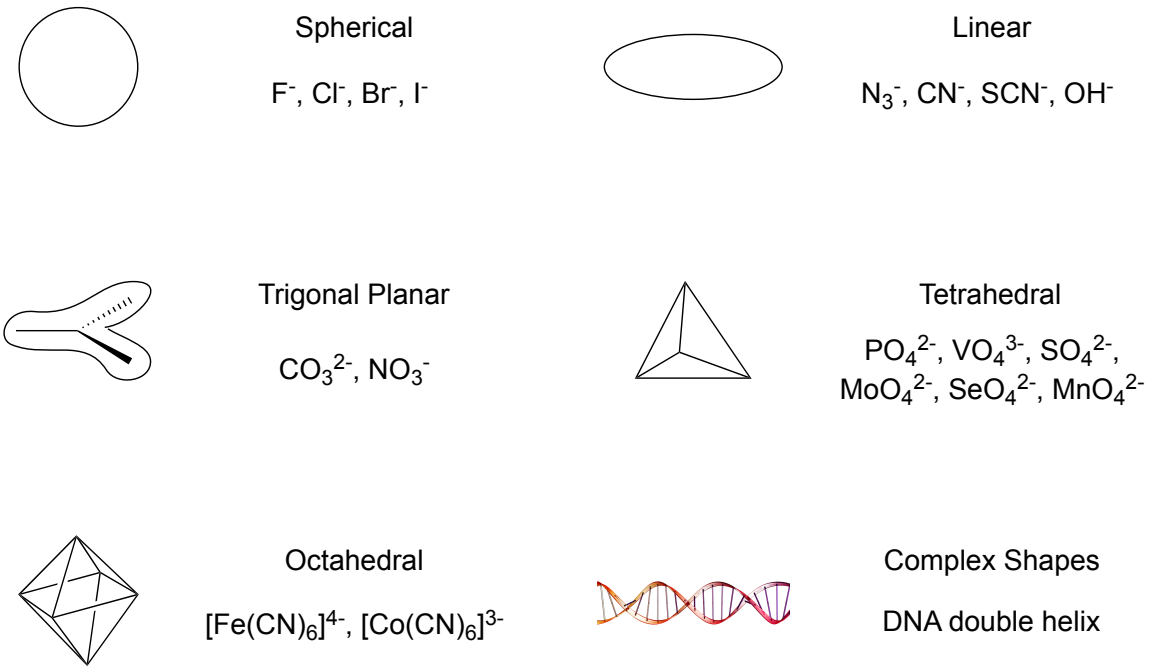

Figure 1.1 Common anion geometries. Figure adapted from Beer *et al.*[9]

1.2 Weak interactions important for anion recognition

Weak interactions determine protein shape and are therefore an essential part of normal protein function. Discreet binding pockets and motifs that have evolved to be highly selective for only a very particular class of substrates come about as a result of a myriad of these non-covalent interactions. The helical shape of DNA is so because of an intricate combination of H-bond donor and acceptor pairs, stacking between the bases, and solvation effects. Weak hydrogen bonding, electrostatic, hydrophobic and Van der Waals interactions all play key roles in protein-substrate and protein-protein interactions. Many reviews and articles addressing these non-covalent interactions have been published,[12-18] the following sections will mainly focus on those that are relevant to anion recognition: hydrogen bonds, electrostatic attraction, and anion-pi interactions.

1.2.1 Hydrogen bonding

The most commonly discussed and arguably the most important weak interactions are hydrogen bonds. Ubiquitous in complex natural systems, almost all biological processes involve hydrogen bonding in some form or another and these interactions have been the topic of extensive study for decades.[19-24] Proteins which act on anionic substrates universally contain highly evolved hydrogen bond networks in their active sites.

Figure 1.2a depicts the pore of a protein in the CLC family of transmembrane chloride channels whose crystal structure was solved in 2002.[25] The ion is coaxed into the pore by four key hydrogen bond donating residues. These attractive interactions pull the chloride into close proximity to an aspartic acid residue which is displaced thus opening the ion channel. During drug design, medicinal chemists often seek to emulate the natural substrate of a biological target and attempt to preserve all attractive forces in the host-guest complex. In one simple example, replacement of the phosphate linker in the natural RNA fragment (Figure 1.2c) with an *N*-acyl sulfonamide in a simple dinucleoside mimic (Figure 1.2d) preserved a key H-bond with His119 and resulted in inhibition of RNase A (Figure 1.2b).[26] All natural anion binding and recognition motifs contain some form of an organized hydrogen bond network, selective and specific to their particular anionic substrate.

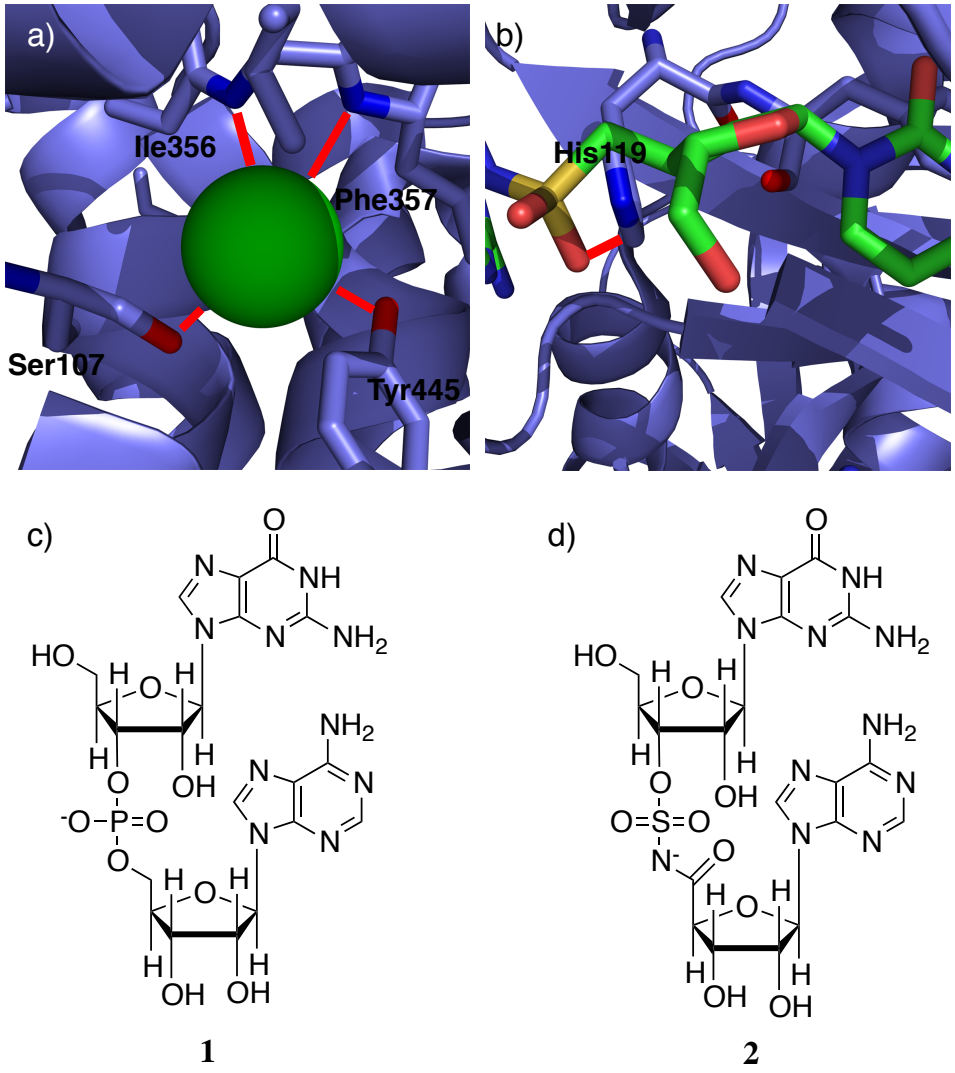

Figure 1.2 a) Crystal structure of chloride (green sphere) bound in the pore of a ClC chloride channel (PDB 1KPL). Key hydrogen bond contacts are observed with surrounding Ile, Ser, Tyr and Phe residues.[25] b) *N*-acyl sulfonamide linked dinucleoside mimic bound to RNase A. A key H-bond between the sulfone of the inhibitor and a nearby histidine is observed in the crystal structure (PDB 2XOI). H-bonds are shown as red lines. c) Natural dimeric RNA fragment d) *N*-acyl sulfonamide functionalized RNA fragment mimic. Both compounds are deprotonated at physiological pH and the mimic displays moderate inhibitory activity against RNase A.[26]

It is not surprising then that synthetic anion receptors, rationally designed to mimic natural anion binding pockets, contain similar hydrogen bond networks almost without exception and several structural and environmental considerations must be taken into account during their design. Given their directional nature, hydrogen bond containing anion receptors allow for easy tuning of size and shape in order to impart

specificity for various anionic guests of interest. Strategies often include increasing alkyl chain lengths between the hydrogen bond donors to create binding cavities for larger guests, introducing degrees of unsaturation to rigidify the host cavity to allow for stronger binding of spherical and planar guests or omitting unsaturation in order to increase flexibility and "floppiness" to facilitate three dimensional anions.

Solvation effects and other ionic species in solution must also be considered when during anion receptor design. Many of the binding studies mentioned in the coming sections are performed in polar organic solvents with bulky counterions to the anion of interest: tetrabutylammonium salts dissolved in DMSO or MeCN are commonplace. Addition of neutral water to these systems diminishes host–guest complexation as the guest anion is better-solvated by the smaller water molecules essentially lowering the amount of guest molecules available for binding. Use of smaller counterions, for example sodium salts, may result in in interactions that could affect guest complexation and selectivity. The protonation state of the host must also be taken into consideration especially in aqueous systems as it is highly pH dependant. These topics will be discussed in the coming sections.

1.2.1a Amides and Sulfonamides

One of the most abundant hydrogen bond donating groups in biological systems are amides. They are also often employed when designing synthetic anion receptors. The more acidic sulfonamides are also commonplace. receptors **1.1a-1.1c** containing two 2,6-diamidopyridine groups were designed by Chmielewski and Jurczak[27] (Figure 1.3) and their binding strength with various anions was determined (Table 1.1). The previously mentioned structural tunability of such hosts is evidenced in this study, as increasing the alkyl chain length between the amide donors increased host cavity size and shape. While the selectivity of **1.1a** for certain guests was minimally affected (~2.3 fold for phosphate

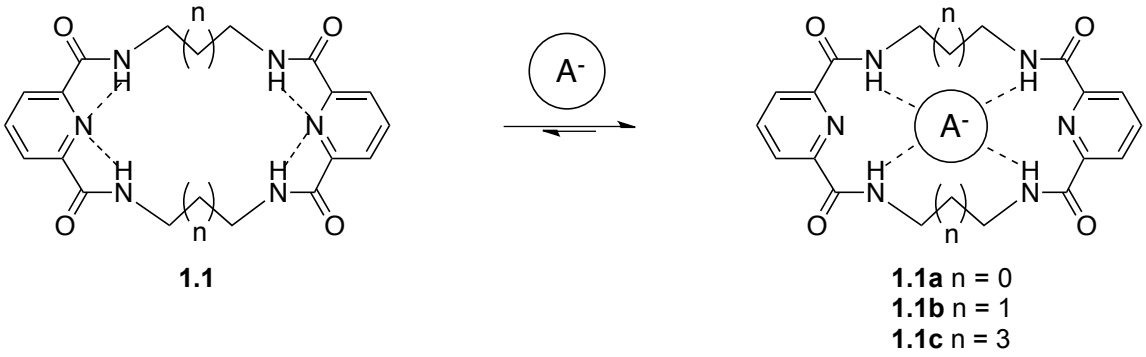

Figure 1.3 Diamidopyridine-based anion receptors. Free host is rigidified by intramolecular amide hydrogen bonding interactions with pyridine nitrogen lone pairs.[27]

Table 1.1 Association constants K_{assoc} (M^{-1}) for the formation of 1:1 complexes of hosts 1.1a, 1.1b and 1.1c with various anions in DMSO-d_6 at 298K.[27] Errors estimated to be <10%. [a] Values taken from ref. 28.

	Guests K_{assoc} (M^{-1})				
Host	$Bu_4N^+ Cl^-$	$Bu_4N^+ PhCOO^-$	$Bu_4N^+ AcO^-$	$Bu_4N^+ H_2PO_4^-$	$Bu_4N^+ HSO_4^-$
1.1a	65[a]	202	2640[a]	1680[a]	<5
1.1b	1930	2283	3240	7410	450
1.1c	18	301	310	450	<5

over acetate with respect to host **1.1b**, binding potency was considerably increased upon construction of the optimally sized binding cavity. Lengthening of the alkyl spacer resulting in a pocket too large and presumably a macrocycle too flexible to effectively preorganize the donors around a central guest (**1.1c)** and essentially abolished binding strength.

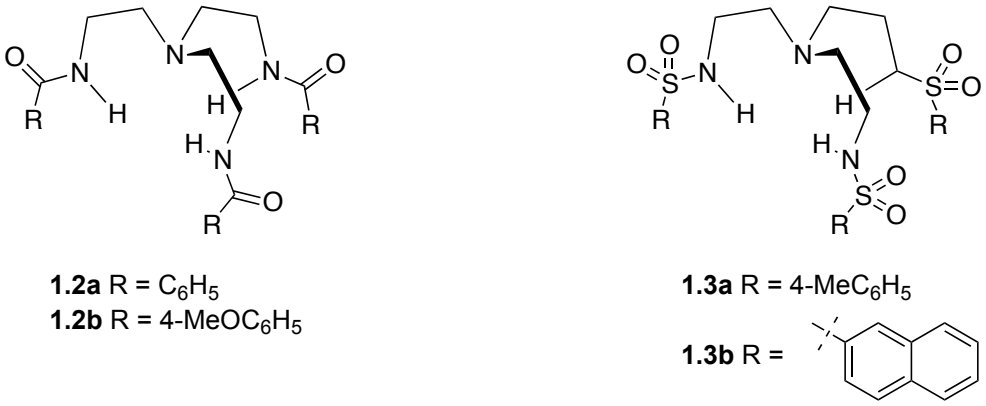

Figure 1.4 *C*-aryl amide and *S*-aryl sulfonamide-functionalized hosts.[29]

Table 1.2 Association constants K_{assoc} (M^{-1}) for the formation of 1:1 complexes between hosts **1.2a**, **1.2b**, **1.3a** and **1.3b** and various anions in acetonitrile-d_3 at 298K. Errors estimated to be 5-10%.[29]

	Guests K_{assoc} (M^{-1})		
Host	$Bu_4N^+ Cl^-$	$Bu_4N^+ HSO_4^-$	$Bu_4N^+ H_2PO_4^-$
1.2a	100	56	870
1.2b	190	73	510
1.3a	540	79	3500
1.3b	1600	38	14200

A study by Reinhoudt *et al.* involved the synthesis of a library of acyclic, C_3 symmetric anion receptors containing either amide or sulfonamide groups (Figure 1.4).[29] The more acidic sulfonamides generally displayed significantly more potent binding affinities for the anions tested, particularly $H_2PO_4^-$ (Table 1.2). The 3-fold symmetry associated with the hosts makes them ideal for tetrahedral anions. This work effectively displayed that, along with the previously discussed host geometry and flexibility, stronger hydrogen bond donating ability also plays an important role in host-guest complexation.

Other, more complex examples of (sulfon)amide-functionalized anion receptors appended to various supramolecular platforms have also been reported displaying a wide range of binding potency and selectivity. Electron deficient *S*-aryl sulfonamides appended to a central six-membered triazine-triazole (**1.4**, Figure 1.5) scaffold displayed

potent binding and selectivity for chloride when compared to nitrate and bromide in $CDCl_3$.[30] Sulfonamide-functionalized cholic acid derived scaffold **1.5** (Figure 1.5) was found to selectively bind chloride with an association constant in the 10^5 M^{-1} range in dichloroethane.[31]

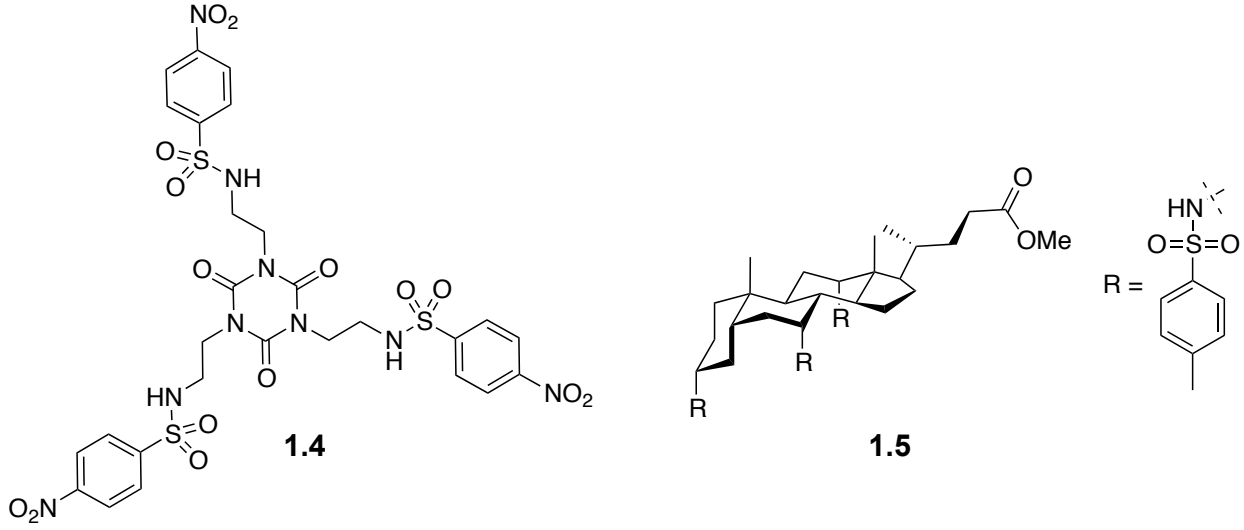

Figure 1.5 Other anion binding constructs containing sulfonamide hydrogen bond donors as the principal binding elements.[30,31]

1.2.1b Ureas and Thioureas

A closely related class of hydrogen bond donors to those described above is the ureas. Having planar donating groups separated by a single carbon atom these binding elements are especially efficient at complexing spherical as well as trigonal planar guests. These groups are very well studied as anion binders and have been incorporated into numerous supramolecular platforms. For example, appending (thio)ureas to calixarene scaffolds has been commonplace in the pursuit of new anion receptors.

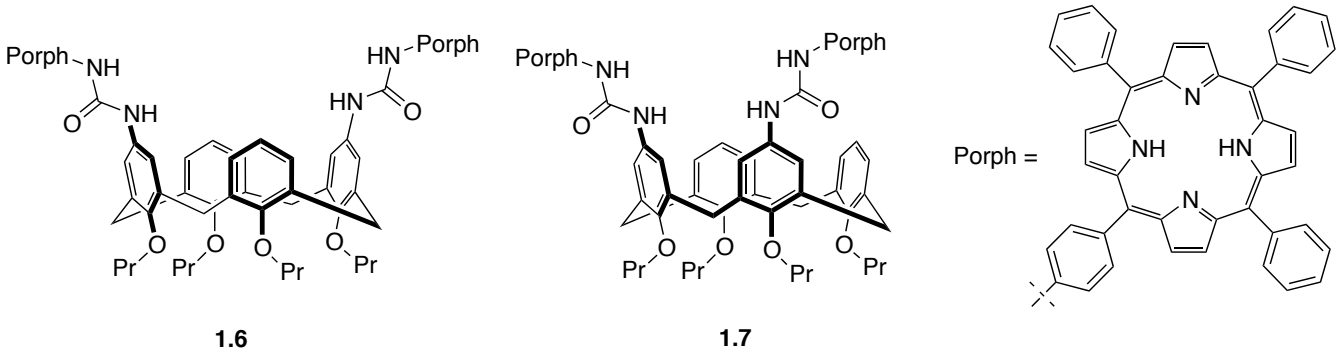

Figure 1.6 Calix[4]arene-based anion receptors affixed with ureas as binding elements.[32]

A study by Lhòtak *et al* involved the construction of calix[4]arene platforms appended with two urea groups at different positions of the upper rim of the scaffold. Attached to the urea functionalities were porphyrin chromophores and binding of various anions monitored by UV-vis titrations in dichloromethane (Figure 1.6).[32] These studies showed that both receptors bound chloride with comparable strength (K_{assoc} = 6.9 × 10^5 M^{-1} and 5.8 × 10^5 M^{-1} for **1.6** and **1.7** respectively). Similarly, bromide was not discriminated against by these hosts (K_{assoc} = 6.9 × 10^5 M^{-1} and 5.8 × 10^5 M^{-1} for **1.6** and **1.7** respectively). These results display the flexibility of the urea-containing linkers and their ability to accommodate both guests regardless of their residing at the 1,2 or 1,3 positions of the calixarene upper rim. Binding diminished with increasing anion diameter (K_{assoc} (Cl^-) > K_{assoc} (Br^-) > K_{assoc} (I^-)) demonstrating the size recognition properties of these particular hosts.

Thioureas have also been incorporated into many different structural contexts as anion binding motifs. The group of Tobe and co-workers constructed cyclic receptors such as **1.8** and **1.9** displaying different substitution patterns about the aryl linkers. It was found that this subtle change in cavity size decreased the binding strength of the larger macrocycle **1.9** with all anions tested by an order of magnitude. All hosts studied showed order(s) of magnitude greater affinity for dihydrogen phosphate over other guests in highly polar DMSO and addition of a third binding site as in **1.10** resulted in a binding constant too high to be measured accurately by ^{1}H NMR titration methods (Figure 1.7).[33]

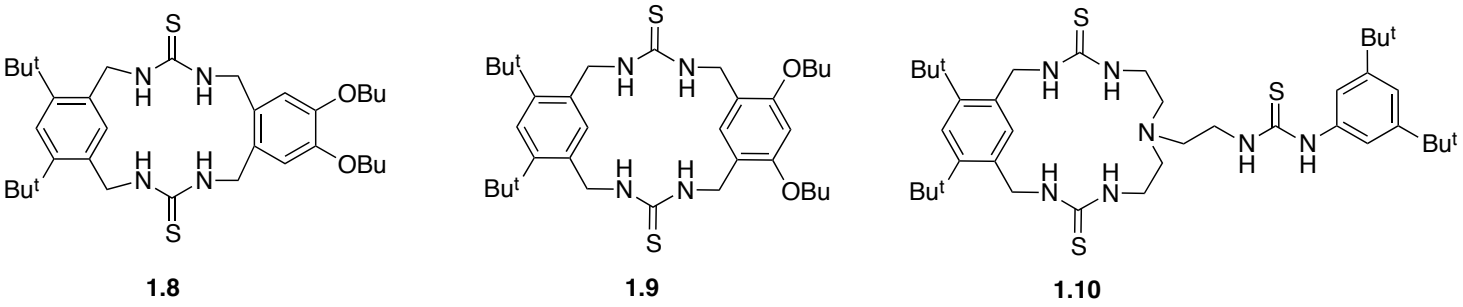

1.8 **1.9** **1.10**

Figure 1.7 Macrocyclic thiourea-functionalized anion receptors selective for dihydrogen phosphate.[33]

In an effort to compare directly the effect of hydrogen bond acidity with respect to anion recognition between ureas and thioureas, Monzani *et al* prepared analogous hosts **1.11** and **1.12** containing each binding element (Figure 1.8). They hypothesized that the more acidic thiourea-functionalized receptor (pK_A thiourea = 21.1, pK_A urea =26.9 in DMSO)[34] would deprotonate in the presence of basic anions such as fluoride, benzoate and acetate while the less acidic urea would not.

1.11 **1.12**

Figure 1.8 Urea and thiourea-functionalized anion receptors.[34]

The hypothesis was confirmed by monitoring the binding events through ^{1}H NMR and UV-vis titration techniques. Noteworthy results were obtained when fluoride and acetates were introduced into solutions of each receptor. Fluoride, benzoate and acetate were found to fully deprotonate the thiourea-functionalized host **1.12**, indicated by a new band forming at 410 nm in the UV-vis spectra with increasing guest addition along with careful monitoring of aromatic proton shifts during ^{1}H NMR titrations. The association constant between **1.12** and fluoride, where hydrogen bonds dominate is equal to the

equilibrium constant between the host-guest complex and the fully deprotonated host. The acetates also fully deprotonate host **1.12** but less efficiently than fluoride, an expected result based on the relative basicities of the anions. In contrast, urea-functionalized host **1.11** remained protonated in the presence of acetates and was deprotonated in the presence of fluoride, but much less efficiently than in the case of **1.12**. These findings begin to aid our understanding of the limitations of such highly acidic systems in the context of anion recognition.

1.2.1c Pyrroles

One of the most commonly observed hydrogen bond donors seen in anion recognition studies in recent years is the pyrrole, which serves both as a recognition element and a heterocyclic scaffold available for further functionalization with the groups mentioned above. The most prevalent example of the pyrrole being utilized as an anion binding element on its own is that of the macrocycle calix[4]pyrrole. Many permutations of this versatile scaffold have been produced in recent years tuned for differing specificities. One of the first examples of a calixpyrrole used as an anion binding agent is compound **1.13** (Figure 1.9) which displayed an association constant of ca. 17,000 M^{-1} toward fluoride, two orders of magnitude stronger than the nearest competitor chloride[35] Non-spherical anions dihydrogen phosphate and hydrogensulfate were also tested and both displayed binding affinities <100 M^{-1} with **1.13**.

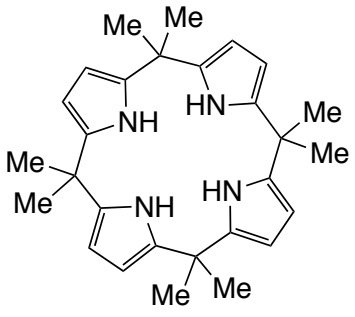

1.13

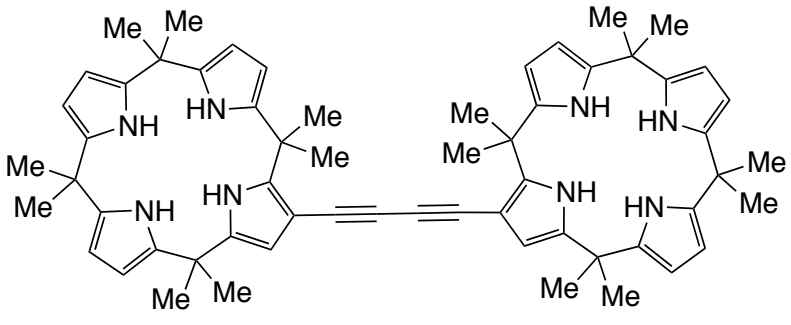

1.14

Figure 1.9 Calixpyrrole anion receptors.[35,36]

Bridged calixpyrroles have also been constructed through monofunctionalization of a pyrrole carbon such as compound **1.14**. Not surprisingly, dimers such as **1.14** display 2:1 binding with singly charged species however when dianionic species with optimal geometries such as isophtalate are introduced into these systems a 1:1 complex is observed. The latter binding stoichiometry is due to a postulated bridging mechanism whereby each oxyanion is recognized by one of the calixpyrroles and the guest is held in the center of a cooperatively bound complex.[36]

While pyrroles on their own as anion binders provide for a versatile area of research in this field, far more interest has been placed in appending other anion recognition elements to the pyrrole platform such as the aforementioned amides and ureas. Brooker *et al.* prepared a series of amide-functionalized pyrrole platforms and investigated their binding affinities toward various anionic guests. Compounds such as **1.15** displayed selectivity toward the benzoate anion[37] while dimer **1.16** functionalized with sulfonamides bound hydrogensulfate with greatest strength (Figure 1.10).[38]

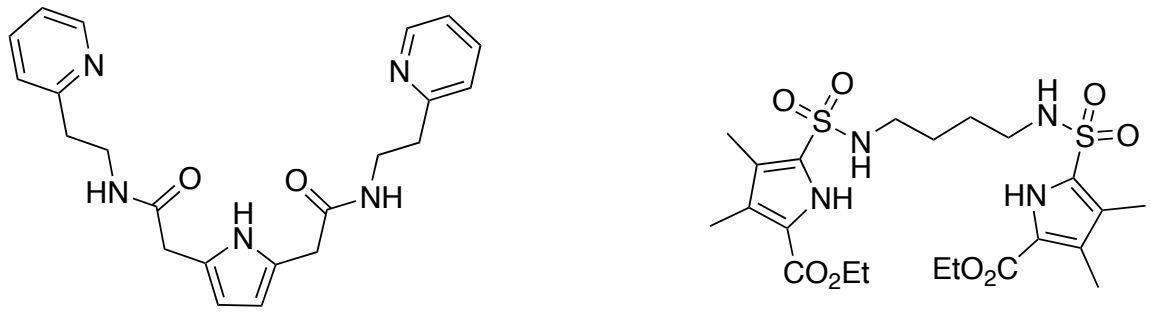

1.15 **1.16**

Figure 1.10 (Sulfon)amide-functionalized pyrroles as anion receptors.[37,38]

Quesada and coworkers constructed amidourea and analogous amidothiourea-functionalized pyrroles **1.17** and **1.18** (Figure 1.11). They discovered that upon addition of certain anions such as fluoride, benzoate, acetate and dihydrogen phosphate, urea-functionalized **1.17** bound the guests with moderate affinities ranging up to approximately 5×10^3 M^{-1} for fluoride. The more acidic thiourea **1.18** however failed to

form a complex with these guests and instead experienced a deprotonation event which was confirmed by X-ray crystal analysis.[39]

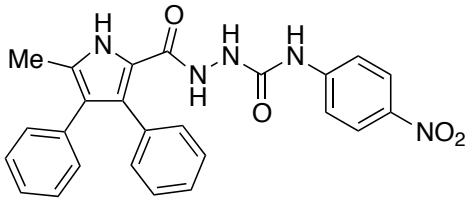

1.17

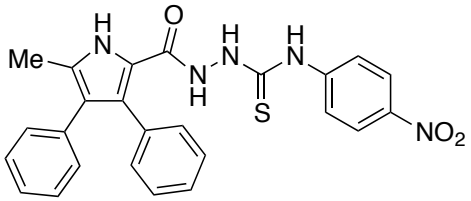

1.18

Figure 1.11 (Thio)urea functionalized pyrroles as anion receptors. Thiourea **1.18** experiences deprotonation upon encountering certain basic anions.[39]

1.2.2 Electrostatic Interactions

The importance of hydrogen bonding in anion recognition chemistry is clear. Oftentimes hydrogen bonding is observed working in cooperation with electrostatic attraction. Nearly always these electrostatic interactions are between the anionic guest and some form of cationic ammonium species. Classic examples of these types of attractive forces are those of the expanded porphyrins. Sessler and coworkers constructed a diprotonated expanded porphyrin **1.19**, commonly reffered to as sapphyrin, which forms stable fluoride salts in MeOH with association constants on the order of 10^5 M^{-1} determined by fluorescence titration experiments (Figure 1.12).[40]

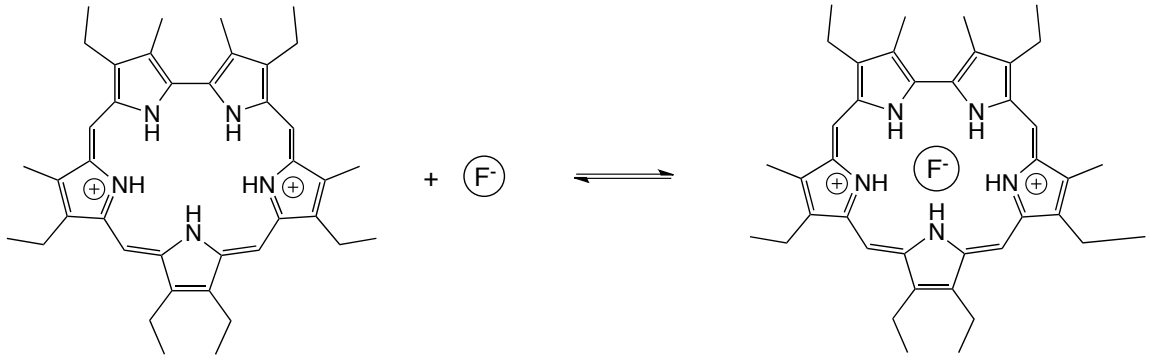

1.19 **1.19 · F⁻**

Figure 1.12 Equilibrium between dicationic sapphyrin 1.19 and the monocationic complex bound with fluoride.[40]

As Beer and Gale note in their review[9] one must be careful to regulate the pH of the interaction environment such that the ammonium species remains protonated but the anionic guest still remains anionic. With this in mind, guanidinium is an ideal candidate for providing favourable electrostatic attractive forces as it is approximately three orders of magnitude more stable than a protonated secondary amine and therefore remains protonated at higher pH values. Guanidinium was incorporated into the constructs **1.20-1.22** (Figure 1.13) which provide the favourable electrostatics along with hydrogen bond donating groups. **1.21** was found to bind 4-nitrobenzoate quite strongly with an association constant of 1.4×10^5 M^{-1} in chloroform.[41]

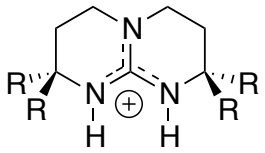

1.20 R = 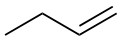

1.21 R = 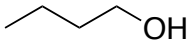

1.22 R = H

Figure 1.13 Bicyclic hosts containing the guanidinium cation.[41]

Transition metals have also been incorporated into host systems to impart positive charge and thus favourable electrostatic attractions toward anionic guests. Steed *et al.* developed a ruthenium-centered monocationic system containing two secondary amine hydrogen bond donating groups (Figure 1.14, compound **1.23**). The system showed moderately strong binding with hydrogensulfate with an association constant of ca. 5×10^3 M^{-1} in chloroform at ambient temperature, roughly five times stronger than the closest competitor nitrate. Introduction of the guest precluded the switch to the anti conformation.[42]

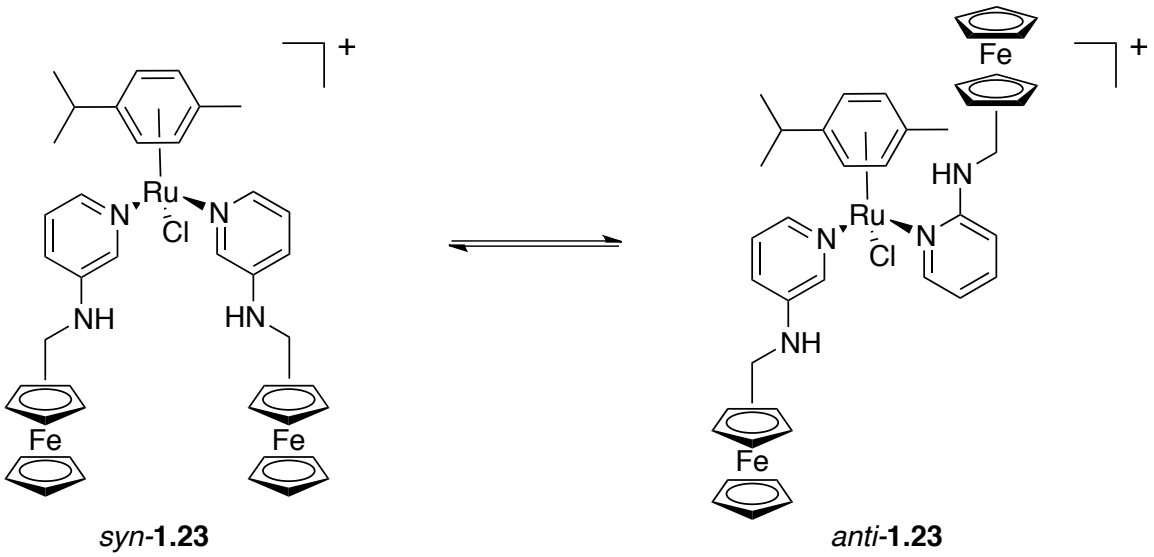

syn-**1.23** *anti*-**1.23**

Figure 1.14 Conformational equilibrium of ruthenium-centered, cationic anion receptor. The equilibrium shifts left upon addition of guest.[42]

1.2.3 Anion-π interactions

A relatively recent area of anion recognition chemistry of interest to the community is that of anion-π interactions. These weak interactions generally involve electron deficient aromatic systems as the recognition elements. The first evidence of these interactions came about through NMR studies in the early nineties by Schneider *et al*. It was discovered that diphenylamine **1.24** positive complexation-induced chemical shifts (CIS) upon being introduced to the dicationic species **1.25** as well as the dianionic species **1.26.** The CIS observed for the aromatic proton signals on **1.24** fully complexed with **1.25** were 0.10 (H_{ortho}), 0.14 (H_{meta}) and 0.24(H_{para}) with a calculated binding energy of 25 kJ mol^{-1}. The CIS observed for the same signals on **1.24** fully complexed with **1.26** were 0.11 (H_{ortgho}), 0.09 (H_{meta}) and 0.08 (H_{para}) resulting in a calculated binding energy of 22 kJ mol^{-1}. The positive magnitude of these CIS valuse indicates downfield shifts in each signal for both complexation events. This is to be expected for the former case due to the electrostatic attraction between the ammonium group and the aromatic π-electrons of **1.24**, often referred to as cation-π interactions, resulting in a deshielding effect.

In the latter case, the magnitude of the CIS as well as the that of the binding energy is unexpected based on the electrostatic repulsion imparted on the aromatic π-

electrons of **1.24** by the nearby sulfonate groups and is attributed to an induced dipole which directs electron density away form the protons of **1.26** resulting in a slight deshielding effect and a complex with stability comparable to **1.24**.[43]

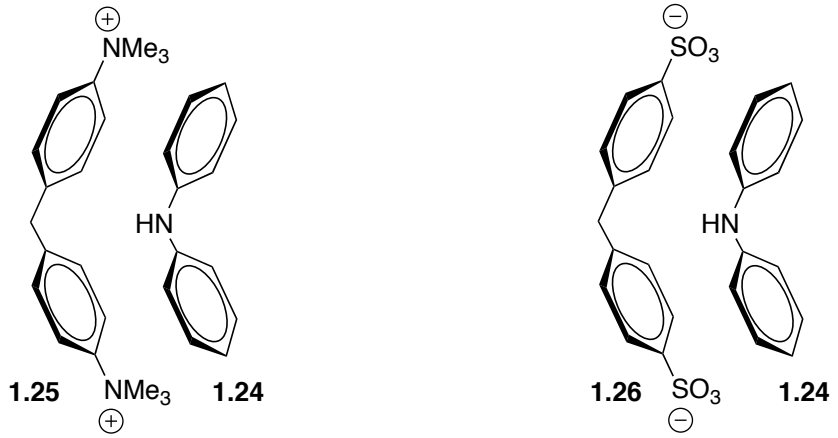

Figure 1.2 Host-guest systems with similar binding energies determined by ^{1}H NMR titrations displaying the first sign that anion-π interactions exist.[43]

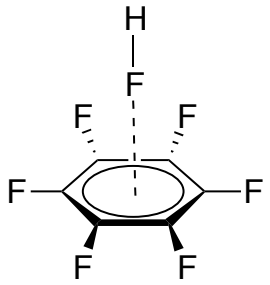

Figure 1.16 Schematic representation of the $C_6F_6\cdots$F-H complex.[44]

These findings sparked computational investigations into such interactions by Alkorta and group in 1997. The system modeled in this case was hexafluorobenzene complexed with H-F (Figure 1.16).[44] The calculated energy of complexation was indeed favourable at -5 kJ mol^{-1}. In the following years several more comprehensive DFT studies were released where many more electron deficient rings were modeled and complexed with many more anions, in all cases favourable binding energies were calculated (Figure 1.17). [43]

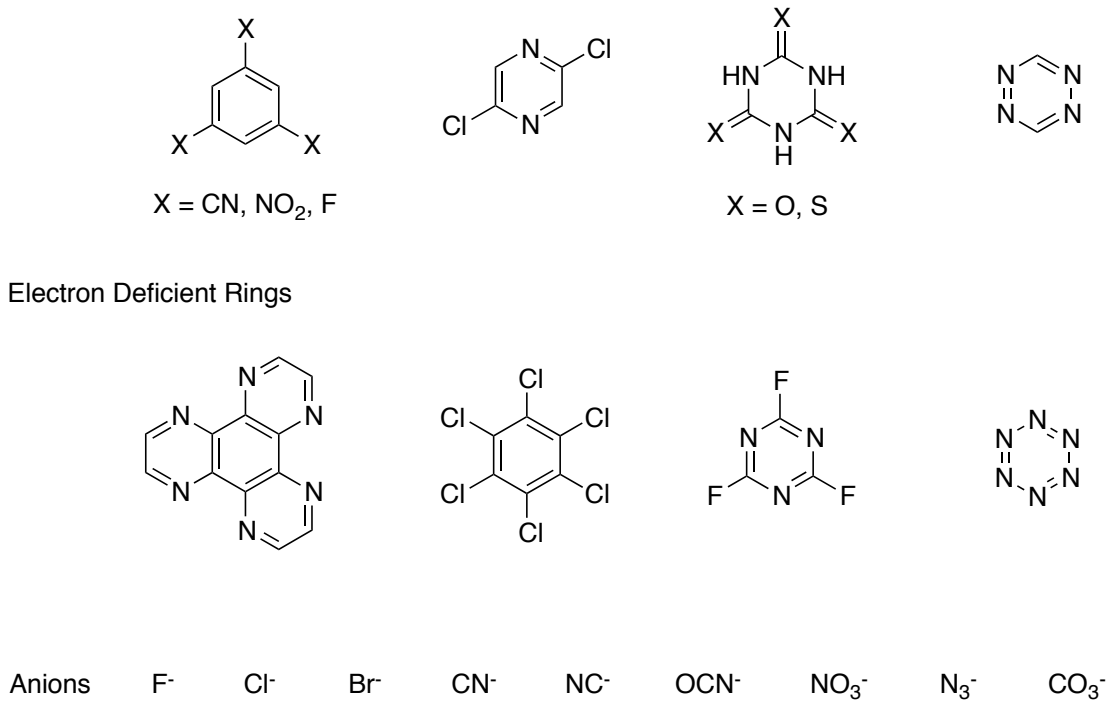

Figure 1.17 Sample of species studied in the more in depth computational investigations of 2002.[43]

These gas phase calculations prompted experimental solution phase binding to be investigated. Johnson and collaborators designed analogous receptors **1.27** and **1.28** containing neutral and electron deficient aromatic rings respectively (Figure 1.18). Upon introduction of anionic species, the fluorinated derivative displayed chemical shifts in the proton NMR leading to calculated association constants of approximately 20-30 M^{-1} for halide guests in chloroform while no shifts were observed in the neutral species.[45]

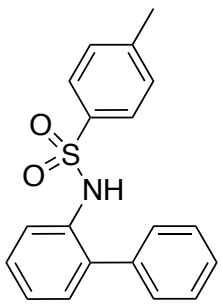

1.27

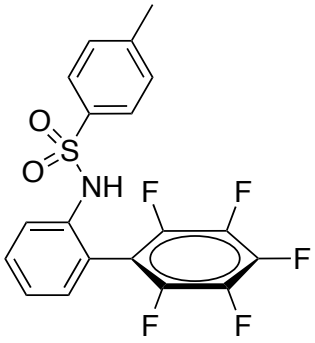

1.28

Figure 1.18 Species employed in solution phase studies of anion-π interactions. **1.28** displayed binding with chloride, bromide and iodide while **1.27** displayed none.[45]

1.3 Functional anion receptors

1.3.1 Sensors

In order to determine whether concentrations of certain anions are within tolerable levels, be it in environmental samples or in living beings, interest in developing new, efficient anion sensors has been burgeoning in recent years. The most common sensing technique employed by far is optical and most sensors contain either a chromophore or fluorophore. A commonly observed chromophore in the literature is the nitrophenyl moiety which has been appended to myriad platforms in order to detect changes in analyte concentration through UV-vis spectroscopy. Teramae and group developed thioureas appended with nitrophenyl group(s) and observed significant bathochromic shifts in the UV-vis spectra upon introduction of acetate (Figure 1.19). The sensor containing two nitrophenyl units (**1.29**) displayed an association constant two orders of magnitude stronger (K_{assoc} = 3.5 × 10^5 M^{-1}) than **1.30** (K_{assoc} = 5.6 × 10^3 M^{-1}) containing only one, as expected.[46]

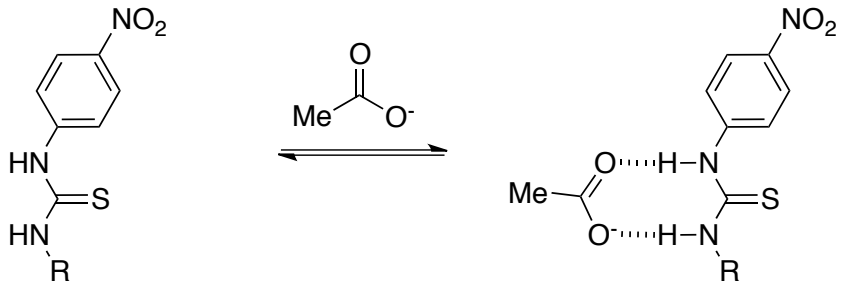

1.29 R = *p*-nitrophenyl

1.30 R = CH_3

Figure 1.19 Colorimetric thiourea-based anion receptors. The more acidic **1.29** containing two nitrophenyl groups bound anions with greater strength.[46]

Calixpyrroles have already been introduced as potent fluoride receptors, and when conjugated to nitrophenyl chromophores can act as fluoride sensors. Receptors **1.31** and **1.32** (Figure 1.20) both displayed bathochromic shifts in dichloromethane upon introduction of fluoride (**1.31** λ_{max} = 391 nm to λ_{max} = 433 nm) (**1.32** λ_{max} = 441 nm to λ_{max} = 498 nm). Colour changes were also seen with host **1.32** in the presence of chloride and dihydrogen phosphate.[47] Other chromophores commonly utilized include aza dyes,[48,49] naphthalenes,[50,51] naphthalimides,[52,53] anthraquinones[54-56] and many others.[57]

Affixing fluorophores to anion binding units is another common way to detect certain analytes. Upon addition of a sample for analysis to the sensor, one can detect whether the analyte of interest is present by detecting changes, either enhancement or quenching, in the emission spectra. While the binding strength of the host may be affected by this structural modification, quantification of analyte concentration can still be achieved through fluorescence titration experimetns. In order to determine the change in binding strength, if any, upon functionalizing the host with a fluorophore, one can conduct ^{1}H NMR titrations on the unfunctionalized "naked" host with the guests of interest.

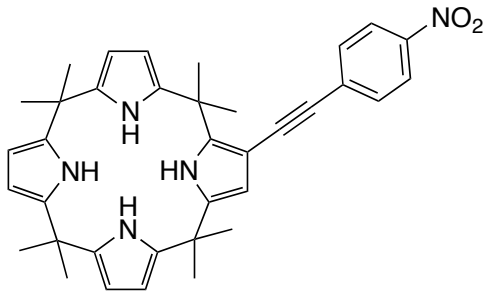

1.31

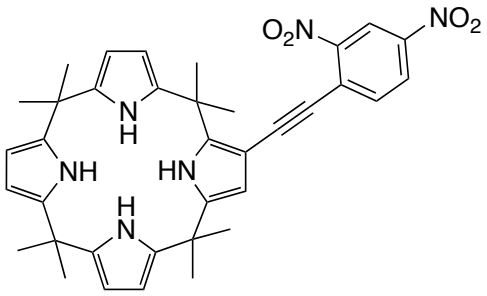

1.32

Figure 1.3 Calix[4]pyrroles conjugated to nitrobezenes, 1.31 is fluoride selective while 1.32 shows changes in its absorption spectrum in the presence of fluoride, chloride and dihydrogen phosphate.[47]

Anthracene is one of the most common fluorophores used to this end because it and many functionalized derivatives are commercially available and its photophysical properties have been thoroughly studied (quantum yield in acetonitrile is 0.36).[58] Again returning to calix[4]pyrrole, anthracene was attached to the macrocycle (**1.33-1.35,** Figure 1.21) through an amide linkage by Gale and colleagues and fluorescence quenching was observed upon the addition of fluoride. Partial quenching was also seen in the presence of chloride and dihydrogen phosphate but the greatest emission quenching was caused by fluoride.[59]

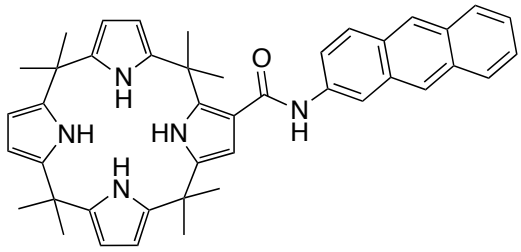

1.33

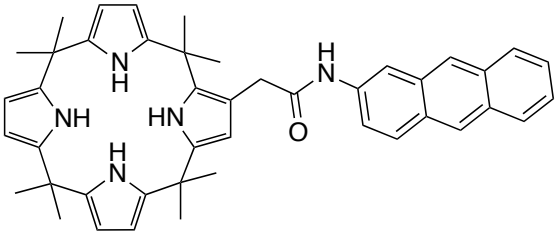

1.35

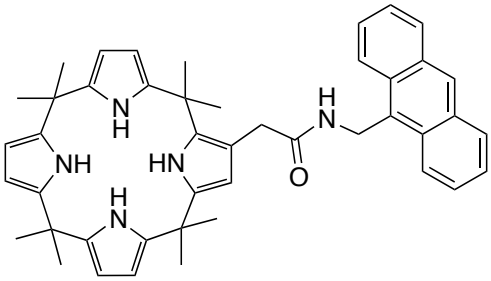

1.34

Figure 1.4 Calix[4]pyrroles linked to anthracenes. All hosts display greates fluorescence quenching in the presence of fluoride, with moderate quenching seen in the presence of chloride and dihydrogen phosphate.[59]

Anzenbacher and coworkers constructed several tripodal anion binders functionalized with common organic fluorophores and found that some of these could serve to differentiate between certain anions based on varying degrees of fluorescence enhancement (**1.36-1.43**, Figure 1.22).[60] Fluorescence titrations revealed similar binding affinities for all hosts towards various anions, halides and oxyanions, all in the 10^6 M^{-1} range in DMSO. The sensors did however exhibit differing emission strength enhancements allowing for differentiation of guests. In order to test their viability to determine anionic species in complex media, the sensors were treated with human blood serum and through the use of a mathematical model known as principal component analysis sensors **1.36-1.39** and **1.40-1.43** were able to differentiate between phosphate, pyrophosphate, AMP and ATP. These results show promise towards the development of a point-of-care method for monitoring phosphate levels in humans.

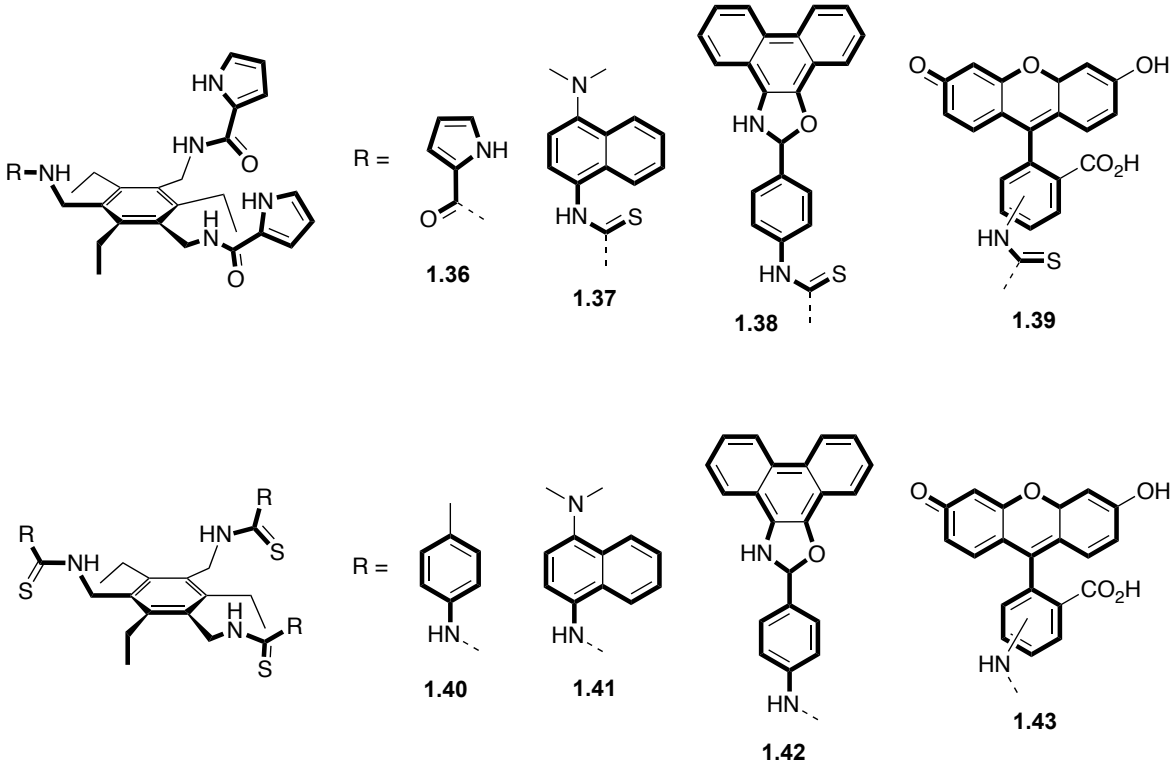

Figure 1.5 Series of fluorescent tripodal hosts able to differentiate between biologically relevant anionic guests.[60] Bold wedges on the host scaffolds used to show perspective, bold lines on the substituents used to illustrate the front edge of a plane[61].

1.3.2 Extractants

As mentioned earlier, there has been growing attention toward creating anion receptors capable of extracting contaminants out from undesired areas, particularly natural bodies of water and nuclear wastes. Of particular concern along with what has been mentioned above is the excess of radioactive waste stored in underground tanks produced during the cold war.[62] A safe way to dispose of this is through a process known as vitrification, whereby the waste is incorporated into a transportable glass and can be stored safely for thousands of years, a process which is impeded by the presence of sulfates. These wastes also contain high concentrations of nitrates, which under standard aqueous-organic extraction conditions enter the organic phase more readily than do sulfates. Moyer, Sessler and coworkers have developed functional cyclo[8]pyrroles **1.44**

and **1.45** which are highly selective towards sulfates and are able to preferentially extract them over nitrates into organic media overcoming the so-called Hofmeister bias (Figure 1.23).[63]

Originally a scale to measure the effects of various salts on protein solubility derived from studies carried out by Franz Hofmeister in the late nineteenth century,[64] the terminology used in this context is used to qualitatively guage water solubility of certain ions. Those that are better solvated induce an overall reduction in the amount of free water molecules in solution, increasing effective protein concentration in solution and eventually causing the protein to precipitate. Sulfates were found to induce precipitation in lower concentrations than nitrates and are hence said to be more water-soluble. Without the presence of a highly selective receptor, sulfates should by this logic be more difficult to extract out of aqueous media than nitrates.

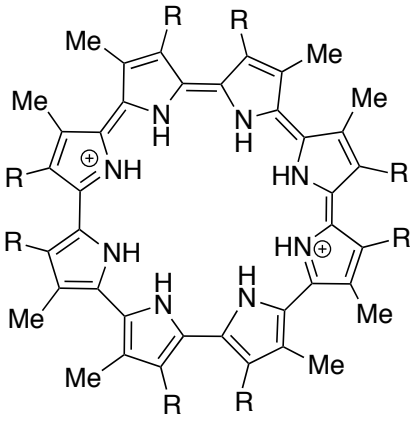

1.44 R = $C_{11}H_{23}$

1.45 R = C_2H_5

Figure 1.6 Cyclo[8]pyrroles developed by Moyer *et al.* The more hydrophobic **1.44** proved to be an exceptional sulfate extractant from aqueous media even in the presence of nitrate anions.[63]

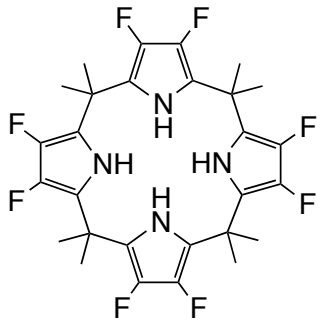

1.46

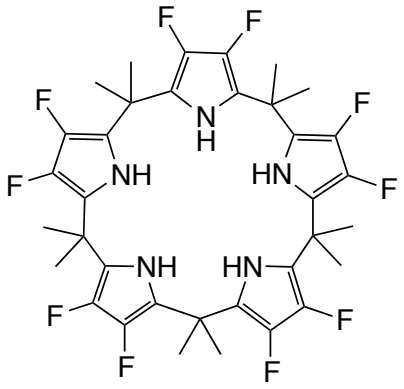

1.47

Figure 1.7 Calixpyrroles extract anions into organic media against the Hofmeister bias.[65]

A similar effect of overcoming the Hofmeister bias was observed with the use of fluorinated calix[4]pyrrole **1.46** and calix[5]pyrrole **1.47** (Figure 1.24). Cesium (counterion chosen based on its relatively high extractability) salts of anions ClO_4^-, I^-, NO_3^-, Br^-, Cl^-, and F^- were dissolved in water at 10 mM and extracted into nitrobenzene in the presence and absence of **1.46** and **1.47.**[65] Extraction efficiency was monitored using ^{137}Cs tracer techniques to measure cesium distribution ($D_{Cs} = [Cs]_{aqueous}/[Cs]_{organic}$). Without the calix[n]pyrroles present, the expected Hofmeister series was observed with respect to extraction efficiency, so the observed extraction order was $ClO_4^- > I^- > NO_3^- > Br^-$. The decreasing extraction efficiency into the organic phase corresponds to the free hydration energy of each species. Perchlorate salts are less water soluble and are therefore extracted into the organic phase more efficiently than bromide salts. In the presence of receptor **1.46**, little discrimination was observed among extraction efficiencies of the halogens iodide, bromide and chloride while calix[5]pyrrole **1.47** displayed a preference for extraction of nitrate and fluoride, overcoming the Hofmeister bias. Extractants such as those described above show great potential for commercial uses in the future.

1.3.3 Transmembrane anion transporters

There has been much focus in recent years on developing novel compounds that can serve as facilitators of anion transport into and out of cells given the various aforementioned disease states caused by misregulation of chloride concentration. Cholapods (ie: **1.48, 1.49**) and cholaphanes (ie: **1.50, 1.51**) have been designed to affect anion, especially chloride transport across the cell wall. They are able to do this because of their hydrophobic steroidal backbone and polar binding sites. Davis and Judd affixed ureas to the steroidal backbone as chloride recognition elements and functionalized the terminal cyclohexane with various polar functional groups (Figure 1.25). It was found that all constructs affected chloride transport into vesicles with compound **1.51** being the most efficient transporter. Computational studies suggest that this partially caged conformation with an extra benzene in the system allows for fewer water molecules to access the anion and the guest is bound more tightly, a supposition backed by binding data. Caged compounds **1.50** and **1.51** exhibit association constants in the 10^8 M^{-1} range with chloride while the others (**1.48** and **1.49**) bind chloride an order of magnitude more weakly.[66]

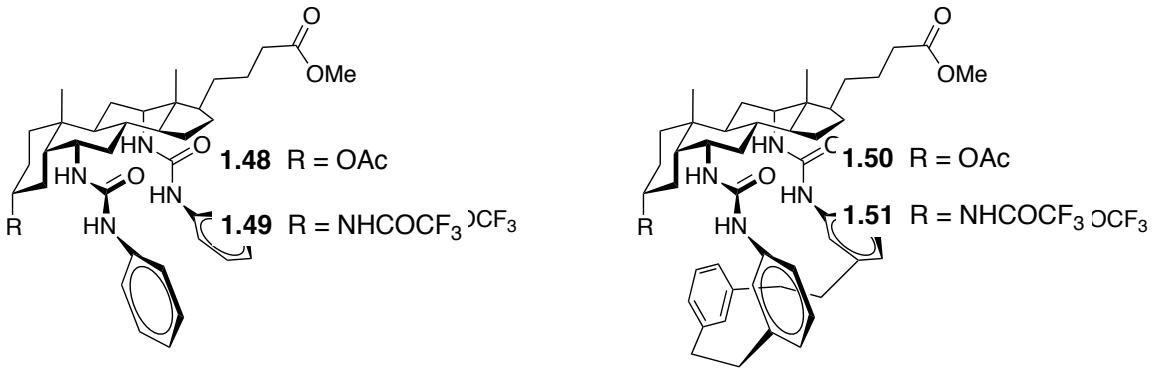

Figure 1.8 Cholapods (left) and cholaphanes (right) affect chloride transport across vesicle membranes.[66]

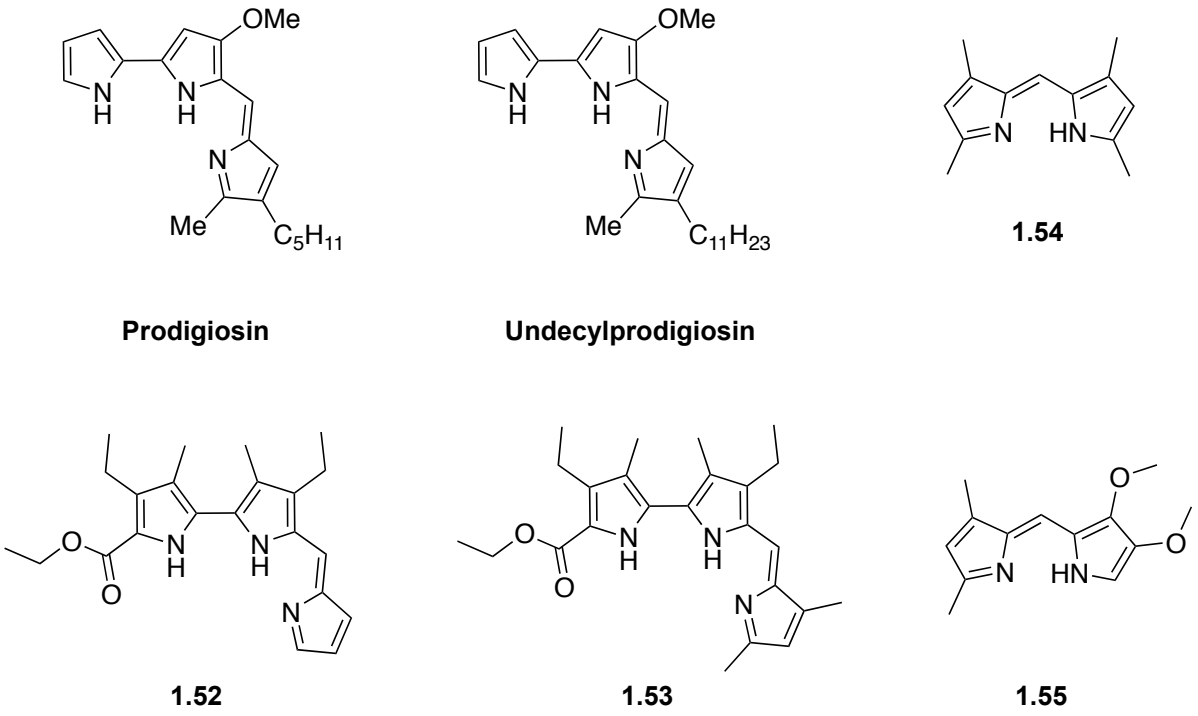

Figure 1.9 Natural products prodigiosin and undecylprodigiosin isolated from *S. marcescens* known as prodiginenes.[67] Synthetic analogs **1.52, 1.53** known as progiosenes developed by Sessler and coworkers.[68] All compounds are thought to affect H^+/Cl^- symport (simultaneous transport in the same direction) across the cell membrane and cause apoptosis of certain cancer cells. Simplified dipyrrins **1.54** and **1.55** have similar effects.[68]

The natural product class of the prodigiosins (Figure 1.26) isolated from the *Serratia marcescens* bacterial family have a bright red pigment and exhibit a wide range of biological activities against bacteria, protozoa and pathogenic fungi. They are also able to induce apoptosis in many different human cancer cell lines but are extremely light sensitive.[67] It is not surprising that given their therapeutic potential, analogs that are more stable are being synthesized and tested for their biological activity. One example among many is the work of Sessler *et al.* who developed several small molecules with the prodigiosin (ie: **1.52, 1.53**) or simplified dipyrrin (ie: **1.54, 1.55**) backbone that displayed activity against A549 human lung cancer cells (Figure 1.26).[68] The mode of action carried out by these compounds is thought to be an H^+/Cl^- symport mechanism whereby one of the nitrogen atoms bears a positive charge and carries an extra proton, further

attracting the chloride ion through favourable electrostatic forces, then releases this proton inside the cell causing a slight drop in pH and subsequent apoptosis of cancer cells.

Anion recognition chemistry is now a rapidly growing field, with efforts to construct new hosts that have medicinal and environmental benefits. The vast number of platforms to which a relatively small selection of binding elements can be affixed has led to myriad constructs that display some of these practical functions described above. As this avenue of research continues to grow, new scaffolds and perhaps new binding motifs will certainly be uncovered and perhaps lead to better and more efficient therapeutics, anion sensors and extractants.

1.4 Summary and key questions

This chapter has demonstrated the motivations for anion recognition, and the structural requirements for the construction of potent anion receptors. Slight changes to host size, location of binding elements and in the case of hydrogen bonding, acidity of the hydrogen bond donor, can significantly alter binding affinity and guest selectivity. Some of the key weak interactions dictating anion recognition properties have been discussed but above all hydrogen bonds are arguably the most important in synthetic receptor design and most prevalent in nature. The purpose of this thesis work is to explore the strong hydrogen bonding capabilities of a collection of functional groups — carboxylic acid bioisosteres — that have been relatively underused in the construction of anion receptors.

The motivation for these studies is propelled by the following questions: can we create new classes of anion binding agents containing the tetrazole molecule? If so, will they be more potent anion binders than those commonly observed in the literature? Will they contain some inherent selectivity toward any biologically relevant anions?

A small sample of functional anion receptors has been described above. These compounds possess anion sensing, aqueous anion extracting and transmembrane anion transport capabilities. Can we incorporate the tetrazole thereby expanding the functional groups at our disposal for anion binding into compounds that have similar functions? I will describe my initial attempts to incorporate the tetrazole on a common supramolecular

scaffold in calix[4]arene (Chapter 2). I will subsequently describe how the results attained in the studies described in chapter 2 led us to construct pyrrolyl-tetrazole hybrids (Chapter 3) followed by extension of the studies in chapter 3 to create pyrrolyl-tetrazoles functionalized with the carbonyl compounds esters and amides (Chapter 4) and discuss some of the possible pitfalls of this motif when applied to biological systems.

Chapter 2. Recognition Properties of Carboxylic Acid Bioisosteres: Anion Binding by Tetrazoles, *N*-Aryl Sulfonamides and *N*-Acyl Sulfonamides on a Calix[4]arene scaffold.

Portions of this Chapter were previously published, and are reprinted with permission from Pinter, T.; Jana, S.; Courtemanche, R. J. M.; Hof, F., Recognition Properties of Carboxylic Acid Bioisosteres: Anion Binding by Tetrazoles, Aryl Sulfonamides, and Acyl Sulfonamides on a Calix[4]arene Scaffold. *J. Org. Chem.,* **2011**, *76* (10), 3733–3741. Copyright American Chemical Society 2011.

This work was conceived of by Thomas Pinter and Fraser Hof.

Synthesis and binding studies of hosts **2.10** conducted by Dr. Subrata Jana.

Synthesis of host **2.9** conducted by Thomas Pinter with work contributed by Rebecca J. M. Courtemanche.

Synthesis and binding studies of all other hosts, CSD data collection and Spartan calculations conducted by Thomas Pinter.

The manuscript was written by Thomas Pinter and Fraser Hof, and this Chapter was adapted from that paper by Thomas Pinter.

2.1 Foreword

Many factors have to be taken into consideration when rationally designing new hosts for anionic guests. As mentioned earlier, spatial orientation of the guest must be complementary to the binding site of the receptor (See figure 1.1). The binding site of the receptor must also exhibit size complementarity with the anionic guest of interest and ideally be easily tunable in order to impart some specificity toward said guest. The importance of the hydrogen bond has been exhaustively demonstrated in recent decades. It is well understood that strong hydrogen bond donors generally make for better anion binding elements. Chapter 1 also highlighted the importance of other non-covalent interactions such as electrostatic forces and the more recently demonstrated anion-π interactions.

The content of this chapter summarizes my efforts to introduce new strong hydrogen bond donating elements that are virtually unexplored in the context of anion binding to a common supramolecular scaffold calix[4]arene, briefly mentioned in chapter 1, in the hopes of generating novel, potent anion receptors. The moieties chosen were tetrazoles and *N*-acyl sulfonamides. Hosts bearing *N*-aryl sulfonamides, anion binding elements which have been thoroughly studied in a wide variety of structural contexts were also prepared as a basis for comparison. We envisaged the rigid, conical binding pocket of calix[4]arene as a suitable center for binding spherical anions of similar size.

2.2 Abstract

Calixarenes are well known supramolecular scaffolds functionalized to bind a variety of guests including metals,[69] cationic amino acids,[70] and anions.[71] In efforts to introduce new anion recognition elements to well understood platforms, I set out to synthesize fourfold symmetric calix[4]arenes functionalized with tertrazoles and *N*-acyl sulfonamides, functional groups virtually unexplored in the world of anion recognition. Four new hosts containing these groups were prepared and their binding properties with a variety of biologically relevant halides and oxyanions determined by ^{1}H NMR titrations. These results were then compared with binding data collected on analogous hosts functionalized with *N*-aryl sulfonamides on the upper rim. The results were not as expected, as the binding was relatively weak for all hosts studied given their presumed

excellent hydrogen bond donating abilities. Curious, I set out to perform computational analyses to determine the optimal binding geometries of these functional groups and discovered that the calix[4]arene platform was less than ideal in presenting these particular binding elements to a guest affixed in the central cavity. I also explored the Cambridge Structural Database of all X-ray crystal structures reported in recent decades and the important dihedral angles in these moieties deviate greatly from optimal when engaging a central guest on calix[4]arene. Of particular interest was the discovery that tetrazoles seem to prefer co-planarity when bound to an aryl neighbour, presumably to maintain conjugation.

2.3 Introduction

In a molecule, when one set of atoms is replaced by another with very similar size, shape, and chemical properties the phenomenon is known as *isosterism*. The concept was first envisaged by Langmuir in the early twentieth century, saying that "….isosteres must contain the same number and spatial arrangement of electrons and therefore the same number of atoms….the differences between isosteres are confined to the charges around the nuclei of the constituent atoms." He correctly predicted the analogy between diazomethane and a ketene which was not proven experimentally until much later.[72] Erlenmeyer expanded these thoughts with some other caveats, not the least of which being the universally taught notion that elements in a common row of the periodic table posses similar properties that he called isosterism.[73] Present definitions of the term include some more specific criteria, including that isosteres should share nearly equal spatial volumes among several other physical properties and should be able to cocrystallyze.[72]

In proteins, the most prominent type of anion present is carboxylate. Negatively charged amino acids are often present at cation-binding hotspots to offer favourable electrostatic attractions. They are also one half of the common salt-bridge binding motif and are present in myriad enzyme substrates and cofactors. Development of drugs and sensors that mimic these substrates often requires the creation of esterified analogues of carboxylates that, upon passage through a cell membrane, are hydrolyzed to the corresponding carboxylate derivative by native esterases. This is an example of a "pro-

drug" strategy. An alternate strategy in drug development is replacement of the carboxylic acid group with a functionally similar moiety, one for which the body lacks the evolved metabolic pathways to effect its degradation. These are known as bioisosteres of carboxylates. Bioisosteres do not necessarily fit the aforementioned classical definitions of isosteres, they do however display similar biological activity *in vivo* and display some similar properties, a common one being pK_a values of acidic protons within the moiety. Common carboxylic acid bioisosteres include *N*-aryl sulfonamides, *N*-acyl sulfonamides, and tetrazoles (Figure 2.1). Utilizing these functional groups in drug development often leads to improved oral availability, metabolic stability and potency relative to carboxylate bearing analogues.[74-76] It follows that a vast number of small molecule therapeutics contain tetrazole,[76,77] *N*-aryl sulfonamide[78,79] and *N*-acyl sulfonamide functionality.[80-82]

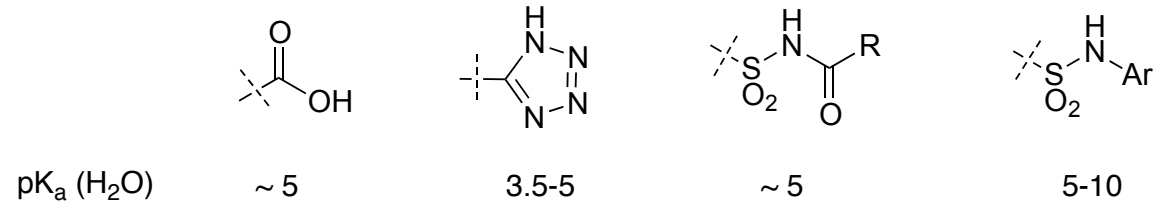

Figure 2.1 Some common carboxylic acid bioisosteres along with their corresponding aqueous pK_a vaues. Left to right: Carboxylic acid, tetrazole, *N*-Aryl sulfonamide, *N*-Acyl sulfonamide.

Representative examples of such replacements in pharmaceuticals on the market include Losartan which is one of the six approved tetrazole-containing angiotensin II type 1 receptor (AT_1) antagonists used for the treatment of hypertension.[77] Sulfanitran has been shown to stimulate transport properties of human multidrug resistance protein 2 (MRP2)[83] and is also an active ingredient in Novastat, a coccidiostat (anti-parasitic) used in the poultry industry.[84] Navitoclax is a potent inhibitor of the antiapoptotic protein Bcl-x_L, overexpression of which is linked to several types of cancer and is currently in phase II clinical trials for the treatment of small cell lung cancer[85] (Figure 2.2).

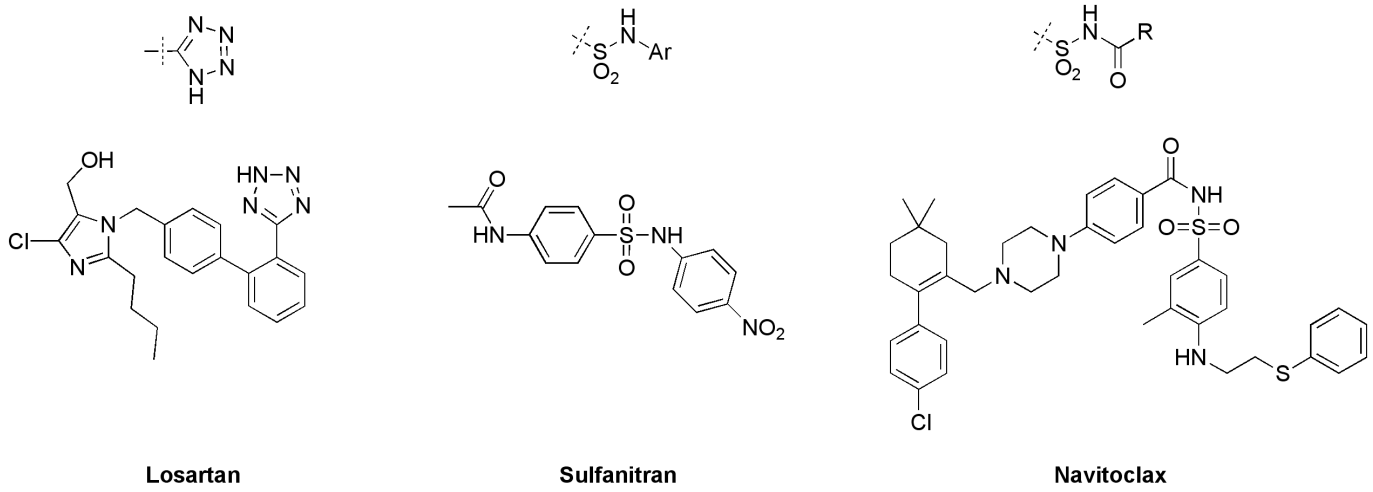

Figure 2.2 Representative drugs Losartan, Sulfanitran, and Navitoclax containing tetrazole, aryl sulfonamide and *N*-acyl sulfonamide functionality respectively.

Our group has relatively recently displayed that a simple tris(tetrazole) host in its neutral, protonated state is among the most potent neutral binders of anions yet reported, several orders of magnitude more potent than its carboxylic acid functionalized analog.[86] Upon learning the superior anion binding capability of the tetrazole over the carboxylic acid when appended to this Anslyn-type tripodal scaffold,[9] efforts were turned to studies that would directly compare the former with the other aforementioned bioisosteres. To study these groups within the context of a well-understood scaffold, syntheses were carried out to affix each of them to calix[4]arene. The binding strength of the resulting hosts were explored with several biologically important halides and oxyanions and determined the roles of functional group conformational preferences on guest binding.

2.4 Synthesis of Host Molecules

The synthesis commenced with the generation of the known calix[4]arene core with no functionalization at the upper rim (**2.2**). This was accomplished through an initial condensation between *p*-tert-butyl phenol and paraformaldehyde followed by the $AlCl_3$ mediated tert-butyl group excision.[87] The lower rim was further functionalized to prevent hydroxyl reactivity and to aid in solubility affording **2.3**, the common intermediate toward all sulfonamide containing hosts (Scheme 2.1) along with **2.4**. The

use of relatively short chains on the lower rim is common, and for studies done in water care must be taken not to attach longer hydrophobic chains to prevent micelle formation.

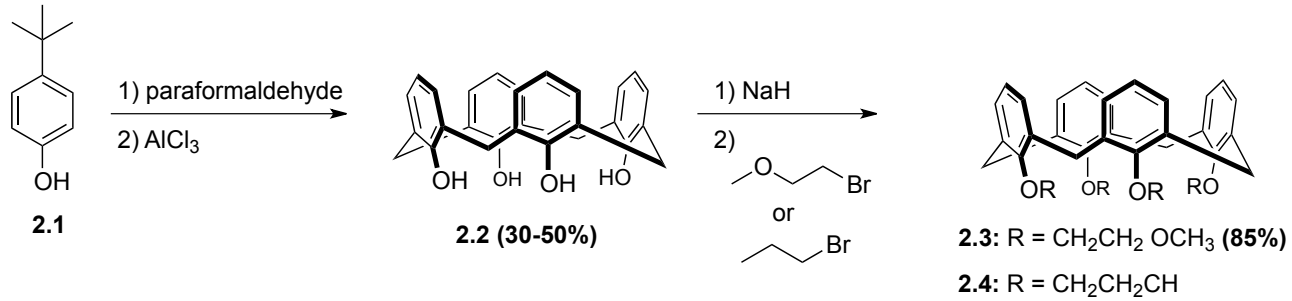

Scheme 2.1 Synthesis of initial calix[4]arene scaffolds

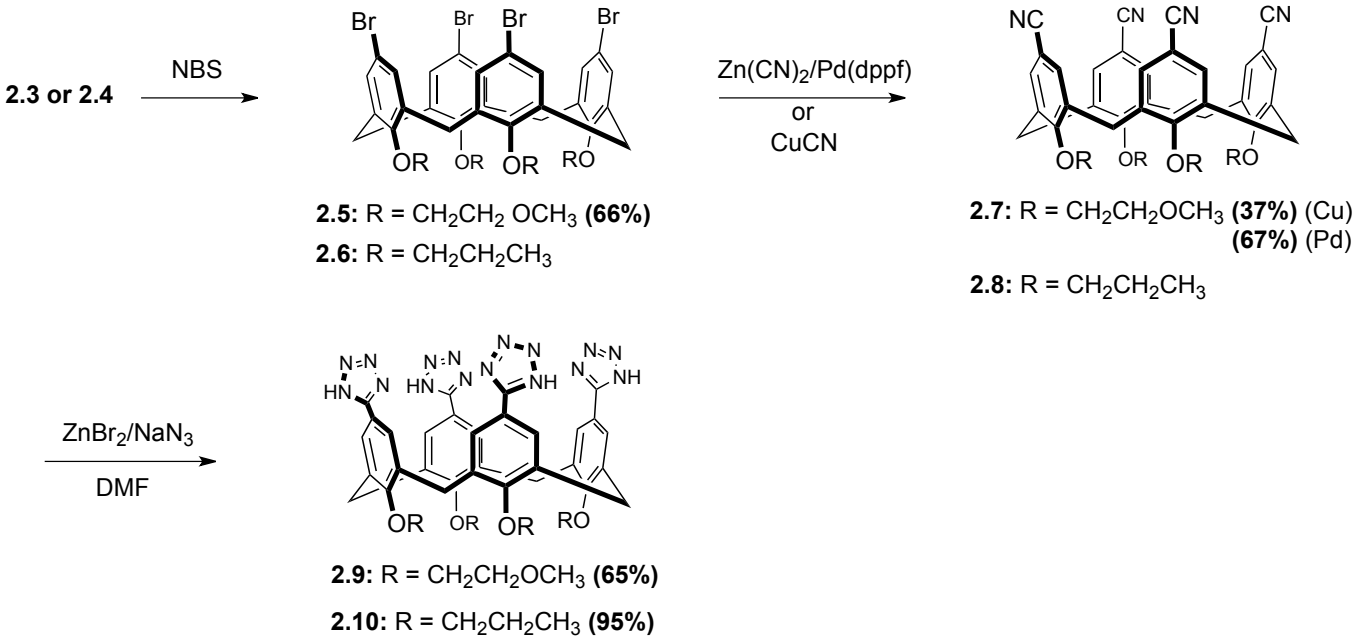

Scheme 2.2 Synthesis of tetrazole-functionalized hosts.

En route to the tetrazole functionalized hosts, intermediates **2.3** and **2.4** were first brominated with *N*-bromo succinimide (Scheme 2.2). Initially, copper catalyzed coupling conditions[88] were attempted to insert the nitrile groups but required extremely elevated temperatures, and were met with low yields and difficult isolation procedures. Attention was then turned to a palladium-mediated procedure which proceeded under much milder conditions and met with ease of isolation and better yields.[89] The final tetrazole-containing constructs were produced as in Scheme 2.2, using a variation on conditions for tetrazole formation developed by Demko and Sharpless.[90] Reactions were shortened in time and increased in yield upon use of microwave irradiation affording the fully tetrazole-substituted hosts **2.9** and **2.10**.

All sulfonamide appended hosts sprouted from the known chlorosulfonylated calix[4]arene **2.11**, generated by treating **2.3** with chlorosulfonic acid.[91] Toluidine and *p*-nitroaniline were selected as the aryl sources to observe any consequence a disparity between electron withdrawing or neutral substituents appended to the aromatic ring would have on binding, and upon reaction with excess aniline in pyridine, hosts **2.12** and **2.13** were isolated (Scheme 2.3).

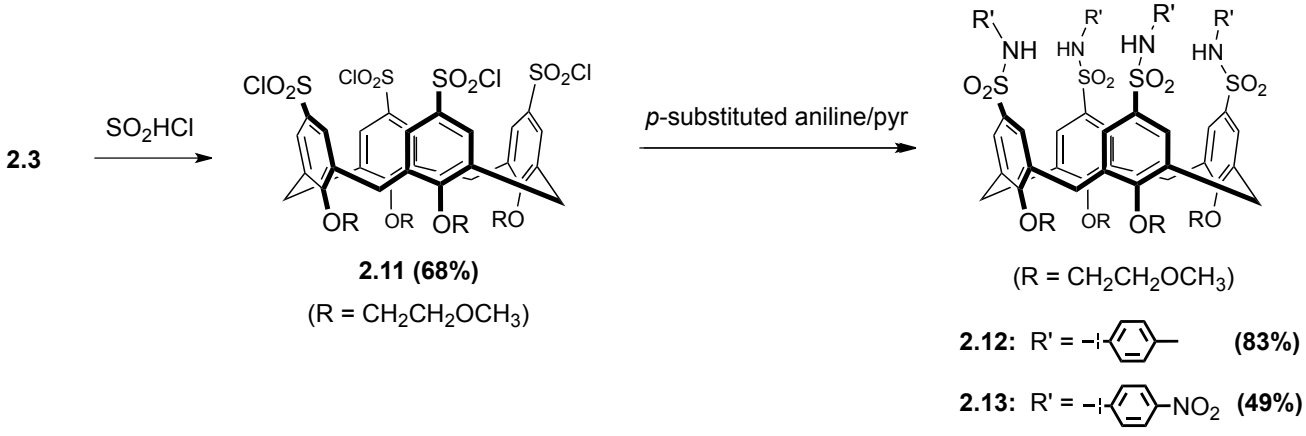

Scheme 2.3 Synthesis of *N*-aryl sulfonamide-functionalized hosts.

An extensive body of literature on the preparation of *N*-acyl sulfonamide exists,[92-97] but we found almost all literature methods incapable of providing the clean reactions and high conversions required in order to isolate significant quantities of the fourfold-symmetric *N*-acyl sulfonamide products **2.15** and **2.16.** Synthesis of the *N*-acyl sulfonamide hosts was first attempted using chlorosulfonylated calix[4]arene **2.11** as the starting material. Reaction of a primary amide (benzamide), and pyridine/DMAP even at reflux failed to produce the desired *N*-acyl sulfonamide product **2.16**. Use of Et_3N or Et_2*i*-PrN in various solvents at elevated temperatures led to complex mixtures and/or extremely slow reaction rates. We then turned our attention to *N*-acylation approaches that start instead with a primary sulfonamide. We created the known primary sulfonamide **2.14**[91] in one step by treating **2.11** with gaseous ammonia, and reacted it with benzoyl chloride in pyridine/DMAP; again, conversions were extremely low and **2.16** could not be isolated from the complex mixture. We attempted to couple **2.14** with benzoic acid using 1-Ethyl-3-(3-dimethylaminopropyl)carbodiimide (EDC) in the presence of tertiary amine bases, but observed instead rapid formation of benzoic anhydride from self-coupling of benzoic acid prior to slow reaction of the resulting anhydride to give some acyl sulfonamide-containing products. Finally, we found that solvent- and base-free conditions in which the primary sulfonamide **2.14** is treated with neat benzoyl chloride or acetyl chloride at high temperatures, proved to be a superb method that produced **2.15** and **2.16** in 98% and 67% yields, respectively (Scheme 2.4).

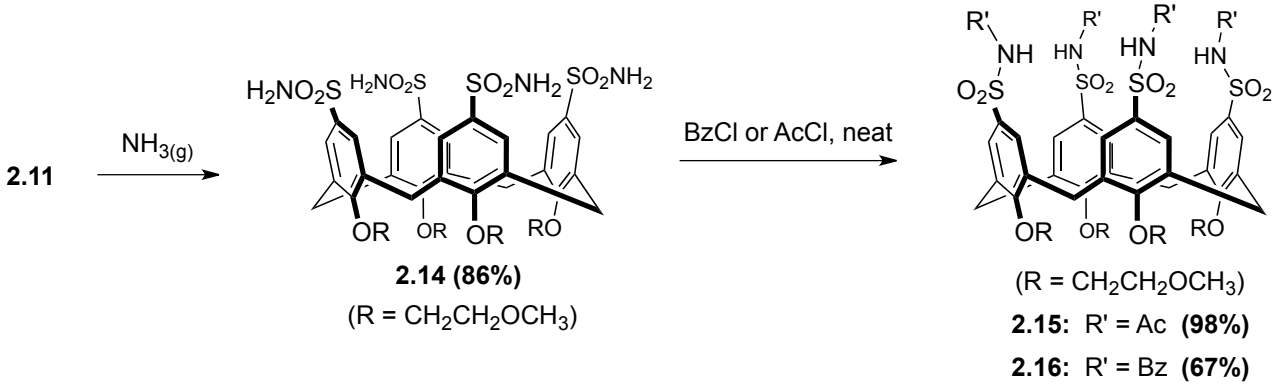

Scheme 2.4 Synthesis of *N*-acyl sulfonamide-functionalized hosts

2.5 Binding Studies

Binding constants were determined by duplicate or triplicate ^{1}H NMR titrations. Host solutions (1 mM) in CD_3CN were first prepared and portions of each were used to make up guest solutions (30–80 mM) in order to ensure that the host concentrations were kept constant throughout the titration. Acetonitrile-*d*3 is one of the most common organic solvents found in the literature when anion binding studies are being performed due to its relatively high polarity and thus ability to dissolve compounds bearing polar groups, in this case the carboxylic acid bioisosteres. Other polar solvent such as DMSO are also used but in the case of moderate or weak attraction between host and guest, it is energetically more favourable for the ions to stay in solution rather than form a complex with the host and little or no binding is observed. These solvents are normally employed when binding in other less polar solvents results in association constants too high to be measured with confidence. Nonpolar solvents such as dichloromethane are also sometimes used but often when functionalized with highly polar groups as in our case the host will not be soluble enough to carry out binding studies. Acetonitrile therefore gives us a basis for comparison with many previously described anion receptors.

Representative binding curves and Job plots for each functional group, along with stacked plots following the downfield shifts of N-H signals for **2.12, 2.13, 2.15,** and **2.16** and aryl C-H signals for **2.9** and **2.10** from which these curves were generated are shown in Figure 2.3. Job's method,[98] also known as the method of continuous variation, is used to determine binding stoichiometry between host and guest. In order to be fully reliable, the method requires an observable parameter which varies during host-guest interaction, in the case of ^{1}H NMR titrations a change in chemical shift ($\Delta\delta$) of any proton signals affected by complexation. It also requires one dominant complex to be formed in solution under the experimental conditions and that ionic strength and that the sum of the total concentrations of host and guest ([Host]+[Guest]) remain constant during the experiment. Equimolar (1 mM) solutions of both host and guest were prepared in CD_3CN and NMR spectra were recorded on samples containing varying volumes of each keeping the total volume constant. The mole fraction of host, defined as χ_H = [Host]•([Host]+[Guest])$^{-1}$ changes throughout the experiment from 100% host solution to 100% guest solution (i.e.

from $\chi_H = 1$ to $\chi_H = 0$). A plot of χ_H against ($\Delta\delta \times \chi_H$) results in a curve on which the value of χ_H at an extremum indicates binding stoichiometry (i.e. an extremum at $\chi_H = 0.5$ indicates a 1:1 binding event, for example). In this experiment the ionic strength does vary slightly among the solutions tested but considering the low concentration of slats this factor is deemed negligible.

Association constants are reported in Table 2.1. The effect of remote substitution on the lower rim was tested by comparing propyl-substituted **2.10** and glycol-substituted **2.9**. The propyl-substituted host **2.10** showed increased binding potency (>2-fold for chloride and tosylate, >10-fold for nitrate) relative to the glycol lower-rim substitution (**2.9**), indicating binding affinity and selectivity depends somewhat on the conformational control provided by lower-rim functionality. Intramolecular lower rim repulsion experienced by **2.10** due to chain length and the presence of free lone pairs on the oxygen atoms would presumably cause the lower rim diameter to expand slightly while simultaneously causing the upper rim to contract. This alteration to the binding cavity size may explain the stronger binding events observed with **2.09** in which these steric and electrostatic repulsions are not present. [99]

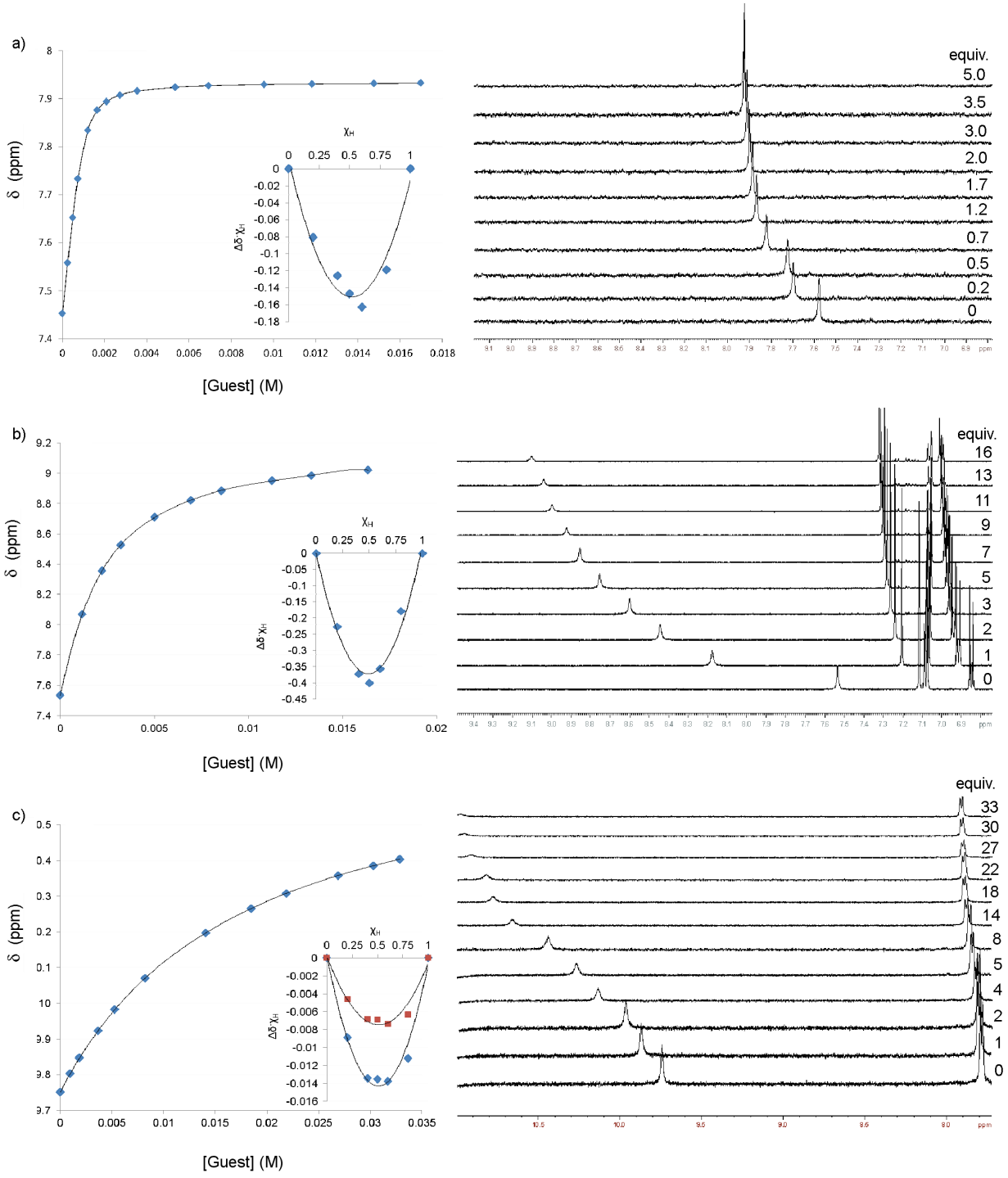

Figure 2.3 Exemplary binding data for each functional group studied. Left: Experimental data fit to a 1:1 binding isotherm arising from titrations of Bu_4N^+ Cl^- into a) = tetrazole host 2.9 at 1 mM, b) = aryl sulfonamide host 2.12 at 1 mM, and c) = acyl sulfonamide host 2.16 at 1 mM. Insets: Job plots for each host plus (◆) = Bu_4N^+ Cl^-. Data for (■) = Bu_4N^+ TsO^- also included for host 2.16. Total concentrations for all Job plots = 5 mM. Right: Stacked plots of partial ^1H NMR (500 MHz) spectra arising from the same titrations. Equivalents of Bu_4N^+ Cl^- added are indicated at far right. Some data points and NMR plots omitted for clarity.

Table 2.1 Association constants K_{assoc} (M^{-1}) in CD_3CN of tetrazole functionalized hosts **2.9-2.10**, aryl sulfonamide functionalized hosts **2.12-2.13** and acyl sulfonamide functionalized hosts **2.15-2.16**. [a]Values reported are the averages resulting from tracking multiple host signals during 2-3 titrations for each host/guest pair. Errors reported are standard deviations. Some signal strength was diminished during the experiments for the less soluble compounds resulting in high errors. Tetrabutylammonium salts were used to aid solubility of the guests and to minimize counterion-host interactions. [b] Insignificant chemical shifts observed during titrations.

	Guests K_{assoc} (M^{-1})[a]					
Host	$Bu_4N^+ Cl^-$	$Bu_4N^+ Br^-$	$Bu_4N^+ I^-$	$Bu_4N^+ TsO^-$	$Bu_4N^+ NO_3^-$	$Bu_4N^+ HSO_4^-$
2.9	3560 ± 1395	804 ± 57	70 ± 9	515 ± 44	328 ± 13	336 ± 12
2.10	8450 ± 983	716 ± 72	62 ± 16	1407 ± 300	5796 ± 1481	656 ± 338
2.12	616 ± 78	116 ± 16	29 ± 12	59 ± 1	39 ± 15	49 ± 1
2.13	1026 ± 52	322 ± 4	41 ± 2	246 ± 11	98 ± 3	183 ± 12
2.15	389 ± 23	94 ± 5	24 ± 7	124 ± 2	55 ± 1	105 ± 4
2.16	112 ± 57	28 ± 4	<10[b]	116 ± 112	75 ± 4	72 ± 11

Affinities ranged up to 8.5×10^3 M^{-1}, with each host showing the highest affinities for chloride among all anions tested (Table 2.1). Given the number of acidic protons in the host molecule this number is surprisingly low, several orders of magnitiude lower than a previously reported tripodal host[86] suggesting that hydrogen bonding is but one of several factors affecting complexation in these systems. In general, tetrazole-functionalized hosts **2.9** and **2.10** bound most anions almost an order of magnitude more tightly than their aryl and acyl sulfonamide analogs **2.12-2.13** and **2.15-2.16**. Among the aryl sulfonamides the binding of nitro-substituted host **2.13** to various guests was tighter than the corresponding methyl-substituted host **2.12**, as expected based on the increased acidity and corresponding increase in hydrogen bond donation ability for **2.13**. This trend was not observed when the comparison was extended to include acyl sulfonamides **2.15** and **2.16**. Although acetyl and benzoyl sulfonamides like **2.15** and **2.16** are several orders of magnitude more acidic than aryl sulfonamides like **2.12** and **2.13**, the binding of anions by acyl sulfonamides was found to be significantly weaker than binding by aryl sulfonamides for all cases tested.

2.6 Discussion

The functional groups of interest in this study are known first and foremost for their acidity. Representative N-H pK_a values are 4.6, 8.5, and 5.2 for exemplary tetrazole,[100] *N*-aryl sulfonamide[101] and *N*-acyl sulfonamide[81] moieties, respectively. The large discrepancies between the anion binding strength of the aforementioned hosts were unexpected and don't follow a simple pK_a trend between the different classes of acid bioisoteres. It was hypothesized that their varying conformations—largely ignored in their simple classification as interchangeable replacements for carboxylic acids—might play a large role in determining their anion-binding affinities. Molecular modeling studies were carried out to investigate the structures of the host-guest complexes. A local minimum was located for each host in which the calixarene is in a perfect "cone" conformation and all four H-bond donor groups engage a central anion symmetrically (Figure 2.4), as well as a collection of local minima for each host involving puckered "pinched cone" calixarene conformations that allow only 3 N-H donors to engage the anion. Despite the gross differences in scaffold conformations, there were similarities in the functional groups' own dihedral angles between both families of complexes. NMR data did not reveal which of the two types of calixarene conformation were operative in solution (it is probably a mixture of both), so instead the role of each functional groups' conformational preferences in host-guest complex formation was investigated.

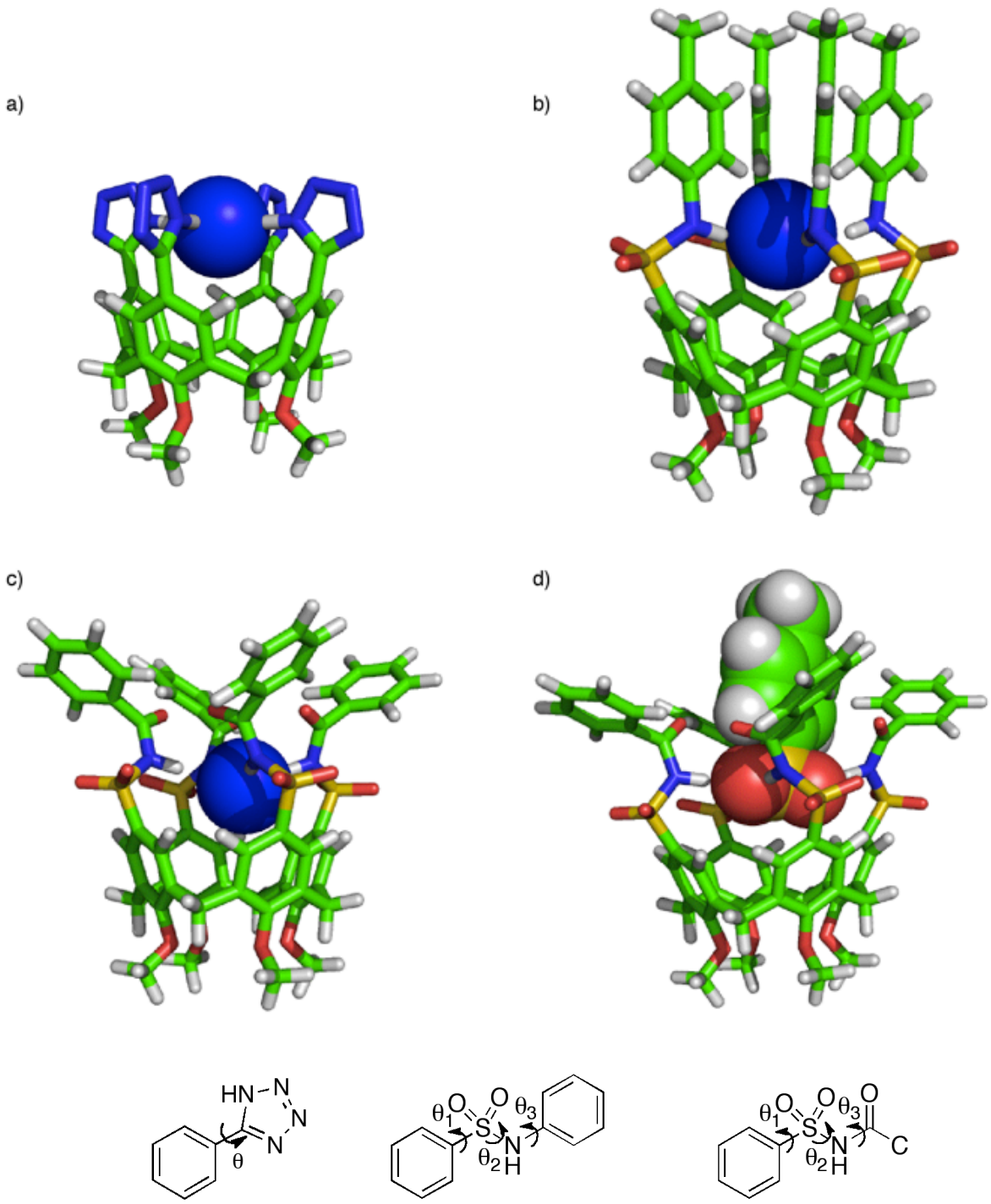

Figure 2.4 Local minima that involve the maximum four host-guest hydrogen bonds for representative host-guest complexes (HF/6-31+G*). Lower-rim substituents have been omitted. a) Tetrazole functionalized host 2.9/2.10 complexed with Cl^-. Calculated average phenyl-tetrazole biaryl dihedral angle $\theta = 86.6 \pm 0.1^o$ b) Aryl sulfonamide functionalized host 2.12 complexed with Cl^-. Calculated average θ_2 and θ_3 dihedral angles 167.9 ± 0.5^o and 50.5 ± 1.0^o, respectively. c) Acyl sulfonamide functionalized host 2.16 complexed with Cl^-. Calculated average θ_2 and θ_3 dihedral angles 162.8 ± 3.8^o and 28.1 ± 8.4^o, respectively. d) Acyl sulfonamide host 2.16 complexed with TsO^-. Calculated average θ_2 and θ_3 dihedral angles 160.5 ± 3.4^o and 11.9 ± 3.0^o, respectively.

The inherent conformational preferences of each of these acid bioisosteres was investigated, isolated and detached from the calixarene, using Hartree-Fock dihedral driving calculations about each rotatable bond in each of the functional groups. These calculations were put on a solid footing of experimental data by mining the CSD for all existing crystal structures containing relevant fragments and determining the relative occurrences of different dihedral angles. The combined computational and data-mining analyses for the key dihedral angles that define the inherent shapes of these bioisosteres are presented in Figures 2.5 (tetrazoles) and 2.6 (aryl and acyl sulfonamides).

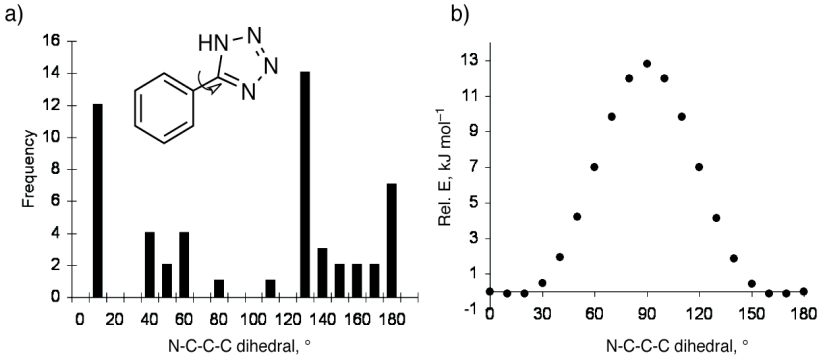

Figure 2.5 a) Histogram generated by a survey of the Cambridge Structural Database (CSD) showing frequencies of biaryl dihedral angles reported in the literature for a simplified phenyl-(5-tetrazole) model. b) Energy diagram calculated at the HF/6-31+G* level of theory when driving the biaryl dihedral angle from 0 to 180^{o} in phenyl-(5-tetrazole).

Computational analysis of phenyl-(5-tetrazole)'s relative energy as the dihedral angle about the biaryl bond is driven from 0 to 180^{o} shows a barrier of 13 kJ/mol on the potential energy surface at an angle of 90^{o}, when conjugation with the benzene ring is broken (Figure 2.5b). Unlike related systems like biphenyl, the potential energy surface remains completely flat until the phenyl-tetrazole bond is twisted ≥30° out of co-planarity. Surveying the CSD for similar fragments (Figure 2.5a) revealed a generally similar trend, with the large majority of structures having a dihedral angle ±50° from co-planar and a paucity of structures with dihedral values near 90°. In this case the CSD data is biased away from co-planarity of tetrazole and arene by the preponderance of crowded

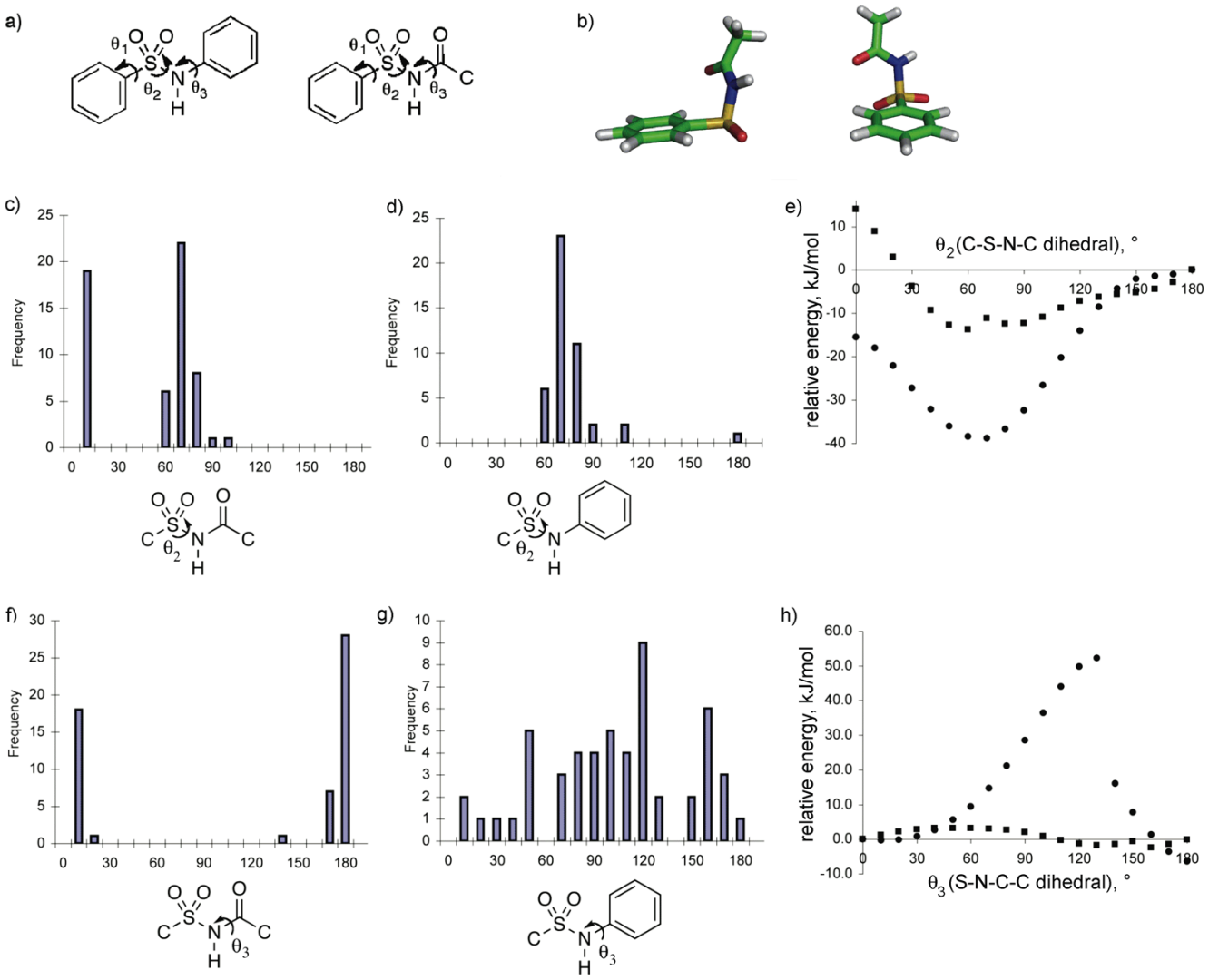

Figure 2.6 a) Labeling of key dihedral angles θ_2 and θ_3 in acyl and aryl sulfonamides. b) Two views of the global minimum energy conformation of a representative acyl sulfonamide fragment, *N*-acetyl benzenesulfonamide. c, d) Histograms showing the frequencies of reported θ_2 dihedral angles for c) acyl sulfonamide fragments and d) aryl sulfonamide fragments from among all structures in the Cambridge Structural Database (CSD). e) Energy profiles calculated for the same fragments while driving θ_2 from 0 to 180° in the acyl sulfonamide (■) and aryl sulfonamide (●) fragments. f, g) Histograms showing the frequencies of reported θ_3 dihedral angles for f) acyl sulfonamide fragments and g) aryl sulfonamide fragments from among all structures in the Cambridge Structural Database (CSD). h) Energy profiles calculated for the same fragments while driving θ_3 from 0 to 180° in the acyl sulfonamide (■) and aryl sulfonamide (●) fragments. All energies calculated at the HF/6-31+G* level of theory.

ortho-substituted 2-(5-tetrazolyl)-biphenyls, as in Losartan (Figure 2.2), in the CSD. Super-imposing this simple angular preference onto the more complex structures of hosts **2.09** and **2.10** reveals why they are less potent than the aforementioned tris(tetrazole) host in spite of the inherent strength of the tetrazole NH---X^- hydrogen bond. The complex of a simplified analog of host **2.10** with Cl^- (Figure 2.4a) demands that this dihedral is near the disfavored 90° angle (costing ~13 kJ/mol per tetrazole) in order for all four tetrazole moieties to engage the guest simultaneously.

The shapes of the aryl and acyl sulfonamides are defined by three important dihedral angles. The conformations of the rotatable carbon-sulfur bonds for aryl sulfone type functionalities (θ_1, Figure 2.6a) have been reported in detail elsewhere, and are similar (at $\theta_1 \sim 90°$) for both classes of compounds.[102,103] The sulfonamide dihedral for rotation about the S-N bond was analyzed (θ_2, Figure 2.6a) along with the amide/aniline dihedrals that define rotation about the neighboring N-C bonds (θ_3, Figure 2.6a) in an attempt to aid in the understanding of the experimental anion binding data that was reported above. Calculated energy profiles show that both acyl sulfonamides and aryl sulfonamides share the same preference for conformation about their S-N bonds (θ_2 = ~60°, Figure 2.6e), although the depths of the energy wells are different. Data from the CSD (histograms in Figures 2.6c and d) show perfect agreement with the calculated angular preferences. In contrast, strong divergence was found in the shape preferences of acyl and aryl sulfonamides about the N-C dihedral θ_3. In acyl sulfonamides, a strong preference for the planar *trans* (θ_3 = 180°) or *cis* (θ_3 = 0°) amide conformations was revealed by both the crystallographic data (Figure 2.6f) and the strong preference for these angles observed in the DFT-calculated potential energy surface (Figure 2.6h). In contrast, the calculations and CSD data show that the rotation of the equivalent bond in the aryl sulfonamides—in this case an aniline N-C type functional group—is essentially a flat potential energy surface with no preferences or barriers to rotation (Figure 2.6h). Again, the CSD data agree, in this case showing that aryl sulfonamides can adopt almost any value for θ_3 with no discrimination between conformations (Figure 2.6g). These data help to evaluate the shapes of the host-guest complexes shown in Figure 2.4. Regardless of the calixarenes' conformations, the acyl and aryl sulfonamides must adopt a conformation wherein θ_2 = 160-170° (calculated values: aryl sulfonamides ~168°, acyl

sulfonamides ~160°, see Figure 2.4) in order to direct their N-H bonds toward the guest. This is disfavoured in both types of sulfonamide, and the larger penalty paid for the acyl sulfonamide (~40 kJ/mol per functional group) must be at least in part responsible for the binding constants we observe for hosts **2.15** and **2.16** being so much lower than would be predicted by their high acidity.

2.7 Conclusion

The experimental binding data show that all three of these carboxylic acid bioisosteres are capable of forming well-ordered complexes with anions using their acidic N-H hydrogen bond donors. Tetrazoles have demonstrated their high inherent affinity for anions, and their ability to outperform carboxylic acids in a prior study[86] and sulfonamides in this study suggests that they should find expanded use as potent binders of anions that operate in a variety of structural contexts. While aryl sulfonamides have been repeatedly explored as anion binders,[45,104,105] acetyl and benzoyl sulfonamides have not. Although the calixarene scaffold employed here does not effectively present the NH groups in a convergent manner, acyl sulfonamides have unique properties that seem to hold promise for their further development. With the newfound knowledge of the tetrazole's strong preference for co-planarity with an aryl partner, our efforts moving forward were to devise constructs where this was in fact the case, and pyrrole seemed a logical idea.

2.8 Experimental Section

2.8.1 General Considerations

Binding Studies: NMR binding studies were performed using 500 and 360 MHz spectrometers for the sulfonamide and tetrazole-containing compounds, respectively. Deuterated acetonitrile was used as purchased from Cambridge Isotope Laboratories. Spectra were referenced to residual solvent. Binding constants were determined by duplicate or triplicate ^{1}H NMR titrations using a 500 MHz spectrometer. Host solutions (1 mM) in CD_3CN were first prepared, and portions of each were used to make up guest solutions (30-80 mM) in order to ensure that the host concentrations were kept constant

throughout the titration. Guest solutions were injected into host solutions incrementally, beginning with 10 μL injections and gradually raising the injection volume to 200 μL until the NMR tube was filled to capacity, resulting in final guest concentrations ranging from 5 to 52 equiv. for strong and weak-binding guests, respectively. Binding constants were determined by monitoring the downfield shifts of N-H protons for sulfonamide-functionalized hosts and aryl C-H protons for tetrazole-functionalized hosts. Chemical shift data was fit to the 1:1 binding isotherm using a program developed by Dr. J.M. Sanderson, Centre for Bioactive Chemistry, Department of Chemistry, Durham University, Durham, U.K. that is available at http://dur.ac.uk/j.m. sanderson/science/downloads.

Proton (^{1}H) NMR spectra were recorded on 500 MHz, 360 MHz or 300 MHz spectrometers, as indicated in each case. Carbon (^{13}C) NMR spectra were recorded 125 MHz, 90 MHz or 75 MHz as indicated in each case. Masses were acquired using high-resolution electrospray ionization mass spectra (HR-ESI-MS). Infrared spectra were recorded on KBr pellets as neat films. All reactions were carried out under nitrogen unless otherwise indicated. Procedures for the preparation of **2.6**,[89] **2.8**,[89] **2.11**[91] and **2.14**[91] have been previously reported.

2.8.2 Synthetic Procedures

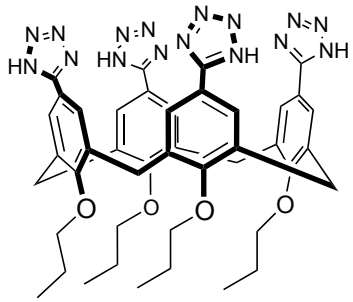

25,26,27,28-Tetrakis(propoxy)-5,11,17,23-tetrakis(tetrazole)calix[4]arene (2.10). 25,26,27,28-Tetrakis(propoxy)-5,11,17,23-tetrakis(cyano)calix[4]arene **2.8** (275 mg, 0.36 mmol), zinc bromide (656 mg, 2.9 mmol), sodim azide (190 mg, 2.9 mmol) were added to a pressure tube conting MeOH (5 mL) and H_2O (5 mL). The tube was sealed and the mixture heated to 140 ^oC for 24 h with vigorous stirring. The reaction was allowed to cool to ambient temperature and 1M HCl (10 mL) and ethyl acetate (10 mL) were added. The mixture was stirred until all solid had dissolved and the aqueous layer was extracted with ethyl acetate (3 × 15 mL). The combined organic layers were evaporated, 0.5 M NaOH (30 mL) added and the mixture was stirred at ambient temperature for 2 h. The resulting zinc hydroxide precipitate was filtered and with vigorous stirring the filtrate was acidified with 1M HCl to pH 1. The crude brown solid was filtered, allowed to air dry and purified by flash chromatography (SiO_2, 10-20% MeOH in CH_2Cl_2 gradient) to afford 180 mg, (95%) of a brown solid. mp: 175°C (dec). IR(KBr, thin film): 2962w, 2922w, 2872w, 1617w, 1559m, 1458m, 1358s, 1213m, 1043w, 1005w, 962m, 896m, 752w, 563w. ^1H NMR (CD_3OD, 500 MHz): δ 1.09 (t, J = 7.4 Hz, 12 H), 2.02 (6, J = 7.5 Hz, 8 H), 3.45 (d, J = 1.7 Hz, 4 H), 4.03 (t, J = 7.3 Hz, 8 H), 4.64 (d, J = 13.7 Hz, 4 H), 7.42 (s, 4 H); ^{13}C NMR (CD_3OD, 125 MHz): δ 10.9, 24.7, 32.04, 78.7, 119.4, 128.8, 137.6, 156.7, 160.9; LR-MALDI-MS: 887.5 (MNa^+, $C_{44}H_{48}N_{16}O_4Na^+$; calc. 887.4); HR-ESI-MS: 865.4175 (MH^+, $C_{44}H_{48}N_{16}O_4H^+$; calc. 865.4123).

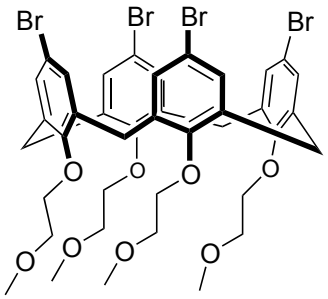

25,26,27,28-Tetrakis(ethoxymethoxy)-5,11,17,23-tetrakis(bromo)calix[4]arene (2.5). Adapted from a previously reported procedure.[23] 25,26,27,28-Tetrakis(ethoxymethoxy)calix[4]arene **2.3** (410 mg, 0.7 mmol) and NBS (623 mg, 3.5 mmol) were stirred in anhydrous DMF (10 mL) for 24 h at room temperature. The reaction was quenched by the dropwise addition of 1 M HCl (6 mL). The precipitate was filtered and recrystallized in MeOH. The crude product was purified by flash chromatography (SiO_2, 3% EtOAc in hexanes) yielding 420 mg (66%) of a white solid. mp: 180-182 °C. IR(KBr, thin film): 2924s, 1572w, 1456s, 1197s, 1127s; ^{1}H NMR ($CDCl_3$, 360 MHz): δ 3.06 (d, J = 13.6 Hz, 4 H), 3.35 (s, 12 H), 3.72 (t, J = 5.0 Hz, 8 H), 4.05 (t, J = 5.3 Hz, 4 H), 4.41 (d, J = 13.5 Hz, 4 H), 6.79 (s, 8 H); ^{13}C NMR ($CDCl_3$, 90 MHz): δ 30.5, 58.6, 71.7, 73.3, 115.5, 131.1, 136.4, 155.3; HR-ESI-MS: 994.9643 (MNa^+, $C_{40}H_{44}O_8Na^+Br_4$; calc. 994.9633).

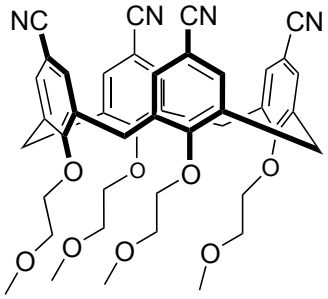

25,26,27,28-Tetrakis(ethoxymethoxy)-5,11,17,23-tetrakis(cyano) calix[4]arene (2.7). Compound **2.5** (450 mg, 0.46 mmol), $Zn(CN)_2$ (950 mg, 8.2 mmol), $Pd_2(dba)_3$ [tris(dibenzylideneacetone)dipalladium(0)] (92 mg, 0.1 mmol), and dppf (128 mg, 0.23 mmol) were added to an oven dried Schlenk flask which was then purged with nitrogen

and evacuated three times. Anhydrous DMF (5.0 mL) was added, the flask sealed and heated at 140 °C for 96 h. The reaction was then allowed to cool to ambient temperature, transferred to a round-bottom flask, and the DMF removed *in vacuo*. The crude black product was purified by flash chromatography (SiO_2, 20% CH_2Cl_2 in EtOAc) yielding 228 mg (67%) of a brown solid. mp: 212 °C. IR(KBr, thin film): 2927w, 2881w, 2819w, 2225s, 1471s, 1125s, 1036s, 895m, 735m; ^{1}H NMR ($CDCl_3$, 360 MHz): δ 3.21 (d, J = 13.9 Hz, 4 H), 3.34 (s, 12 H), 3.71 (t, J = 4.43 Hz, 8 H), 4.15 (t, J = 4.8 Hz, 8 H), 4.54 (d, J = 13.8 Hz, 4 H), 6.99 (s, 8 H); ^{13}C NMR ($CDCl_3$, 90 MHz): δ 30.5, 58.9, 71.8, 74.2, 107.3, 118.4, 132.7, 136.0, 160.0; HR-ESI-MS: 779.3054 (MNa^+, $C_{44}H_{44}N_4O_8Na^+$; calc. 779.3057).

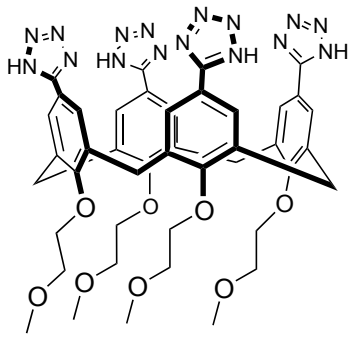

25,26,27,28-Tetrakis(ethoxymethoxy)-5,11,17,23-tetrakis(tetrazole)calix[4]arene (2.9).

Compound **2.7** (275 mg, 0.36 mmol), zinc bromide (656 mg, 2.9 mmol), sodim azide (190 mg, 2.9 mmol) were added to a pressure tube containing MeOH (5 mL) and H_2O (5 mL). The tube was sealed and the mixture heated to 140 ^{o}C for 24 h with vigorous stirring. The reaction was allowed to cool to ambient temperature and 1M HCl (10 mL) and ethyl acetate (10 mL) were added. The mixture was stirred until all solid had dissolved and the aqueous layer was extracted with ethyl acetate (3 × 15 mL). The combined organic layers were evaporated, 0.5 M NaOH (30 mL) added and the mixture was stirred at ambient temperature for 2 h. The resulting zinc hydroxide precipitate was filtered and with vigorous stirring the filtrate acidified with 1M HCl to pH 1. The crude brown solid was filtered, allowed to air dry and purified by flash chromatography (SiO_2, 10-20% MeOH in CH_2Cl_2 gradient) yielding 220 mg (65%) of a yellow solid. mp: 230-

232 °C (dec). IR(KBr, thin film): 2923m, 1616w, 1559m, 1460s, 1456s, 1220w, 1123m, 1040m; ^{1}H NMR (Acetone-d_6, 300 MHz): δ 3.43 (s, 12 H), 3.46 (d, *J* = 13.6 Hz, 4 H), 3.92 (t, *J* = 4.7 Hz, 8 H), 4.32 (t, *J* = 4.7 Hz, 8 H), 4.78 (d, *J* = 13.6 Hz, 4 H), 7.53 (s, 8 H); ^{13}C NMR (CD_3OD, 75 MHz): δ 31.8, 59.0, 73.2, 75.1, 119.3, 128.6, 137.5,156.5, 160.7; HR-ESI-MS: 951.3735 (MNa^+, $C_{44}H_{48}N_{16}O_8Na^+$; calc. 951.3739).

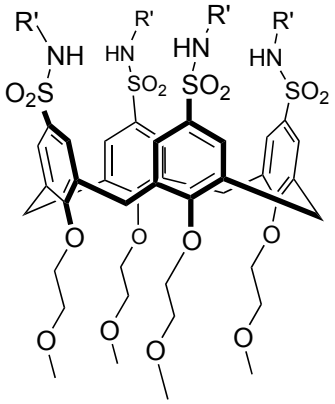

2.12: R' = 

2.13: R' = 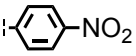

General procedure for the preparation of aryl sulfonamide substituted calix[4]arenes **2.12** and **2.13**:

A flask containing chlorosulfonyl calix[4]arene **2.11** (50 mg, 0.048 mmol), the appropriate *p*-substituted aniline (0.77 mmol), and pyridine (4 mL) was heated to 70^{o}C with stirring. The reaction was left to stir for an additional 8 h at which point it was quenched with 1 M HCl (10 mL) and diluted with CH_2Cl_2 (15 mL). The organic layer was washed with 1 M HCl (3 × 10 mL), dried ($MgSO_4$), filtered and concentrated *in vacuo*. The crude products were purified by flash chromatography (SiO_2, 10% MeOH in CH_2Cl_2).

25,26,27,28-Tetrakis(ethoxymethoxy)-5,11,17,23-tetrakis(*p*-toluenesulfamoyl)calix[4]arene (2.12). Brown solid; yield = 53 mg, (83%); mp: 140-144 °C; IR(KBr, thin film): 3251 m, 2923m, 1511s, 1463m, 1451 M, 1332m, 1301 M, 1264m, 1149s, 1105m; ^{1}H NMR ($CDCl_3$, 300 MHz): δ 2.28 (s, 12 H), 3.08 (d, 4 H, *J* =

13.7 Hz), 3.25 (s, 12 H), 3.64 (t, 8 H, *J* = 4.4 Hz), 4.08 (s, 8 H), 4.46 (d, 8 H, *J* = 13.7 Hz), 6.90-7.23 (m, 24 H); ^{13}C NMR (CD_3CN, 75 MHz): δ 20.9, 31.5, 58.6, 72.5, 74.8, 123.9, 128.2, 130.7, 135.2, 135.5, 136.3, 136.4, 161.0; HR-ESI-MS: 1355.3998 (MNa^+, $C_{68}H_{76}N_4O_{16}S_4Na$, calc. 1355.4037).

25,26,27,28-Tetrakis(ethoxymethoxy)-5,11,17,23-tetrakis(4-Nitrobenzenesulfamoyl)calix[4]arene (2.13). Yellow solid; yield: (49%); mp: 140-144 °C; IR(KBr, thin film): 2926w, 1595s, 1520s, 1495m, 1464m, 1343s, 1264w, 1150s, 1106m; ^{1}H NMR (CD_3CN, 300 MHz): δ 3.15 (s, 12 H), 3.31 (d, 4 H, *J* = 13.7 Hz), 3.65 (t, 8 H, *J* = 4.6 Hz), 4.13 (t, 8 H, *J* = 4.6 Hz), 4.50 (d, 4 H, *J* = 13.5 Hz), 7.22 (m, 16 H), 8.14 (m AA'XX', 8 H), 8.38 (s, 4 H); ^{13}C NMR (CD_3CN, 75 MHz): δ 31.4, 58.6, 72.5, 75.0, 119.7, 126.3, 128.1, 134.4, 136.8, 144.8, 144.8, 161.6; HR-ESI-MS: 1479.2854 (MNa^+, $C_{64}H_{64}N_8O_{24}S_4Na$, calc. 1479.2814)

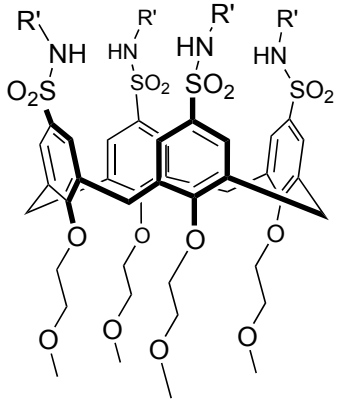

2.15: R' = Ac

25,26,27,28-Tetrakis(ethoxymethoxy)-5,11,17,23-tetrakis (acetylsulfonamido)calix[4]arene (2.15). A flask containing compound **2.14** (80 mg, 0.082 mmol) and acetyl chloride (3 mL) was brought to reflux with stirring. The mixture was stirred for an additional 24 h, and the acetyl chloride was removed *in vacuo* yielding 92 mg (98%) of a white solid that was used without further purification. mp: 150-154 ^{o}C (dec). IR (KBr, thin film): 3220w, 2921w, 1686s, 1449s, 1419 m, 1343 m, 1266 m, 1151s, 1108s, 1044 m. ^{1}H NMR (acetone-d_6, 300 MHz): δ 3.39 (s, 12H), 3.52 (d, 4H, *J*=13.5Hz), 3.88 (t, 8H, *J*=4.8Hz), 4.33 (t, 8H, *J*=4.8Hz), 4.72 (d, 4H, *J*=13.5Hz), 7.50 (s,

8H),10.28 (s, 4H). C^{13} NMR (CD_3CN, 75 MHz): δ 24.0, 31.2, 58.9, 72.6, 75.3, 128.7, 134.8, 136.6, 161.6, 170.3. HR-ESI-MS: 1163.2567 (MNa, $C_{48}H_{60}N_4O_{20}S_4Na$, calc'd 1163.2581).

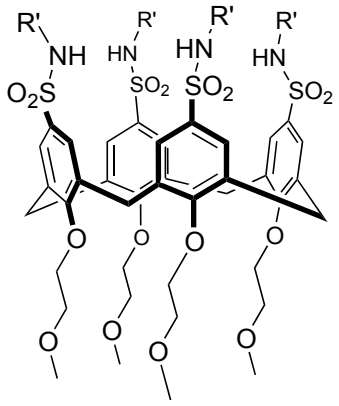

2.16: R' = Bz

25,26,27,28-Tetrakis(ethoxymethoxy)-5,11,17,23-tetrakis (benzoylsulfonamido)calix[4]arene (2.16). A flask containing compound **2.14** (45 mg, 0.046 mmol) and benzoyl chloride (5 mL) was heated to 140 ^oC with stirring. The mixture was stirred for an additional 72 h and was then concentrated to near dryness *in vacuo*. Et_2O (5 mL) was added, and the resulting precipitate was filtered and air-dried. The white solid (43 mg, 67%) was collected and used without further purification. mp: 260-265 ^oC (dec). IR (KBr, thin film): 2922w, 1699s, 1454s, 1435s, 1347 m, 1262 m, 1155s, 1108w. ^1H NMR (CD_3CN, 500 MHz): δ 3.28 (s, 12H), 3.48 (d, 4H , *J*=13.7Hz), 3.77 (t, 8H, *J*=4.6 Hz), 4.24 (t, 8H, *J*=4.3Hz), 4.63 (d, 4H, *J*=13.5Hz), 7.48 (t, 8H, *J*=7.7 Hz), 7.53 (s, 8H), 7.62 (m, AA'XX', 8 H), 7.80 (m, AA'XX', 8 H), 9.77 (s, 4 H). ^{13}C NMR (CD_3CN, 125 MHz): δ 31.5, 58.8, 72.6, 75.2, 129.3, 129.3, 129.7, 133.7, 134.2, 134.5, 136.4, 161.9, 166.3. HR-ESI-MS: 1411.3231 (MNa, $C_{68}H_{68}N_4O_{20}S_4Na$, calc'd 1411.3207).

Chapter 3

Pyrrolyl-tetrazole: A new, planar anion binding motif outperforms the common amidopyrrole

Reprinted with permission from Courtemanche, R. J. M.; Pinter T.; Hof, F., Just add tetrazole: 5-(2-Pyrrolo)tetrazoles are simple, highly potent anion recognition elements *Chem. Commun.,* **2011**, *47*, 12688-12690. Copyright Royal Society of Chemistry 2011.

This work was conceived of by Thomas Pinter and Fraser Hof.

Synthesis and binding studies of hosts **3.2** and **3.11**, and Spartan calculations were conducted by Rebecca J. M. Courtemanche and Thomas Pinter.

Synthesis and binding studies on amidopyrrole 3.4 conducted by Fraser Hof.

and Synthesis of bipyrrole 3.6, and overall data analysis were conducted by Thomas Pinter.

The manuscript was written by Thomas Pinter and Fraser Hof, and this Chapter was adapted from that paper by Thomas Pinter.

3.1 Foreword

Our previous work with tetrazoles, and *N*-acyl sulfonamides led to the realization that the highly acidic tetrazole has a penchant to be in a co-planar conformation with its aryl neighbour when directly bonded to it. It has been shown in chapter one that the pyrrole has fast become a gold standard of functional groups when designing anion receptors. It follows then that a new class of potent and perhaps selective anion receptors could be designed based on a linked pyrrolyl-tetrazole binding motif. Amide-functionalized pyrroles (amidopyrroles) are structurally related species that have been used as anion recognition motifs. One of the over-arching themes of this thesis is that acid bioisosteres offer a chance to improve upon the much more commonly used amide-type binding groups. Based on our knowledge of the superior hydrogen bond donating ability of the tetrazole over *N*-aryl sulfonamides on a calix[4]arene scaffold (Chapter 2), our hypothesis was that a simple amide-to-tetrazole swap in already-established amidopyrrole anion binders would lead to new and more potent receptors.

3.2 Introduction

Despite the previously discussed importance of anion recognition (Chapter 1) the vast majority of anion receptors are constructed by assembly of only a few different, well understood anion-binding functional groups that include amides,[105-107] sulfonamides,[45,104] and (thio)ureas.[46,54,109] Pyrrole (**3.7**) is a dominant player in anion recognition, represented by many derivatized pyrroles[110-112] and related pyrrolic ring systems.[113-116] Triazoles, easily assembled by "click" reactions of alkynes and azides,[117,118] have recently been added to this toolkit as agents that bind anions via their electron-deficient CH group.[119,120] A related heterocycle, tetrazole, is relatively under-used as a neutral binder of anions but is attractive for many reasons. Tetrazoles are easily assembled by variants of the "click" reaction that involve almost any organic nitrile being treated with NaN_3 under a variety of conditions.[74,90,121,122] Further, tetrazoles are potent anion-binding elements that operate well in a variety of structural contexts because their acidic NH bears a much larger partial positive charge than other amide-like groups and heterocycles.[86,123,124]

3.3 Abstract

To explore the use of tetrazoles as anion binding elements, we constructed the simple bidentate 5-(2-pyrrolyl)tetrazole receptor (**3.2**) and compared it with analogous pyrrole-2-carboxylic acid, pyrrole-2-amides and 2-2'-bipyrrole (**3.6**), a nearly identical compound geometrically. In our intital exploratory studies, this new host outperformed the others, binding chloride with at least 10-fold greater affinity. We then made a direct comparison of binding affinity for an array of anions between **3.2** and **3.6**. Similar results were observed with one exception, the more basic anion benzoate seemed to deprotonate the tetrazole-functionalized host after a threshold concentration of the guest was reached, a phenomenon discussed in chapter 1.

A second host containing two tetrazoles on either side of the pyrrole was also constructed and similar binding studies carried out. This new receptor bound anions several orders of magnitude more strongly than analogous diamidopyrroles and displayed a fleeting 1:2 (Guest:Host) binding event with addition of chloride. A similar deprotonation event as described above seemed to take place with addition of benzoate. Computational studies once again reveal that presumed intramolecular interactions and conformational preferences make the tetrazole a more energetically favourable moiety for cooperative anion binding with a neighbouring pyrrole.

3.4 Synthesis and binding studies of 5-(2-pyrrolyl)tetrazole.

5-(2-pyrrolyl)tetrazole (**3.2**) is a nearly isosteric analog of 2,2'-bipyrrole (**3.6**) that is readily prepared from commercially available 2-cyanopyrrole in one step by treatment with Et_3NHCl/NaN_3 (Scheme 3.1).[125] Control compounds pyrrole-2-carboxylic acid **3.3**, simple pyrrolyl amide **3.4,** and 2,2'-bipyrrole **3.6**[126] were either commercially available or prepared by established routes.

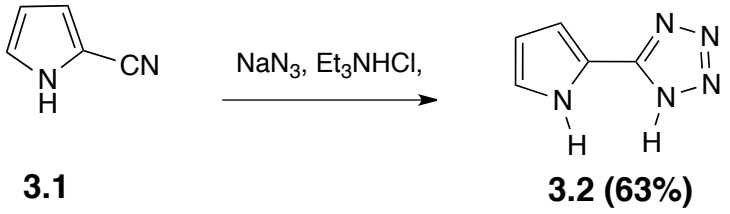

3.1 **3.2 (63%)**

Scheme 3.1 Synthesis of 5-(2-pyrrolyl)tetrazole.

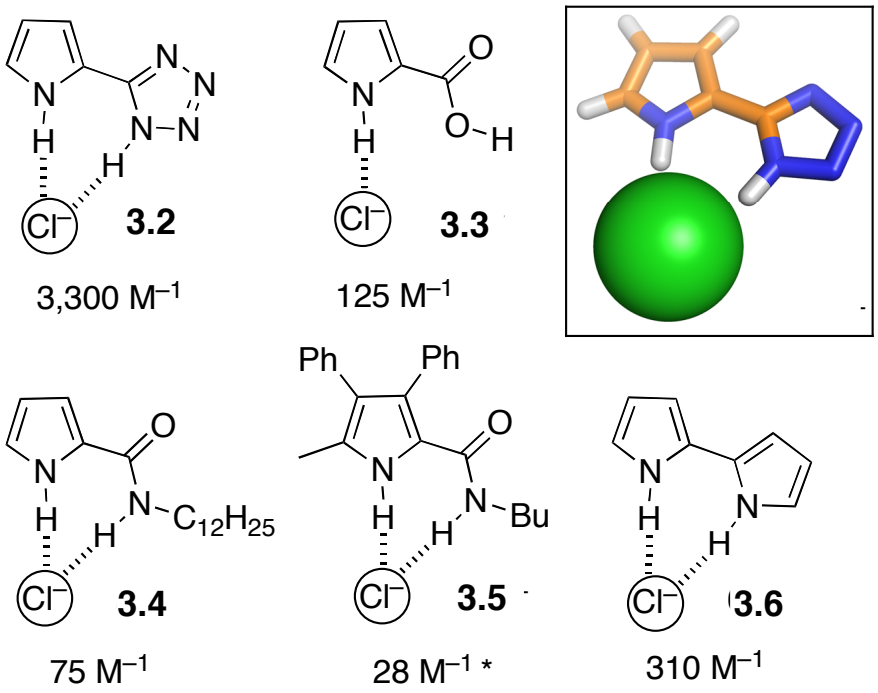

Figure 3.1 Pyrrole based hosts and their association constants for Cl^- determined in CD_3CN. Inset: Calculated structure of **3.2**·Cl.

Solutions of hosts **3.2**, **3.3**, **3.4**, and **3.6** in CD_3CN were titrated with Bu_4N^+ Cl^- in order to take a preliminary look at the success of this design. Chemical shift data were fit to 1:1 binding isotherms to determine K_{assoc} values that revealed striking differences between the anion-binding potency of **3.2** and the control compounds (Figures 3.1 and 3.3). We explain the difference between the binding strength of tetrazole-functionalized **3.2** (3,300 M^{-1}) and carboxylic acid-functionalized **3.3** (125 M^{-1}; 26-fold weaker) on the

basis of the stereoelectronic effects that favor the *syn* conformation of the carboxylic acid OH.[86,127] In a host like **3.3**, a *syn* carboxylic acid OH diverges from the binding pocket and can't cooperate with the pyrrole NH to bind a single Cl^- anion. As for the tetrazole-moiety, calculations in the gas phase suggest that the conformation in **3.2** which favours anion binding and essentially emulates this disfavoured rotamer of **3.4** is actually energetically beneficial (Figure 3.2).

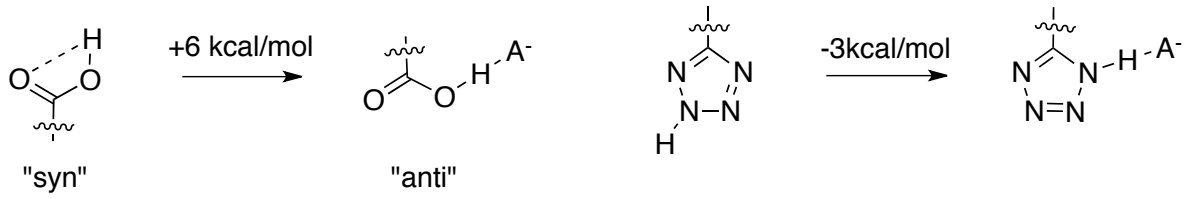

Figure 3.2 Syn and anti geometries of a carboxylic acid. The less favoured *anti* conformation required for anion binding causes a decrease in K_{assoc}. Dashed line indicates stabilizing intramolecular hydrogen bond.

The pyrrolyl amide **3.4** does not suffer from this particular conformational problem, but its Cl^- affinity is low nevertheless. Our determined value for **3.4**•Cl^- (K_{assoc} 75 M^{-1}) is similar to that reported for related host **3.5** published by Gale (K_{assoc} 28 M^{-1}, determined in CD_3CN containing 0.03% H_2O), and both are >40-fold weaker than **3.2** ($\Delta\Delta G$ = 2.2 kcal mol^{-1}). These hosts differ from **3.2** in both conformation and acidity; calculations suggest that both factors play a role in driving stronger binding by **3.2**. The relatively low affinities of each of these pyrrole-amide hosts arises because their global minimum energy conformations are governed by the antiparallel orientation of pyrrole and amide dipoles (that also can be considered a weak intramolecular NH---O=C hydrogen bond) that hold them in an *anti* conformation in which pyrrole NH and amide NH are divergent (Figure 3.3).[74,86,128-132] We calculated the relative energies of **3.2** and **3.4** in their NH-divergent ("*anti*") and NH-convergent ("*syn*") conformations by energy minimizations at the HF/6-311+G** level of theory as implemented in Spartan '06 (Wavefunction, Inc.) (Figure 3.4). Both prefer the *anti* conformation, but **3.2** pays a smaller penalty (+5.5 kcal mol^{-1}) than **3.4** (+6.1 kcal mol^{-1}) to reorient itself into the *syn* conformation required for anion binding. This difference of 0.6 kcal mol^{-1} makes up

~25% of the ≥44-fold difference (ΔΔG ≥ 2.2 kcal mol^{-1}) observed between **3.2**•Cl^- and **3.4**•Cl^-; the remainder likely arises as a result of the inherently greater acidity and H-bonding capability of the tetrazole relative to the amide. We examined acidity in particular by comparing **3.2** to its nearly isosteric, but far less acidic, analog 2,2'-bipyrrole **3.6** (Table 3.1)**.** Again, the 5-(2-pyrroyl)tetrazole **3.2** wins out by a significant margin, binding Cl^- more strongly than does **3.6** by an order of magnitude (ΔΔG = 1.4 kcal mol^{-1}).

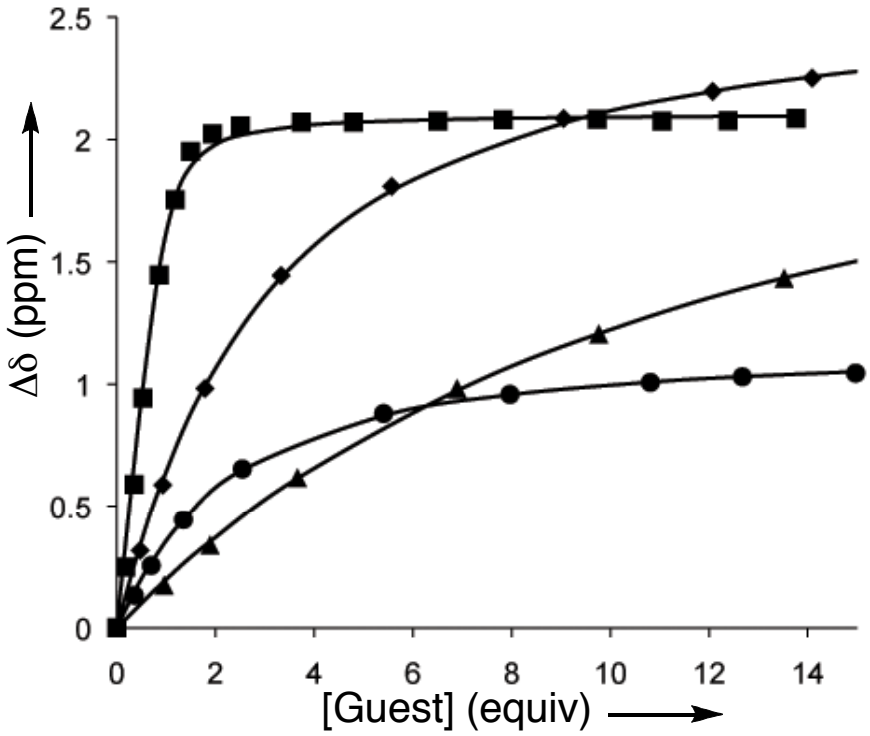

Figure 3.3 Chemical shift data (points) and fitted 1:1 binding isotherms (lines) that arise upon titration of Bu_4N^+ Cl^- into CD_3CN solutions of hosts 3.2 (■), 3.3 (●), 3.4 (▲), and 3.6 (◆). Job plots confirm 1;1 binding stoichiometry (see electronic supporting information ref. 124).

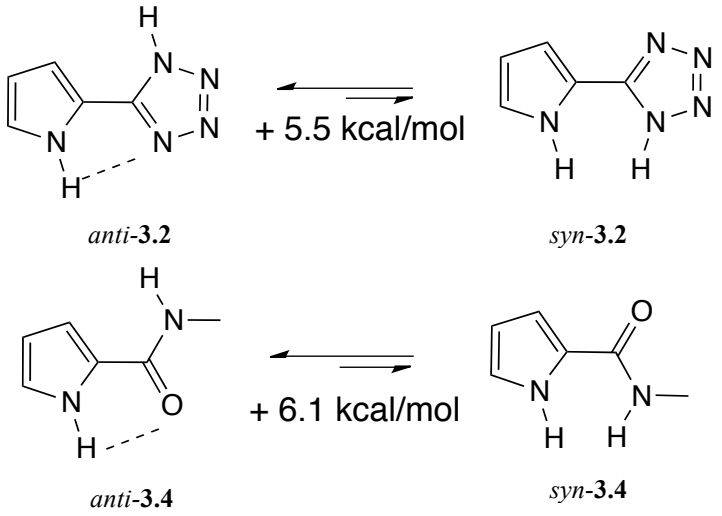

anti-**3.2** *syn*-**3.2**

anti-**3.4** *syn*-**3.4**

Figure 3.4 Calculated energies of pyrrolyl-tetrazole (**3.**2) and amidopyrrole (**3.**4) hosts. An energetic penalty of +0.6 kcal/mol is paid by **3.4** to orient it into the *syn* position in order for both donors to engage the anion. Dashed lines indicates proposed hydrogen bond interactions which stabilize the conformations unable to offer two hydrogen bond donors.

In order to examine the scope of anion binding by this new motif, we carried out NMR studies of **3.2** with a variety of halides and oxyanions, both in anhydrous CD_3CN and in CD_3CN containing 1% (v/v) H_2O. Addition of BzO^- to tetrazole-containing **3.2** gave rise to curves that could not be fit to 1:1, 2:1, or 1:2 binding isotherms, along with disappearance of the tetrazole NH when ~2 equivalents of BzO^- had been added.[124] Job plots (carried out as described in section 2.5) were complex (i.e. had multiple extrema) and not supportive of any n:m binding stoichiometry (Figure 3.5). These data are in line with those reported by other groups for other combinations of acidic hosts and carboxylate anions, in which initial (strong) binding is followed by proton transfer from host to guest that is partially driven by the formation of a strong $RCOO^-$•••HOOCR complex.[133-137]

Table 3.1 Affinities of 5-(2-pyrrolo)tetrazole **3.2** and bipyrrole **3.6** for various anions.[a]

Guest	K_{assoc} for **3.2** in CD_3CN (M^{-1})	K_{assoc} for **3.6** in CD_3CN (M^{-1})	K_{assoc} for **3.2** in 1% H_2O/ CD_3CN (M^{-1})	K_{assoc} for **3.6** in 1% H_2O/ CD_3CN (M^{-1})
Cl^-	3300 ± 1200	310 ± 10	890 ± 100	71 ± 5
Br^-	450 ± 50	50 ± 3	110 ± 15	21 ± 2
I^-	17 ± 3	3 ± 1	< 3	< 3
TsO^-	900 ± 50	37 ± 4	420 ± 120	16 ± 1
NO_3^-	160 ± 20	19 ± 1	60 ± 9	7 ± 1
BzO^-	p.t.[b)]	1500 ± 200	p.t.[b)]	260 ± 30

[a] Guests were titrated as their Bu_4N^+ salts into solutions of hosts in the stated solvent system. Chemical shift data for all nuclei that displayed significant chemical shifts were fit to 1:1 binding isotherms to arrive at K_{assoc} values. Experiments were done in duplicate or triplicate. Values reported are averages of all nuclei from all experiments. Errors reported are standard deviations. [b] p.t. = evidence of proton transfer between host and gest, see text.

All other (less basic) anions studied produced NMR titration data that fit well to 1:1 binding isotherms to give K_{assoc} values (Table 1). To evaluate better the potency of **3.2**, we also studied 2,2'-bipyrrole (**3.6**) with the complete set of anions because it has a nearly identical hydrogen bonding geometry to **3.2**.[138] Chemical shift data for bipyrrole **3.6** fit well to 1:1 binding isotherms to give K_{assoc} values for all anions tested (Table 3.1), with no evidence of proton transfer to BzO^- (as expected). A 1:1 stoichiometry of complexation was confirmed by Job plots for Cl^- and BzO^-. Comparison of these two hosts' K_{assoc} values reveals that tetrazole substitution in **3.2** gives rise to significantly higher affinities for all anions than **3.6** but also limits the scope of anions with which **3.2** can form stable complexes. A maximum difference of ~25-fold was observed for TsO^- in both solvent systems presumably due to peripheral lone pair interactions with the pyrrole N-H donor. This study also illustrates the impact of increasing solvent polarity as addition of 1% (v/v) water to the system which shifts the equilibrium between dissolved anion and host-guest complex (i.e. K_1, Figure 3.5) left decreased binding affinites by an order of magnitude in all cases.

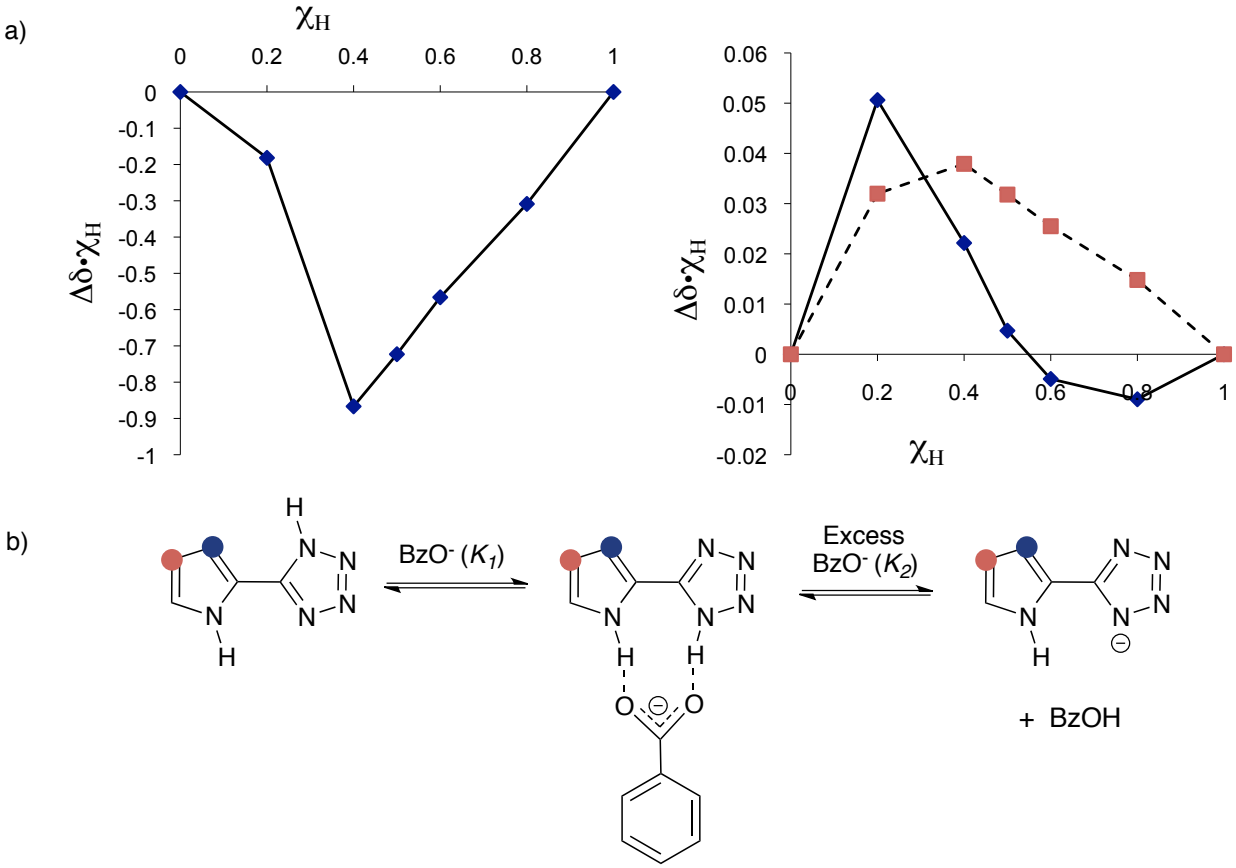

Figure 3.5 a) Job plots of the **3.2**•OBz^- system, no reasonable n:m binding stoichiometry could be extracted from the data. b) Proposed stepwise equilibria resulting in eventual host deprotonation. K_1 (χ_H = 0.2) and K_2 (χ_H = 0.4) are reported by pyrrolic C-H signals labelled with blue and red respectively. The pyrrolic N-H signal reports on both binding events..

3.5 Synthesis and binding studies of 2,5-*bis*(tetrazolyl)pyrrole

Finally, we carried the synthesis of 2,5-*bis*(tetrazolyl)pyrrole **3.11** (Scheme 2) using literature conditions to arrive at 2,5-dicyanopyrrole **3.10**.[139,140] Freshly distilled pyrrole (**3.7**) was formylated at the 2-position under Vilsmeier-Haack conditions and the resulsting aldehyde masked as an α,β-unsaturated ester. The 5-position was subsequently formylated under the same conditions and the conjugated ester then hydrolyzed to produce dialdehyde **3.9** which was then converted to dinitrile **3.10** via *in situ* aldoxime formation by refluxing it in the presence of hydroxylamine hydrochloride, triethylamine and phthalic anhydride. The final *bis*(tetrazole) **3.11** was constructed as before using sodium azide and triethylammonium chloride.

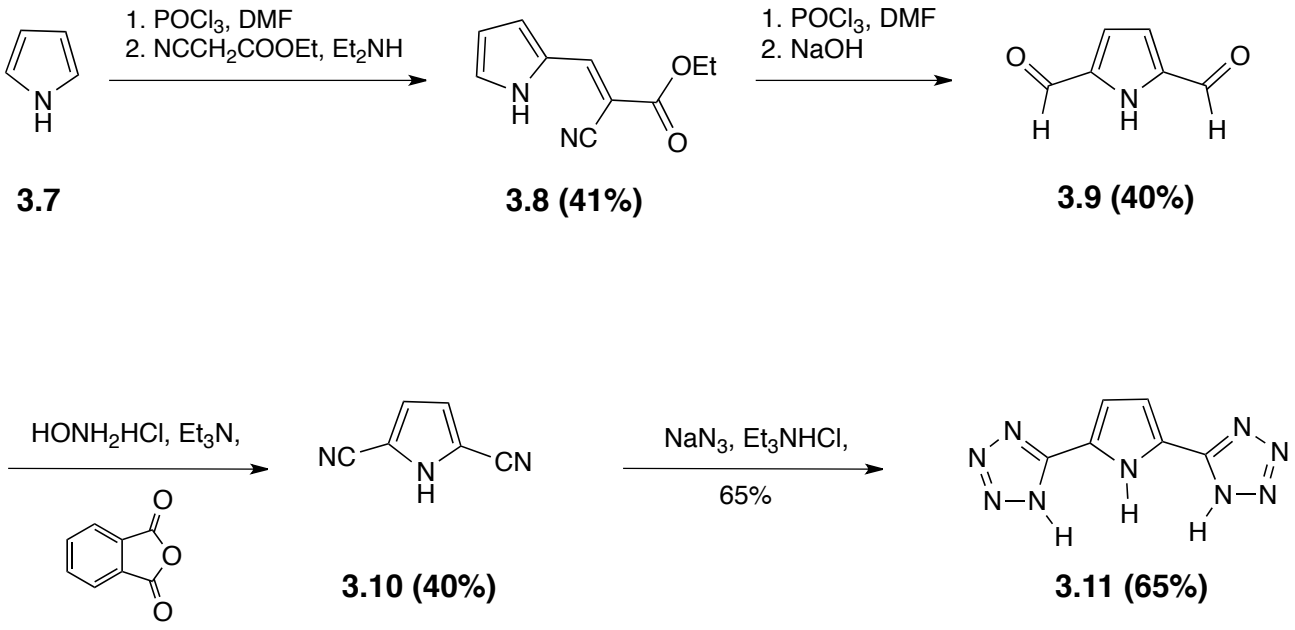

Scheme 3.2 Synthesis of 2,5-*bis*(tetrazolyl)pyrrole **3.11**

NMR studies in 1% H_2O/CD_3CN and in pure CD_3CN show the formation of 1:1 complexes with significantly increased association constants relative to host **3.2** for all anions (Table 3.2), demonstrating that both tetrazole NH's and the central pyrrole NH can cooperate to bind complementary anions as suggested by models (Figure 3.7). Titration with BzO^- again gave rise to data suggesting binding followed by proton transfer. In pure CD_3CN, titrations with Cl^- gave rise to data that indicated mixed 1:1 and 1:2 (H:G) complex formation.

The simple titration data was best fit to binding isotherms including both the formation of 1:1 and 1:2 complexes, with the expected strong 1:1 complex formation (K_{11} = 26,300 M^{-1}) followed by a much weaker binding of a second equivalent of Cl^- (K_{12} = 780 M^{-1}). Job plot analysis also indicated mixed complex formation, but in an unconventional way: the Job plot tracking the chemical shift of the pyrrolic NH had its maximum at 0.5, indicating 1:1 binding, while the plot tracking the pyrrolic CH had a maximum at 0.3, indicating 1:2 binding (Figure 3.6a). Mixed Job plot results of this type must be interpreted with caution. In this case, our hypothesis is that the

pyrrolic NH reports largely on the formation of the 1:1 complex while the chemical shift of the CH arises largely due to the binding of the second equivalent of Cl^- as the equilibrium between the **3.11**•Cl^- and **3.11**•$(Cl^-)_2$ shifts further right with incresing guest addition (Figure 3.6b). This theory is consistent with the calculated structures for **3.11**•Cl^- and **3.11**•$(Cl^-)_2$ (Figure 3.7), as are the relative magnitudes of the experimentally determined values of K_{11} and K_{12}.

Table 3.2 Affinities of *bis*(tetrazole) 3.11 for various anions.[a]

Guest	K_{assoc} for **3.11** in CD_3CN (M^{-1})	K_{assoc} for **3.11** in 1% H_2O/CD_3CN (M^{-1})
Cl^-	K_{11} 26,300 ± 2,300	6,500 ± 500
	K_{12} 780 ± 120	
Br^-	1,500 ± 430	1,100 ± 50
I^-	1,100 ± 130	650 ± 50
TsO^-	34,000 ± 3,500	3,000 ± 1,000
NO_3^-	1,600 ± 300	900 ± 300
BzO^-	p.t.[b]	p.t.[b]

[a] All values are for K_{11} unless otherwise indicated. Guests were titrated as their Bu_4N^+ salts into solutions of hosts in the stated solvent system. Chemical shift data for all nuclei that displayed significant chemical shifts were fit to 1:1 or 1:2 binding isotherms to arrive at K_{assoc} values. Experiments were done in duplicate or triplicate. Values reported are averages of all nuclei from all experiments. Errors reported are standard deviations. [b] p.t. = evidence of proton transfer between host and gest, see text.

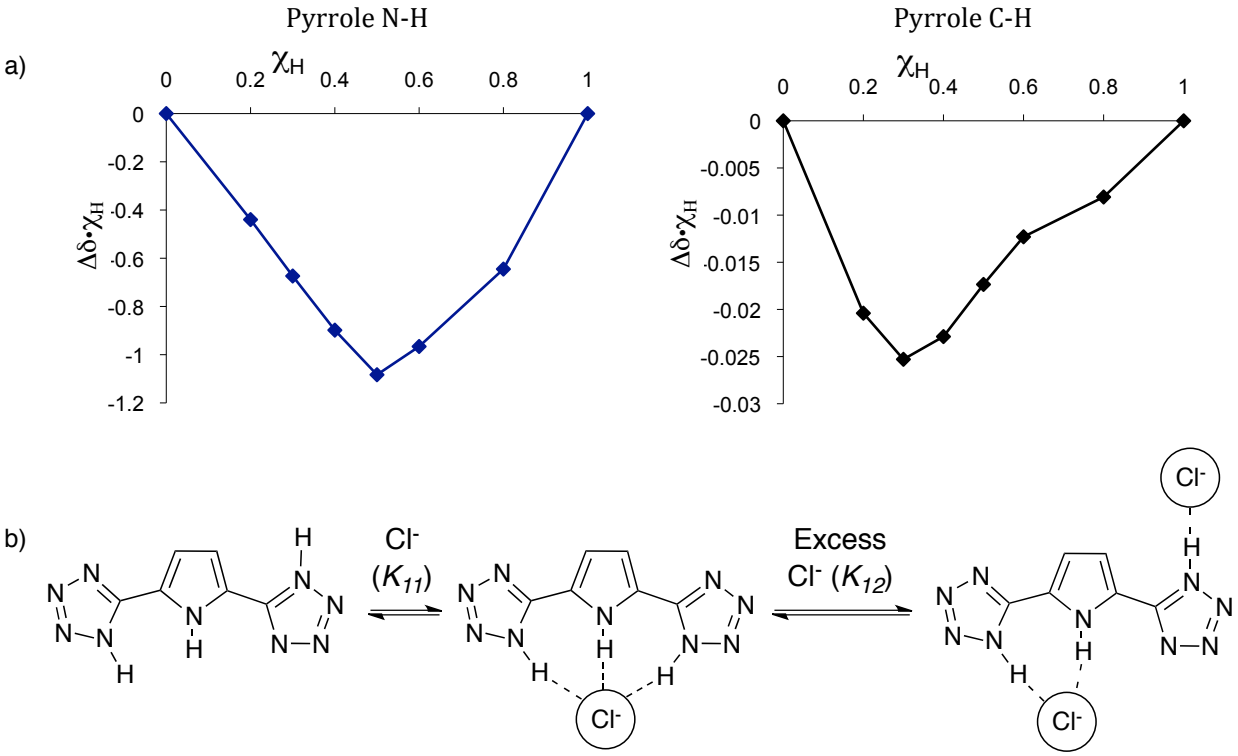

Figure 3.6 Job plots for the binding events 3.**11**•Cl^- and 3.**11**•$(Cl^-)_2$. Tracking the shifts of the pryyole N-H signal suggests it mainly reports on the former (extremum at mole fraction = 0.5) while tracking the pyrrole C-H signal suggests it mainly reports on the latter (extremum at mole fraction = 0.3). b) Equilibrium representing the binding events. Molecular symmetry precludes the possibility of two separate curves for the pyrrolic C-H signals as in figure 3.5. The pyrrolic N-H remains locked in a 1:1 stiochiometry with chloride during the course of guest addition.

Host **3.11** also displays an altered guest-binding preference relative to **3.2** in pure CD_3CN, showing its highest affinity for the oxyanion TsO^- (K_{assoc} = 34,000 M^{-1}) instead of Cl^-. Molecular models (HF/6-311+G**) suggest that Cl^- can't hydrogen bond to the peripheral tetrazole NH's of **3.11** as effectively as does the larger TsO^- anion (Figure 3.7). In **3.11**•Cl^- the distance between the tetrazole NH donor and Cl^- acceptor is $d_{N\text{-}Cl}$ = 3.41 Å, or 0.11 Å *longer* than the sum of van der Waals radii (half of the shotest distance observed in crystals betweem nuclei of atoms of the same nature belonging to different molecules).[141,142] In **3.11**•TsO^- the equivalent hydrogen bonding distances are $d_{N\text{-}O}$ = 2.813 and 2.815 Å, which are

0.25 Å *shorter* than the sum of van der Waals radii. With that said, the "normal" selectivity of Cl^- over TsO^- is observed in 1% H_2O/CD_3CN, making it incautious to interpret these selectivities exclusively in terms of host-guest contacts observed in gas-phase calculations.[143] In this case more guest is held in the bulk solvent than in pure CD_3CN reducing the magnitude of K_{11} for all guest studied. Under these conditions **3.11**•$(Cl^-)_2$ cannot form and the stability of the **3.11**•(Cl^-) complex is stronger than that of **3.11**•(OTs^-).

Whatever the details of host-guest complexation, stoichiometries, and geometries, it is clear that the addition of tetrazoles has a consistently strong and favorable influence on the anion binding properties of the pyrrole scaffold. The potency of the 5-(2-pyrrolyl)tetrazole motif in this setting is most clearly demonstrated by a simple comparison of the K_{11} of **3.11** for Cl^- in CD_3CN (26,300 M^{-1}) to the reported value for the closely related pyrrole *bis*(amide) **3.12** (138 M^{-1}),[138] a *nearly 200-fold increase* in affinity that arises from a simple tetrazole-for-amide swap.

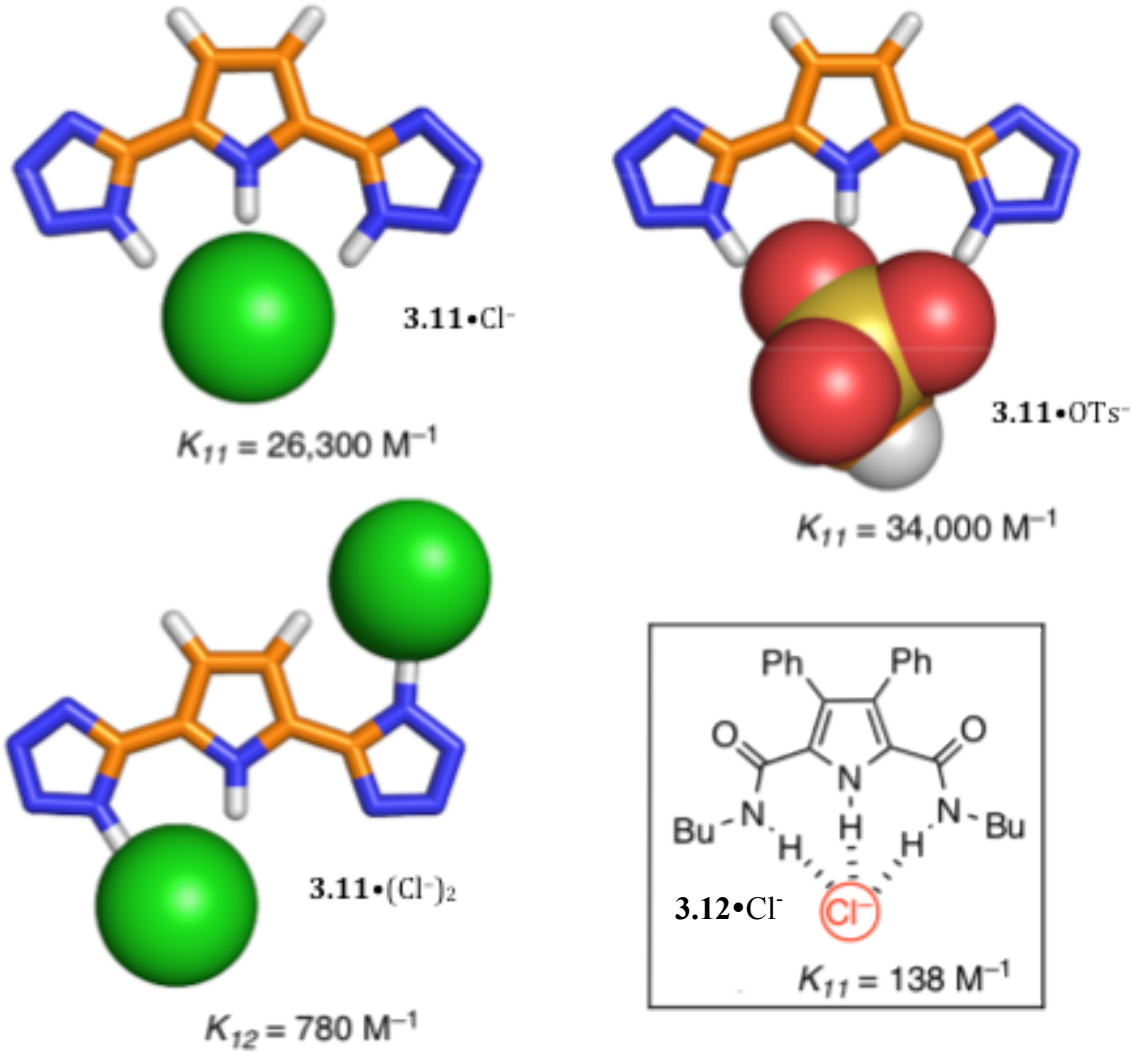

Figure 3.7 Calculated structures and stepwise binding constants for complexes of **3.11** with Cl^- and TsO^- (truncated as methanesulfonate for calculations). Inset: structure and K_{11} value for reference host **4.3.**

3.5 Conclusions

Pyrroles offer a richness of photochemical and electrochemical properties,[144-147] as well as diverse possibilities for synthetic derivatization, that have driven researchers to incorporate them into myriad anion hosts and sensors.[111,148,149] Yet the potencies of simple, acyclic pyrrole-based anion receptors can be orders of magnitude weaker than their urea, squaramide, and indolocarbazole counterparts.[128,129,150] Tetrazoles are prized as metabolically stable carboxylic acid bioisosteres in medicinal chemistry[71] and have shown promise as organocatalysts,[130] but their favorable recognition properties have been

ignored with few exceptions.[86,123,131,132,151-153] Like other acidic recognition elements, tetrazoles are inherently limited to moderately basic anions. But the tradeoff for this limited scope is the ability to create potent receptors quickly and easily without complex synthetic steps like macrocyclizations and strapping reactions. Host **3.2** is derived from host **5** via a tetrazole-for-amide swap, as host **3.11** is derived from host **3.12**. We envision that this conservative modification could be applied as a general and synthetically simple improvement that will provide orders-of-magnitude affinity enhancements for a large number of other amide and urea-based anion-binding hosts.

3.6 Experimental Section

3.6.1 General Considerations

2-pyrrolo-carbonitrile was used as purchased from Aldrich. 2,5-dicyanopyrrole was prepared from pyrrole by the methods reported in references 136 and 137. Melting points are uncorrected. Infrared spectra were recorded from thin films on KBr plates or KBr pellets. Proton (^{1}H) NMR spectra were recorded on 500 MHz or 300 MHz spectrometers, as indicated in each case. Carbon (^{13}C) NMR spectra were recorded at 125 MHz or 75 MHz as indicated in each case. NMR spectra were referenced to signals for deuterated solvent bearing residual protons. High-resolution electrospray ionization mass spectra (HR-ESI-MS) were recorded on a Quadrupole-ToF mass spectrometer using 2,2'-bipyridine as a lockmass reference.

3.6.2 Synthetic Procedures (Both procedures adapted from ref. 125)

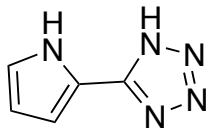

5-(2-Pyrrolo)tetrazole (3.2). 2-pyrrole carbonitrile (385 mg, 4.18 mmol), NaN_3 (541 mg, 8.32 mmol), and $Et_3N \cdot HCl$ (1.122 g, 8.15 mmol) were added to a 250 mL round bottom flask. Toluene (50 mL) was added and the reaction stirred and heated at reflux under N_2 overnight. The reaction was cooled to room temperature and the reaction mixture was extracted with H_2O (3 × 30 mL). Concentrated HCl was added dropwise to the aqueous layer until pH = 1 and a precipitate formed. The mixture was then extracted with ethyl acetate (3 × 30 mL), dried over $NaSO_4$ and concentrated to dryness on a rotary evaporator, which gave the product (357 mg, 63%) as a pale pink solid. mp 223-225°C. IR: 3290*s*, 3157*w*, 3012*w*, 2909*w*, 2832*w*, 2752*w*, 2673*w*, 2578*w*, 2502*w*, 1790*w*, 1708*w*, 1636*s*, 1541*m*, 1469*s*, 1445*sh*, 1350*w*, 1268*w*, 1209*m*, 1129*s*, 1073*m*, 1054*s*, 1033*m*, 998*m*, 903*w*, 736*w*, 701*w*, 675*w*, 589*m*. ^{1}H NMR (CD_3CN, 300 MHz): δ 12.64 (*br s*, 1 H); 10.21 (*br s*, 1 H); 7.05 (*td*, *J* = 2.6, 1.5, 1 H); 6.84 (*ddd*, *J* = 3.8, 2.5, 1.4, 1 H); 6.33 (*dt*, *J* = 3.3, 2.5, 1 H). ^{13}C NMR (DMSO-d_6, 75 MHz): δ 149.4; 122.6; 115.6; 110.9; 109.7. HR-ESI-MS (MH^+ *m/z*): calc. for $C_5H_6N_5^+$ 136.0623, found 136.0623.

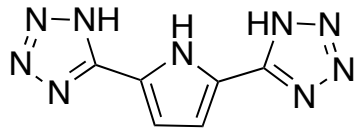

Pyrrole-2,5-*bis*(5-tetrazole) (3.11). 2,5-dicyanopyrrole (100 mg, 0.85 mmol), NaN_3 (222 mg, 3.42 mmol), $Et_3N \cdot HCl$ (470 mg, 3.42 mmol), and toluene (15 mL) were added to a round bottom flask. The reaction mixture was stirred under N_2 and heated at reflux for 24 h. After cooling to room temperature, the reaction mixture was extracted with H_2O (3 × 10 mL) and acidified to pH 1 with 1 M HCl to cause a precipitation of the product. Filtration isolated the pure product as a pale pink solid (113 mg, 65%). Mp 153°C

(decomp.). IR: 3266*s*, 3137*w*, 3103*w*, 3053*w*, 2929*w*, 2817*w*, 2705*w*, 2588*w*, 1625*s*, 1527*m*, 1412*m*, 1325*w*, 1272*w*, 1255*w*, 1163*w*, 1152*w*, 1102*w*, 1074*w*, 1037*m*, 995*w*, 931*sh*, 909*m*, 811*m*, 741*m*, 696*w*, 618*w*, 433*w*. ^{1}H NMR (DMSO-d_6, 500 MHz): δ 16.53 (*s*, 1 H); 12.81 (*s*, 1 H); 6.98 (*d*, *J* = 2.25, 1 H). ^{13}C NMR (DMSO-d_6, 75 MHz): δ 149.1; 119.9; 112.5. HR-ESI-MS (MH^+ *m/z*): calc. for $C_6H_6N_9^+$ 204.0746, found 204.0746.

3.6.3 NMR Binding Studies

^{1}H NMR titrations were done on a μL Bruker DRX 500 MHz spectrometer using CD_3CN purchased from Cambridge Isotope Laboratories. Guests were used as their Bu_4N^+ salts and were dried *in vacuo* over P_2O_5 before use. Binding constants were determined by duplicate or triplicate titrations using host solutions of 0.5–4 mM. Guest solutions were prepared using the host solutions themselves to ensure that [host] remained constant during the titrations. Guest concentrations were 8–20 times the concentration of host solutions, and were added into the host solutions beginning with 10 μL increments and increasing to a final incremental volume of 500 uL. Titration curves were generated by plotting the change in chemical shift of protons on the host molecule against the concentration of guest. The chemical shift data was fit to 1:1 or 1:2 binding isotherms using a Microsoft Excel macro by Dr. J.M. Sanderson and the Centre for Bioactive Chemistry, Department of Chemistry, Durham University, Durham, UK which is freely available at http://dur.ac.uk/j.m.sanderson/science/downloads. Job plots were carried out in CD_3CN using total concentrations of ([host] + [guest]) as indicated.

Chapter 4. The pyrrolyl-tetrazole binding motif appended with amides: a new class of diversifiable anion binding agents

Portions of this Chapter were previously published, and are reprinted with permission from Pinter T.; Simhadri, C.; Hof F.; Dissecting the complex recognition interfaces of potent tetrazole- and pyrrole-based anion binders. *J. Org. Chem.,* **2013**, *78*, 4642-4648.

This work was conceived of by Thomas Pinter and Fraser Hof. Initial synthesis of hosts **4.7**, **4.10** and **4.11** were conducted by Chakravarthi Simhadri, (Scheme 4.1).

Revised syntheses of **4.10** and **4.11** (Scheme 4.2, Scheme 4.3), binding studies of all hosts, Spartan calculations and overall data analysis were conducted by Thomas Pinter.

The manuscript was written by Thomas Pinter and Fraser Hof and this Chapter was adapted from that paper by Thomas Pinter.

4.1 Foreword

The remarkable strength of the pyrrolyl-tetrazole binding motif has been demonstrated, however the ability of this binding element to be derivatized has been inhibited by the installation of two tetrazoles on the pyrrole scaffold. In order to impart the potential for diversification one tetrazole must be replaced by an element that can show variety. Given the knowledge that amidopyrroles are observed as abundant anion binding agents in the literature, combining amides with this new pyrrolyl-tetrazole motif would allow for this goal.

4.2 Abstract

Tetrazoles are potent anion binders. We report here a new family of tetrazole-pyrrole-amide hosts that arise when a tetrazole is incorporated as a new binding element alongside the well-known amidopyrrole anion-binding scaffold. In addition to reporting three new, modular synthetic routes that can be used to access these structures, we also report that the new hosts are highly potent binders of chloride. Along the way, we carried out studies of a pyrrole-ester control compound that, surprisingly, bound anions almost as strongly as did the amide analogs. This led us to investigate further the relative importance of the amide NH in halide binding. We report that, despite the regular appearance of this close amide NH---Cl contact in previously published calculated and experimental X-ray structures, the amide NH in this family of anion hosts does not hydrogen bond strongly to chloride in solution.

4.3 Introduction

Our studies discussed in chapter three proved the hypothesis that tetrazoles when bound in a co-planar fashion to an aryl neighbor would prove to be potent anion recognition elements, in particular chloride. Indeed, a single tetrazole bound to pyrrole as in **3.2** was able to bind chloride with equal strength as calix[4]arene **2.9** containing four tetrazole binding elements. The tetrazoles of the latter were forced into an unfavourable conformation (with conjugation to their respective benzene partners broken) in order to engage chloride and as a consequence binding strength was significantly diminished.

Tridendate host **3.11** outperformed **2.9** with respect to chloride binding by an order of magnitude.

A single unadorned tetrazole (**4.1,** Figure 4.1) is a stronger anion binder[86] than many more elaborate, multi-dentate hydrogen bond donating hosts (e.g. **3.2**, **3.5**, and **3.12**) (Figure 4.1).[124,154] One tetrazole-containing anion-binding motif that we have previously reported is represented by the pyrrole-tetrazole hybrids **3.2** and **3.11**, which are some of the most potent and simple anion recognition motifs in the pyrrole family. Mono-tetrazole **3.2** binds chloride 120-fold stronger than does analogous monoamide **3.5**, and *bis*(tetrazole) **3.11** binds chloride almost 200-fold stronger than does its closely analogous *bis*(amide) **3.12** (Figure 4.1).[154] Given this data, I set out to construct a new family of pyrrole-based hosts that contain both amides and tetrazoles (hosts **4.9** and **4.10**), as well as ester-functionalized host **4.7** (see Scheme 1). These hosts show generally high affinities for HSO_4^-, and even higher affinities for Cl^-, and allow us to dissect out energetic influences of different groups at the recognition interface. Whereas *bis*(tetrazole) **3.11** leaves no room for diversification of the host molecule, leaving one site open to functionalization with the ultimate goal of tetrazole insertion at the other site should result in rapid access to a wide variety of new hosts containing our pyrrolyl-tetrazole binding motif._

4.4 Synthesis

We developed multiple routes to the selective installation of both tetrazole and ester/amide functionality at the 2- and 5-positions of pyrrole (**3.7**). The first strategy (Scheme 4.1) began with the synthesis of ethyl pyrrole-2-carboxylate (**4.5**) achieved through a Vilsmeier-Haack formylation of pyrrole (**3.7**), silver oxide oxidation and DCC coupling to ethanol. Ester **4.5** was then cyanated with chlorosulfonyl isocyanate[155] to give **4.6** and finally tetrazole formation was realized upon treatment with NaN_3 and NH_4Cl (generating HN_3 *in situ*) to produce host **4.7**. Hydrolysis of the ester provided highly polar carboxylic acid **4.8**, and subsequent EDC-mediated coupling to *p*-toluidine or *p*-methoxybenzylamine gave amide-functionalized hosts **4.9** and **4.10**, respectively. One

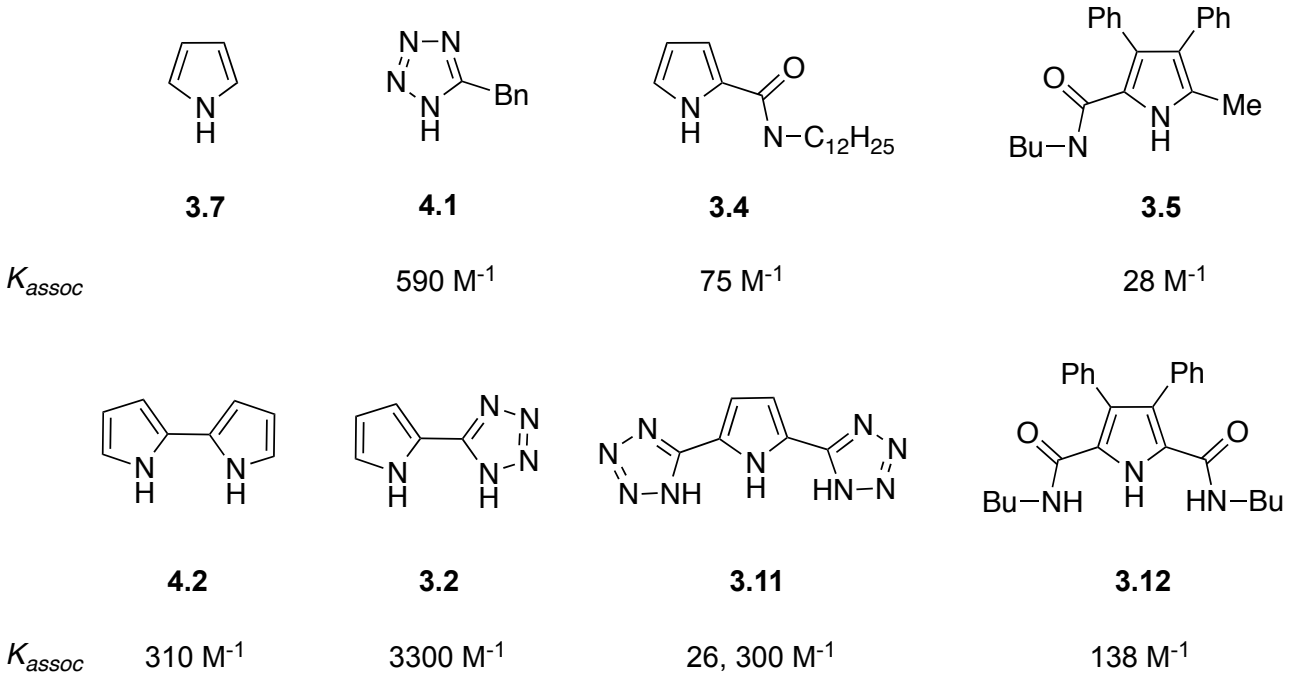

Figure 4.1 Structures of pyrrole (**3.7**) and related anion receptors, along with the 1:1 binding constants for the complexation of Cl^- in CD_3CN that have been previously reported in the literature (see text). (Bn = Benzyl)

shortcoming in this route was the poor regioselectivity of the cyanation of **4.5**, where substitutions at the 4-position (undesired) and 5-position (desired) were observed at approximately a 3:2 ratio that persisted despite efforts to optimize conditions.

During the course of these investigations we found the ethoxy group in **4.6** could be displaced directly by certain primary amines at high temperature, raising the possibility of a more direct synthetic route. To take advantage of the higher reactivity for methyl esters in direct ester-to-amide conversions, we switched to a route starting with methyl-2-pyrrole carboxylate **4.11**, and cyanated as before to give **4.12**. Direct displacement of the methoxy group was achieved by stirring **4.12** in neat *p*-methoxybenzylamine at 120^{o}C for 2 days, which cleanly provided amide **4.13** in >80% yield. Standard tetrazole forming conditions as described above gave the final product **4.10** in only four steps from commercially available material **4.12** (Scheme 4.2).

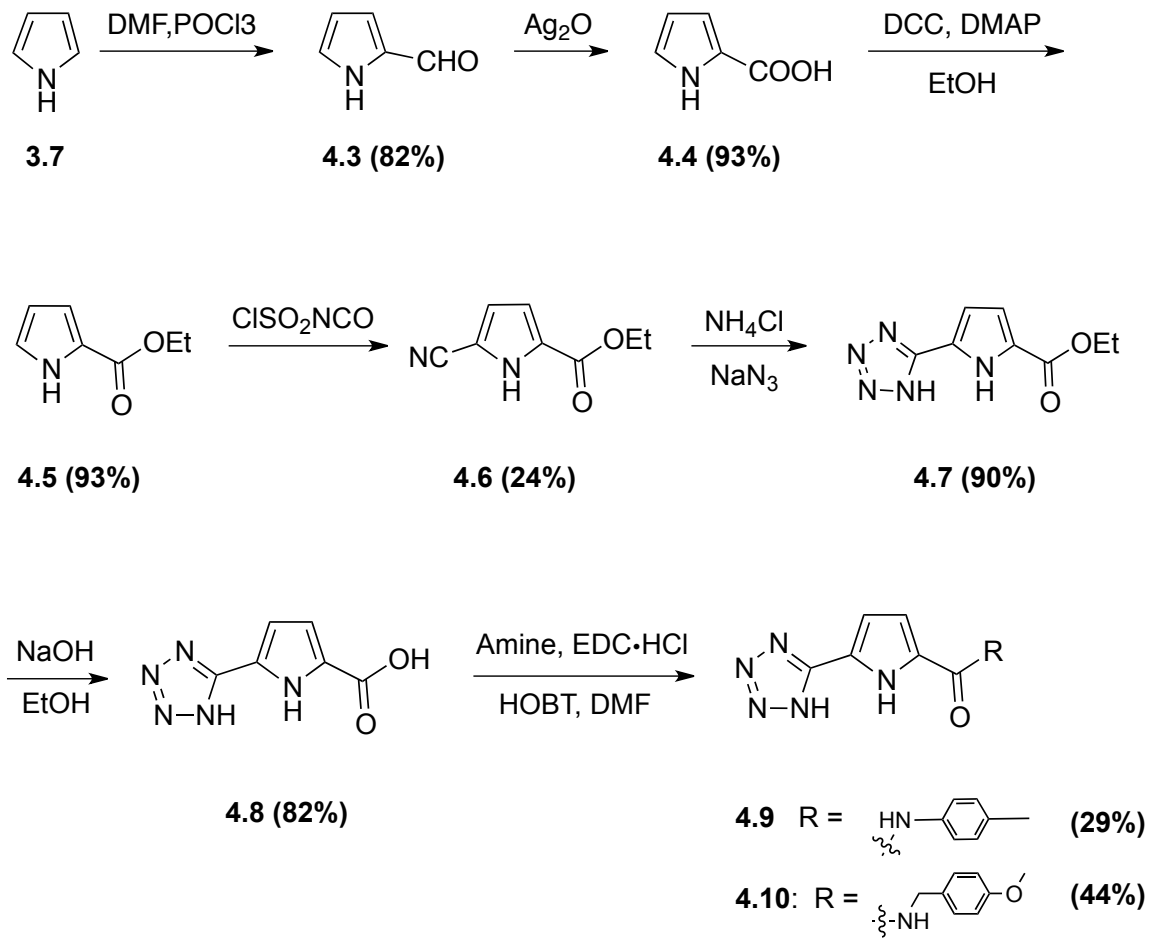

Scheme 4.1 Initial synthetic approach to hosts **4.8**, **4.9**, and **4.10**.

Attempting synthesis of host **4.9** via the direct amidation met with disappointing results, as stirring precursor **4.12** in molten *p*-toluidine even at temperatures in excess of 150°C for several days resulted only in recovery of starting material. Looking back at the initial synthetic plan (Scheme 4.1), I then envisaged two alternate routes to construct *N-aryl* amide-functionalized host **4.9**. Path A involves first ester hydrolysis of the intermediate **4.12** to give carboxylic acid **4.14**. EDC coupling to toluidine gives amide **4.15** and completion of the synthesis is achieved through tetrazole insertion as described above (Scheme 4.3, Path A). Following Path B requires initial insertion of the tetrazole

to afford **4.16** followed by ester hydrolysis yielding **4.8** and finally EDC mediated acid-amine coupling (Scheme 4.3, Path B). I completed both synthetic routes, and found that Path A proved to be the superior option. This is one of many examples encountered during this thesis work that teaches the general lesson that the tetrazole formation is best left as the last step when possible, as highly polar tetrazole-containing intermediates such as **4.8** can be difficult to purify and/or dissolve for subsequent reactions. This is evidenced by the poor yields in the last steps of both of Scheme 4.1 and Scheme 4.3 (Path B). Scheme 4.3 (Path A) circumvents this problematic intermediate resulting in a much more convenient synthesis.

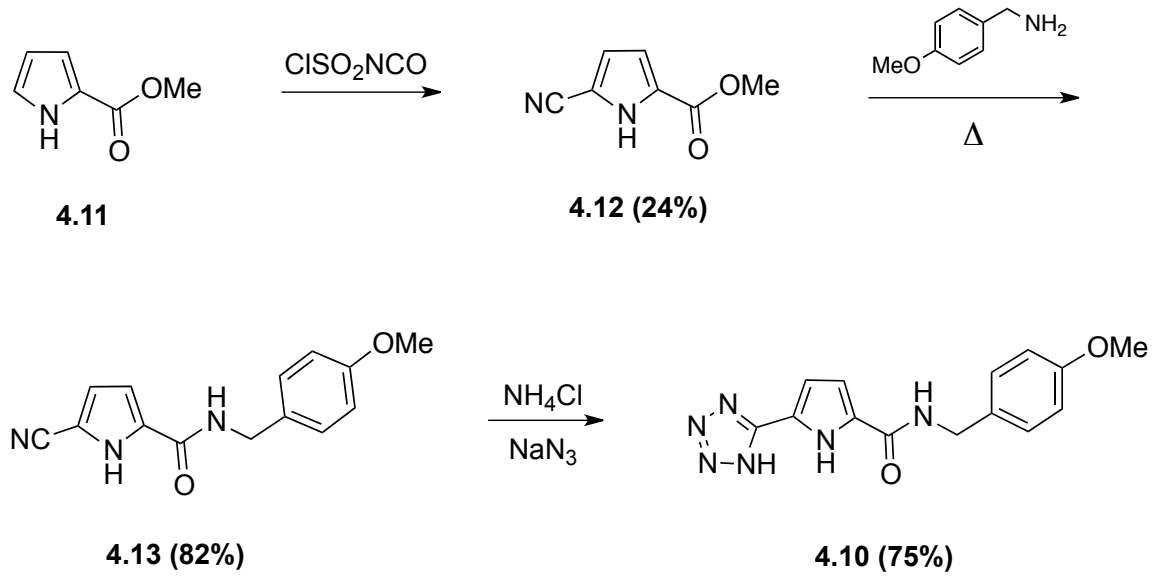

Scheme 4.2 Synthesis of amidopyrrole **4.10.**

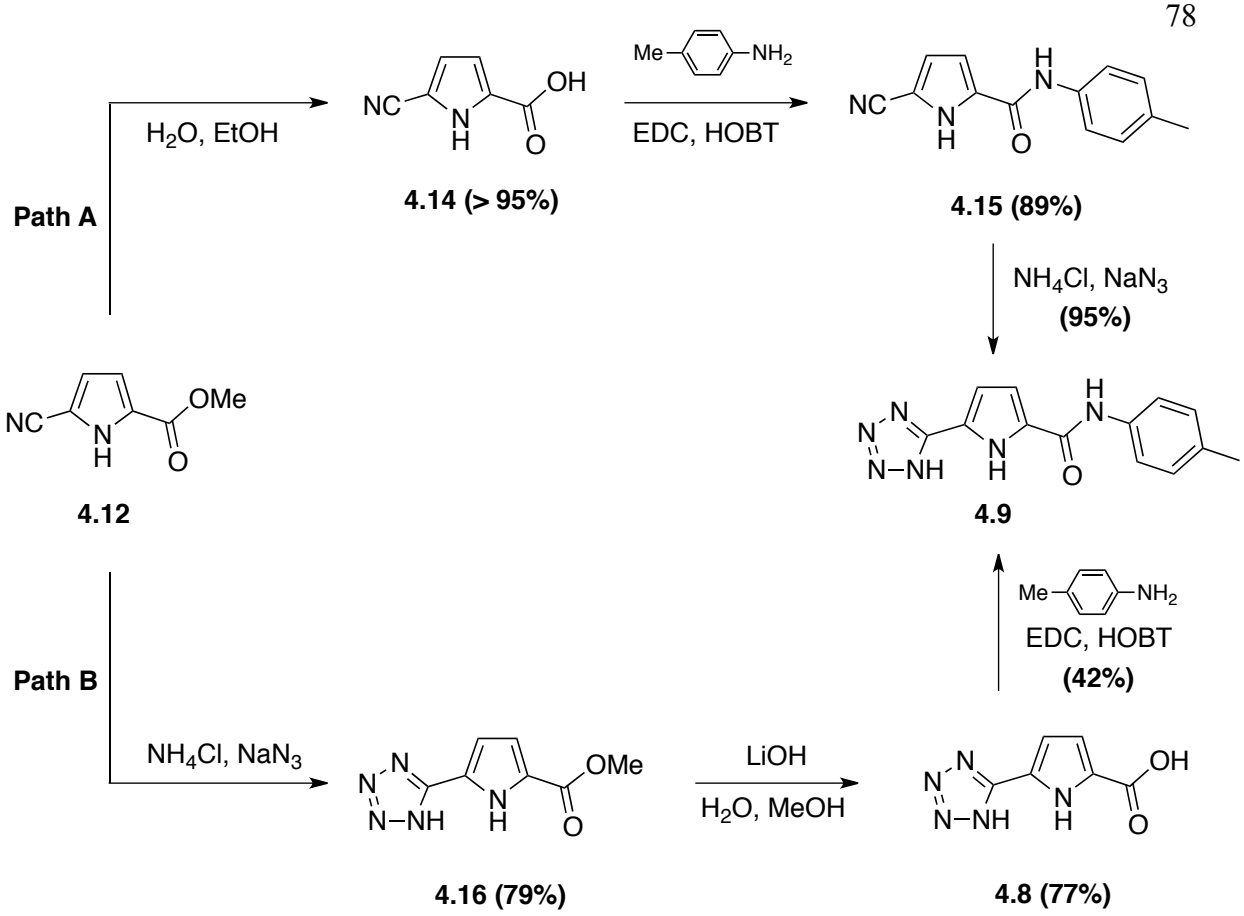

Scheme 4.3 Two synthetic routes to amidopyrrole **4.9** Path A was found to be superior.

4.5 NMR-based binding studies and molecular modeling studies

^{1}H NMR titrations were used to determine the anion-binding capabilities of hosts **4.7**, **4.9**, and **4.10**. Studies were carried out in CD_3CN, as this solvent allows comparisons to the broadest set of values for other pyrrole-containing hosts reported in the literature. Briefly, anionic guests were added as their Bu_4N^+ salts, and the resulting host chemical shift changes were fitted to 1:1 or 2:1 (H:G) binding isotherms using HypNMR (Protonic Software, 2008). (This software was purchased after the research in Chapters 2 and 3 was completed, because it offers an option to display residuals that increases one's confidence in quality of the model and the fit.) Binding stoichiometries under these conditions were cleanly 1:1 for all complexes except those of host **4.10** and Cl^- which showed a small contribution from 2:1 (H_2G) complex formation (Figure 4.2). Our choices of binding stoichiometries for curve fitting were confirmed by Job plot[98] data for all three hosts with Cl^-, and for

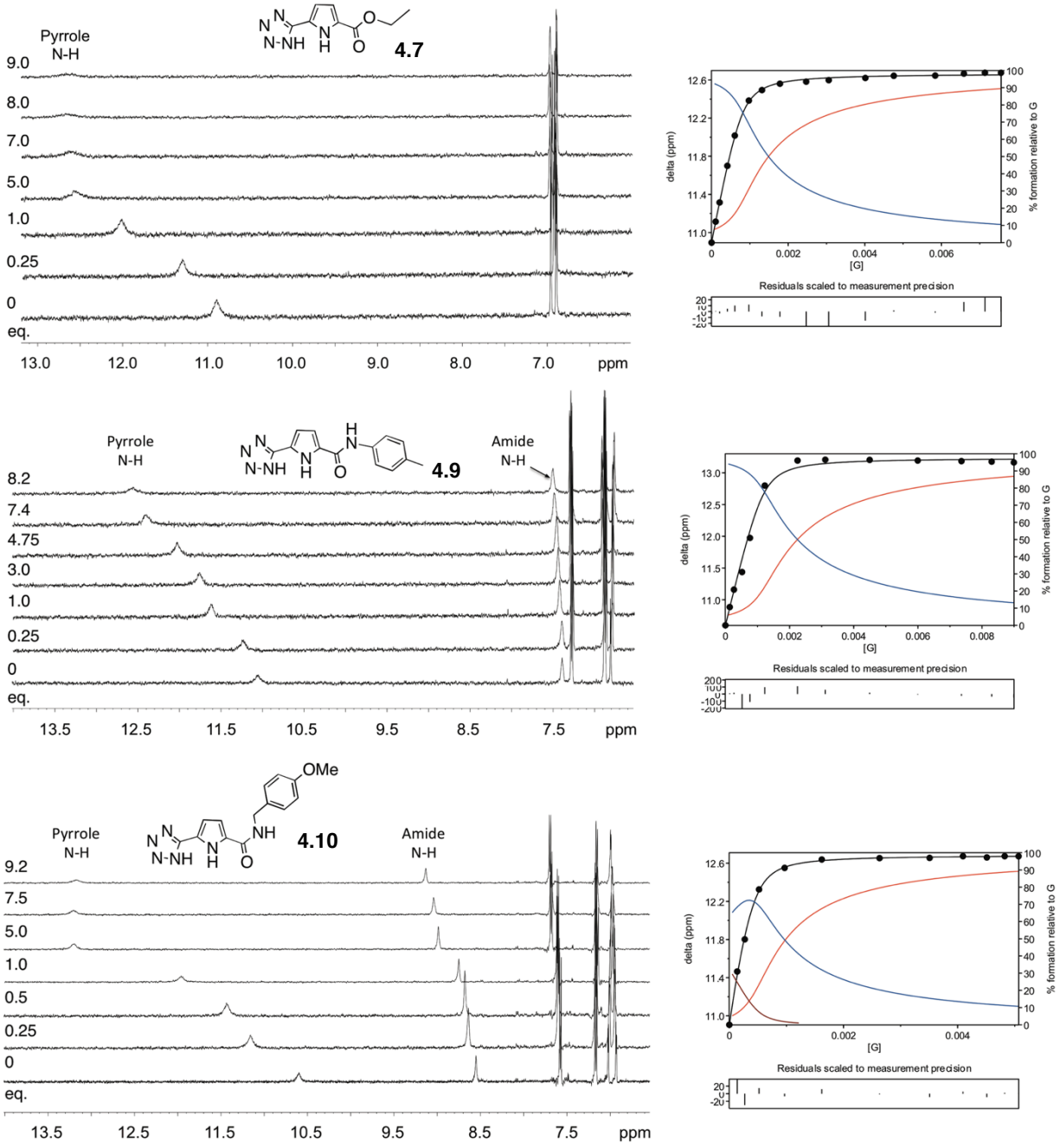

Figure 4.2 Left: Excerpts of stacked ^{1}H NMR (500 MHz) plots following pyrrole (downfield singlet) and amide (upfield singlet) signals for each host in this study. Titrations in these examples were performed in CD_3CN with $Bu_4N^+Cl^-$ as the guest (see experimental section for details). Right: Representative binding curves following the pyrrole N-H and speciation plots (see text) (black points = experimental chemical shift data, black line = fitted chemical shift data, red line = [1:1 complex], blue line = [free host], brown line = [2:1 host:guest complex]). An initial small increase in free host **4.10** (blue line) is observed correlating with a decrease in the 2:1 host:guest complex (brown line) with guest addition as the 2:1 complex is broken freeing some host molecules to form additional 1:1 complexes.

hosts **4.7** and **4.10** additionally with Br^- and HSO_4^-. The resulting association constants between the hosts studied and various anionic guests are given in Table 1. Representative stacked plots and binding curves are shown in Figure 4.2. (Residuals indicate standard deviation for each data point. The apparent trend of the residuals derived from binding measurements with **4.7** is indicative of an incorrect fitting model being used which is acceptable as a 1:1 model generated useful data and other fitting models would not compute).

4.5.1 Halide binding

All hosts showed similar high affinities for chloride and lowest for iodide. The ability of **4.7** to bind Cl^- and Br^- as well as do amides **4.9** and **4.10** was unexpected, as its ester oxygen atom lone pairs must be in close proximity to anions engaged by the central pyrrole NH. Even more surprising, when picturing a repulsive, close O---Cl^- contact, is that **4.7** is 5.5-fold more potent than its unsubstituted parent compound **3.2**.[120] The best interpretations of these data are that a) the O---Cl^- contact for **4.7** is long enough not to destabilize the complex significantly, and b) the electron-withdrawing nature of the ester acidifies the pyrrole NH and thereby increases the strength of pyrrole NH---Cl^- hydrogen bond. The pyrrole NH in free **4.7** is 0.8 ppm downfield of the chemical shift of the same NH in parent host **3.2**, giving further support to this line of reasoning.

So what are the amide NH's in **4.9** and **4.10** in fact doing in the exceptionally stable 1:1 complexes of each host with Cl^-? Comparison to host **4.7**, which has no amide NH's but has similar Cl^- affinity, would suggest that they aren't strongly involved in hydrogen bonding to the anion. Upon binding Cl^- the amide NH's in **4.9** and **4.10** shift downfield by only 0.5 and 0.2 ppm, respectively, as fitted $\Delta\delta_{max}$ values; host **4.9** in particular shows a barely detectable experimental downfield shift (Figure 4.2). Much larger downfield shifts of ~2 ppm are normally observed upon formation of NH---Cl^- hydrogen bonds. The answer then, would seem to be that the amides serve mainly as electron withdrawing groups that increase the strength of pyrrole NH---Cl^- hydrogen bonding in a manner analogous to the ester in host **4.7**. Given the similarity of the amido-pyrrole motifs in **4.9** and **4.10** with the large number of previously published amido-

pyrrole hosts in the literature, we wondered if this lesson could tell us something about this broader set of hosts. Literature hosts **3.4**,[124] **3.5**,[154] and **3.12**[154] bind Cl^- with affinities of 28–138 M^{-1} in CD_3CN. Some substantial part of these affinities are routinely attributed to amide NH---Cl^- hydrogen bonds. Close contacts between amide NH and anionic guest are always observed in calculated host-guest structures, and are sometimes also observed in x-ray co-crystal structures of the host-guest complexes.[7] To understand these motifs better, we carried out control titrations that revealed that even unsubstituted pyrrole (**3.7**) and ethyl-2-pyrrole carboxylate (**4.5**) bind to Cl^- with significant affinity ($K_{assoc} \geq 10$ M^{-1}). More importantly, the pyrrole N-H signals in compounds **3.7** and **4.5** experience downfield shifts of ≥2 ppm when saturated with chloride, while smaller shifts are observed for amide protons in **3.4**, **3.5**, or **3.12** that resemble more the small shifts we detect for **4.9** and **4.10**. When considering all lines of evidence, it is clear that the amides in **4.9** and **4.10** don't contribute strong H-bonds to halide guests, and that a similar interpretation is probably justified for most of the many amido-pyrrole hosts that have been reported.[7,156]

4.5.2 Oxyanion binding

But the amides do not always remain innocent. Host **4.9** shows moderately strong binding for the oxyanions HSO_4^-, TsO^- (Tosylate), and NO_3^- that is stronger in each case than that of ester-functionalized host **4.7**. Host **4.9** shows four-fold stronger binding for TsO^- than NO_3^-. Conversely, **4.10** displayed an approximately 1.5-fold weaker binding for TsO^- than NO_3^-. In a general sense, amides **4.9** and **4.10** show better aptitude for engaging the varied geometries of oxyanions than does ester **4.7**. The amide NH chemical shifts inform us on the possible formation of NH---O hydrogen bonds in these various host-oxyanion complexes. The largest complexation-induced shifts of the amide NH are seen for TsO^-, while insignificant shifts are seen for NO_3^-. These shifts offer direct experimental evidence of amide NH---anion hydrogen bonding (or lack thereof), but we can't draw simple connections between observed affinities and the presence or absence of the aforementioned hydrogen bonds. Again, these results raise questions about the roles of amide NH's in oxyanion binding by previously reported amido-pyrrole hosts. An X-ray crystal structure of a *bis*(amidopyrrole) (**3.12**) in complex with benzoate reveals all

H-bond donors engaging the guest. In this complex, one benzoate oxygen is engaged by both the pyrrole N-H and one amide N-H, with H----O bond lengths varying by less than 1 Å.[157] The remaining amide N-H and guest oxygen are separated by a distance virtually identical to the pyrrole-guest bond length demonstrating that each H-bond donor contributes nearly equally to guest stabilization. In an indole-based system that included pendant urea and amide groups, a similarly weak participation of the amide N-H in guest binding was also observed.[158] The binding constants of **3.12** with chloride and benzoate were determined to be 138 and 2500 M^{-1} respectively. Conversely, mono-amide **3.5** shows affinities of 28 and 202 M^{-1}, respectively, for the same two guests, a clear indication that a third hydrogen bond donor is necessary for strong binding of oxyanions.

Table 4.1 Binding constants for the hosts studied obtained via ^{1}H NMR titrations in CD_3CN.[a]

Host	Cl^-	Br^-	I^-	HSO_4^-	OTs^-	NO_3^-
4.7	18, 000 ± 2300	1700 ± 260	85 ± 21	130 ± 13	950 ± 7	440 ± 35
4.9	31, 000 ± 4600	1800 ± 100	71 ± 11	1500 ± 230	3000 ± 98	750 ± 85
4.10	K_{11} = 23, 000 ± 4700 K_{21} = 820 ± 11	1300 ± 700	150 ± 23	1200 ± 58	770 ± 49	1120 ± 12

[a] All values are for K_{11} unless otherwise noted. All titrations were done in duplicate or triplicate, and the errors reported are standard deviations. Host solutions of 0.5–1 mM were first prepared, and then also used as solvent to make the titrant solution (containing 8–15 mM of each guest). The guest solutions were titrated into the host until a point of saturation was reached.

4.5.3 2:1 complexation by 4.10

The **4.10**·Cl^- complex, indicated by Job plot to be a 2:1 host:guest binding event, was fit to a 2:1 (H_2G) binding isotherm using HypNMR. The results show a K_{11} value of 2×10^4 M^{-1}, similar to those seen for **4.7**•Cl^- and **4.9**•Cl^-, and a K_{21} value ~two orders of magnitude weaker. No other titration data collected in this study could be fit well to any analogous 2:1 isotherm. The 2:1 complex only exists when a large excess of host is present, and only about 2% of it is present in solution after 1 equivalent of guest is added (Figure 4.2).

4.6 Molecular Modelling

Molecular modeling was conducted to investigate further the conclusions drawn from solution phase data (Figure 4.3) as attempts at isolating crystals suitable for x-ray analysis failed. Local minimum energy structures were identified for the chloride complexes of **4.7**, **4.9**, and **4.10**, including the H_2G complex posited for **4.10**. All structures have reasonable bond lengths and angles, and notably, all complexes of amide-containing hosts have local minima with amide NH groups forming hydrogen bonds to Cl^-. Heavy atom (N---Cl) separations with respect to guest and tetrazole NH were 3.35 and 3.32 Å for hosts **4.9** and **4.10** respectively; guest and pyrrole nitrogen were observed to be 3.21 and 3.18 Å for hosts **4.9** and **4.10**, respectively; guest and amide nitrogen were observed to be 3.55 and 3.58 Å for hosts **4.9** and **4.10**, respectively. As with many other previously reported amido-pyrrole examples,[7,156] the calculated N---Cl contacts for amides, while moderately long, would suggest an energetically favorable contact between these groups that the NMR data tell us must not exist in solution.

Modeling the H_2G complex for **4.10** revealed a local minimum in which two of the benzyl amide functionalized hosts (**4.10**) bound chloride in their hydrogen bond-donating clefts orthogonally to one another, but this structure could not be identified as a local minimum for the other hosts. It can be seen in the model (Figure 4.3a) that an edge-to-face interaction between the two aromatic rings is occurring. The methylene linker in **4.10** allows for an extra degree of rotational freedom relative to the more rigid host **4.9**. It is possible that this additional aromatic-aromatic contact is the reason why **4.10** forms weak, but measurable 2:1 complexes with Cl^- while **4.9** does not.

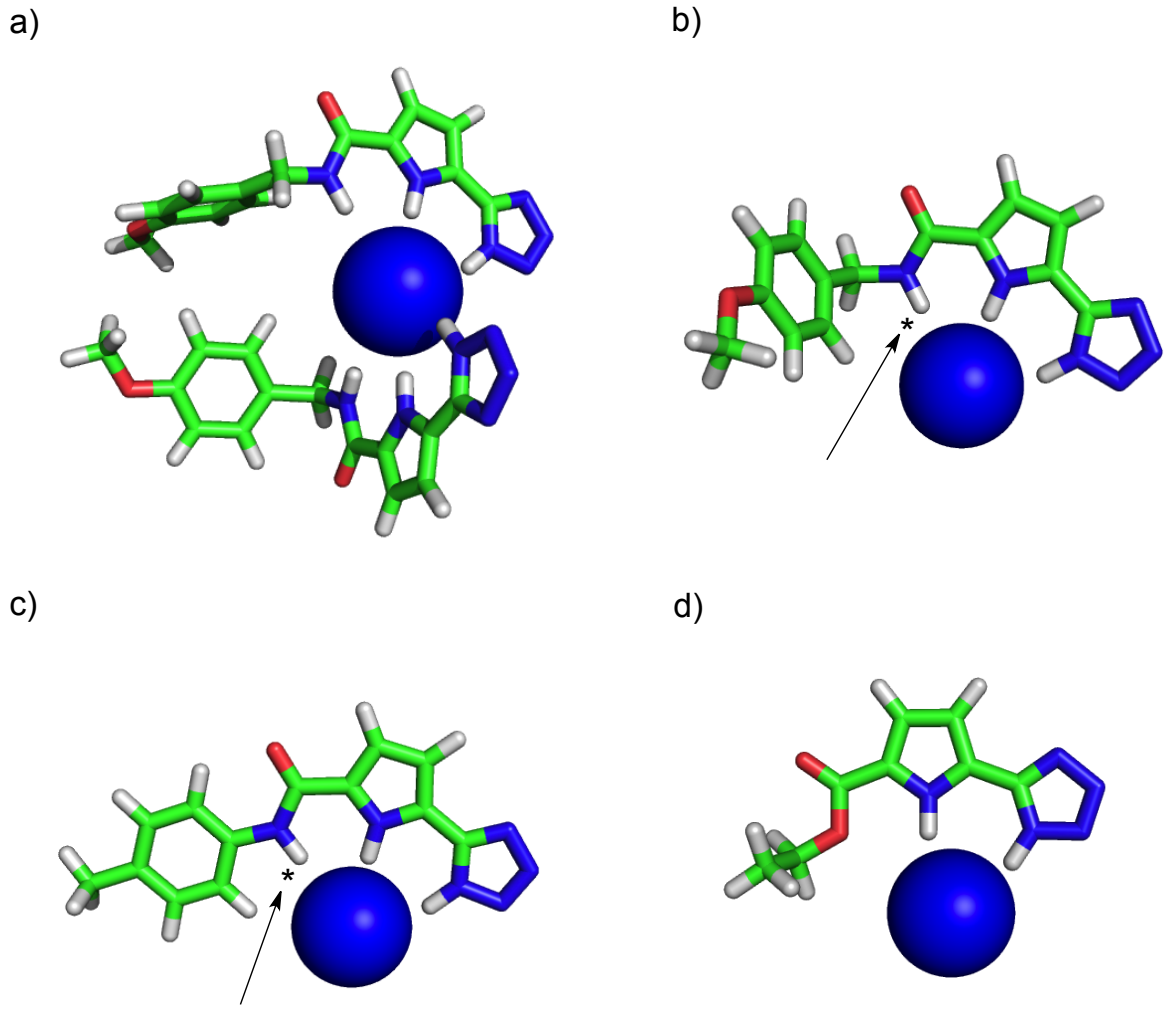

Figure 4.3 Local minima identified for the host-guest complexes with Cl^- by calculations at the HF/6-31+G* level of theory. a) The 2:1 complex observed between host **4.10** and chloride. b) The 1:1 complex between host **4.10** and chloride. c, d) The 1:1 complexes of the other two hosts with chloride. Hydrogen bonds that are suggested by calculated structures but whose energetic importance is refuted (or diminished) by solution-phase data are marked with an asterisk (*).

4.7 Conclusions

We have synthesized a new class of anion recognition elements containing tetrazole and amide functionalities at the 2- and 5-positions of pyrrole. These compounds were able to outperform common *bis*(amidopyrroles) such as **3.12** in chloride recognition by a wide margin. Further, a 2:1 host:guest complex was observed between **4.10** and chloride due to a key edge-to-face interaction between the appended *p*-methoxybenzyl moieties. Of particular importance, we found that an extra amide-type hydrogen bond

donor does not increase halide affinity significantly in this family of hosts, and probably does not make strong hydrogen bonds to halides in solution. Previous studies have shown this to be true in similar systems such as indole analogues of amidopyrroles. Also to our surprise, we observed that the association constants of hosts **4.7**, **4.9**, and **4.10** for chloride are relatively comparable, and also similar to that of *bis*(tetrazole) **3.11**. These data suggest that adding a third H-bond donor does not significantly affect the stability of the complex, but that it is the electron withdrawing nature of tetrazole, ester, or amide functionalities at the 2-position of a pyrrole that can have a profound, favorable influence on binding affinities. In any case, the introduction of tetrazoles clearly produces some of the most potent halide-binding hosts in the pyrrole family. In other areas of the chemical sciences, authors extol the virtues of tetrazoles' high stability in biological systems and high degree of usefulness as pharmacological agents.[74] We continue to explore the possibility that tetrazoles might find utility as anion-binding therapeutic and/or sensing agents in biological settings.

4.8 Experimental Section

4.8.1 General Considerations

Proton (^{1}H) NMR spectra were recorded on 500 MHz, 360 MHz, or 300 MHz spectrometers, as indicated in each case. Carbon (^{13}C) NMR spectra were recorded at 125 MHz, 90 MHz, or 75 MHz as indicated in each case. All NMR binding studies were performed on a 500 MHz spectrometer. HR-ESI-MS was obtained at the UVic Genome BC Proteomics Centre on a LTQ Orbitrap in positive ionization mode unless otherwise indicated. Melting points are uncorrected. All molecular modeling was performed using Spartan '04 or Spartan '06 (Wavefunction, Inc.) at the HF/ 6-31+G* level of theory. Microwave reactions were carried out in a Biotage Initiator 2.5 microwave reactor at the temperatures indicated.

4.8.2 Synthetic Procedures

General procedure for pyrrole cyanation:

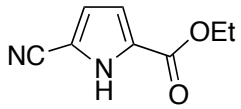

Ethyl-5-cyano-1*H*-pyrrole-2-carboxylate (4.7). Ethyl-1*H*-pyrrole-2-carboxylate (**4.6**) (500 mg, 3.6 mmol) dissolved in 10 ml : 7 ml anhydrous MeCN : DMF was cooled (-40^{o}C) Chlorosulfonyl isocyanate (0.94 ml, 10.8 mmol) was added dropwise and the reaction allowed to warm to ambient temperature. After 24 h, poured over ca. 100 g of ice containing 20 ml of 2 M NaOH. The ice was allowed to melt and the aqueous layer extracted with DCM (3 × 50 ml). The combined organic phases were dried over $MgSO_4$, filtered and concentrated. The crude brown solid was purified (SiO_2, 2:1 Hexanes: EtOAc) yielding 126 mg of **4.7** (0.77 mmol, 21%) as a pale brown solid. mp: 82-84 °C; IR(KBr, thin film): 3349s, 3132w, 2990w, 2921w, 2233s, 1689s, 1568s, 1270s, 1205w, 1107; ^{1}H NMR ($CDCl_3$, 300 MHz): δ 1.37 (t, 3H, J = 7.11Hz), 4.35 (q, 2H, J = 7.11 Hz), 7.12 (m, 1H), 7.42 (m, 2H), 10.40 (s, 1H); ^{13}C NMR ($CDCl_3$, 75 MHz): δ 14.4, 61.6,

95.2, 115.5, 117.8, 124.4, 129.2, 160.6; HR-ESI-MS: 187.04810 (MNa^+, $C_8H_8N_2O_2Na^+$; calc. 187.04781).

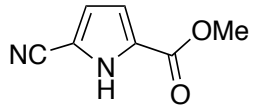

Methyl-5-cyano-1*H*-pyrrole-2-carboxylate (4.13). The general procedure for pyrrole cyanation was applied to methyl-1*H*-pyrrole-2-carboxylate (**4.12**). mp: 140-142 °C; IR(KBr, thin film): 3300s, 3100w, 2990w, 2325w, 2150s, 1701s, 1568s, 1495s, 1270s, 1205w, 750s; ^{1}H NMR ($CDCl_3$, 300 MHz): δ 3.90 (s, 3H), 7.12 (dd, J = 2.52 Hz, 1.50 Hz, 1H), 7.41 (dd, J = 3.21 Hz, 1.46 Hz, 1H), 9.57 (s, 1H); ^{13}C NMR (Acetone-d_6, 75 MHz): δ 52.1, 95.3, 116.0, 118.0, 125.1, 130.9, 160.7; HR-ESI-MS: 173.03222 (MNa^+, $C_7H_6N_2O_2Na^+$; calc. 173.03211).

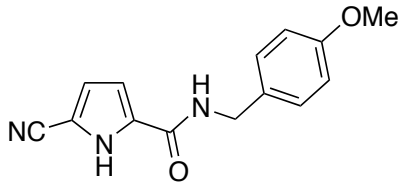

5-cyano-*N*-(4-methoxybenzyl)-1*H*-pyrrole-2-carboxamide (4.14). A mixture of Methyl-5-cyano-1*H*-pyrrole-2-carboxylate **(4.13)** (50 mg) dissolved in *p*-methoxybenzylamine (3 ml) was heated to 120^{o}C and stirred for 2 days. The reaction was allowed to cool and 20 ml of EtOAc was added. The organic phase was washed with 1 M HCl (5 × 15 ml), dried ($MgSO_4$) and concentrated leaving pure **4.14** (45 mg, 89%) as a pale brown solid. mp: 235 °C (dec); IR(KBr, thin film): 3370m, 3174s, br, 2225s, 1634s, 1538w, 1512m, 1436w, 1253m, 1150w; ^{1}H NMR (DMSO-d_6): δ 3.69 (s, 3H), 4.33 (d, J = 6.01 Hz, 2H), 6.85 (d, J = 6.84 Hz, 2H), 7.14 (d, J = 1.19 Hz, 1H), 7.17 (d, J = 7.17 Hz, 2H), 7.64 (d, J = 1.11 Hz, 1H), 8.72 (t, J = 5.95 Hz, 1H), 12.43 (s, 1H). ^{13}C (DMSO- d_6): 41.5, 55.1, 91.9, 112.3, 113.7, 116.5, 127.9, 128.6, 129.1, 131.3, 158.3, 159.2. HR-ESI-MS: (-ve): 254.09353 (M-H, $C_{14}H_{12}N_3O_2^-$, calc'd: 254.09359)

General procedure for tetrazole formation:

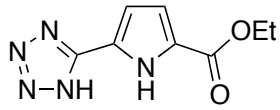

Ethyl-5-(5'-tetrazolyl)-1*H*-pyrrole-2-carboxylate (4.8). Ethyl 5-cyano-1*H*-pyrrole-2-carboxylate **4.7** (25 mg, 0.15 mmol), NaN_3 (19.2 mg, 3.2 mmol), NH_4Cl (17.1 mg, 3.2 mmol) and anhydrous DMF (1 ml) were added to a microwave vial. The vessel was purged with argon, sealed, vortexed at maximum speed for 1 min and placed in a microwave reactor at 110°C for 1 h. The mixture was transferred to a separatory funnel with 30 ml of saturated $NaHCO_3$, the aqueous layer washed with 30 ml EtOAc and subsequently acidified to pH<1 with conc. HCl. The aqueous layer was then extracted with EtOAc (3 × 20 ml) and the combined organic extracts dried ($MgSO_4$), filtered and concentrated. The crude brown solid was triturated in $CHCl_3$ and the insolubles filtered and air-dried yielding 28 mg (90%) of **4.8** as a pale brown solid. mp: 220 °C (dec.); IR(KBr, thin film): 3279m, 2993w, 2981w, 1722s, 1611w, 1475w, 1290m, 1503m, 1763m; ^{1}H NMR ($CDCl_3$, 300 MHz): δ 1.39 (t, 3H, J = 7.11Hz), 4.36 (q, 2H, J = 7.11 Hz), 6.86 (d, 1H, J = 4.05 Hz), 6.98 (d, 1H, J = 4.11 Hz); ^{13}C NMR (MeOD, 90 MHz): δ 14.7, 61.8, 113.0, 117.2, 121.9, 127.7, 151.4, 162.0; HR-ESI-MS: 208.08278 (MH^+, $C_8H_9N_5O_2H^+$; calc. 208.08287).

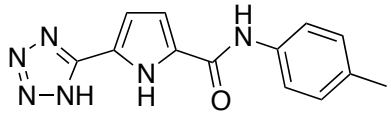

Compound 4.10. The general procedure for tetrazole formation was applied to compound **4.16**. mp: 190 °C (dec); IR(KBr, thin film): 3180s, br, 1654s, 1625s, 1602s, 1535s, 1449m, 1332m, 815m; ^{1}H NMR (DMSO-d_6, 300 MHz): δ 2.28 (s, 3H), 7.15 (d, J = 8.40 Hz, 2H), 7.50-7.79 (m, 4H), 10.00 (s, 1H), 12.30 (s, 1H); ^{13}C NMR (DMSO-d_6), 90 MHz): δ 20.5, 108.2, 109.6, 120.0, 122.6, 128.1, 129.1, 132.3, 136.5, 151.1, 158.4; HR-ESI-MS: 291.09652 (MNa^+, $C_{13}H_{12}N_6ONa^+$; calc. 291.09651).

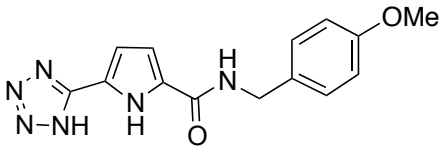

Compound 4.11. The general procedure for tetrazole formation was applied to compound **4.14**. mp: 235 °C (dec); IR(KBr, thin film): 3291s, br, 2932w, 1615s, 1514s, 1568m, 1249m; ^{1}H NMR (MeOD, 300 MHz): δ 3.78 (s, 3H), 4.49 (s, 2H), 6.83-6.98 (m, 4H), 7.28 (m, 2H); ^{13}C NMR ($CDCl_3$, 90 MHz): δ 43.5, 66.7, 102.9, 112.9, 113.2, 114.9, 120.4, 129.9, 131.0, 132.0, 160.5, 162.4; HR-ESI-MS: 321.10692 (MNa^+, $C_{14}H_{14}N_6O_2Na^+$; calc. 321.10701).

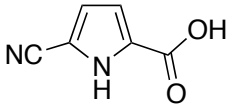

5-carboxy-1*H*-pyrrole-2-carbonitrile (4.15). To a mixture of Methyl-5-cyano-1*H*-pyrrole-2-carboxylate **(4.13)** (50 mg, 0.4 mmol) in H_2O/EtOH (1 ml/2ml) was added LiOH (47.9 mg, 2 mmol). The mixture was heated at reflux with stirring for 2 h then cooled to room temperature. 10 ml of EtOAc was added and the organic layer washed with 1 M HCl (3 × 10 ml). The organic layer was dried ($MgSO_4$), filtered and concentrated leaving pure **4.15** in quantitative yield. mp: 185°C (dec); IR(KBr, thin film): 3239s, br, 3131s, 2920m, 2236s, 1674s, 1454m, 1121s; ^{1}H NMR (DMSO-d_6, 300 MHz): δ 7.11 (s, 1H), 7.77 (s, 1H), 12.67 (s, 1H); ^{13}C NMR (DMSO-d_6, 90 MHz): δ 93.7, 115.5, 117.3, 125.2, 129.7, 161.5; HR-ESI-MS: 135.02021 ($M\text{-}H^-$, $C_6H_3N_2O_2^-$; calc. 135.01945).

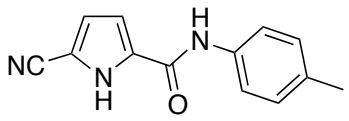

5-cyano-*N*-(*p*-tolyl)-1*H*-pyrrole-2-carboxamide (4.16). 5-carboxy-1*H*-pyrrole-2-carbonitrile (4.15) (40 mg, 0.29 mmol), EDC•HCl (1-Ethyl-3-(3-dimethylaminopropyl)carbodiimide·HCl) (90 mg, 0.58 mmol) HOBT (Hydroxybenzotriazole) (60 mg, 0.44 mmol) and *p*-toluidine (38 mg, 0.35 mmol) were dissolved in anhydrous DMF (5 ml) and stirred at room temperature for 18 h. Ethyl acetate (15 ml) was added and the organic phase washed with 1m HCl (3 × 10 ml). The organic layers were combined, dried ($MgSO_4$) and concentrated. The product was purified (SiO_2, 2:1 EtOAc:Hex) yielding 58 mg (89%) of **4.16** as a brown solid. mp: 185 (dec); IR(KBr, thin film): 3239s, br, 3131s, 2920m, 2236s, 1674s, 1454m, 1121s; ^{1}H NMR (Acetone-d_6, 300 MHz): δ 2.29 (s, 3H), 7.15 (m, 2H), 7.30 (m, 2H), 7.62 (m, 2H), 7.72 (m, 2H), 9.34 (s, 1H), 11.64 (s, 1H); ^{13}C NMR (Acetone-d_6, 920 MHz): δ 20.0, 93.9, 112.5, 115.5, 120.1, 128.4, 129.0, 129.2, 136.4, 157.7; HR-ESI-MS: 226.09748 (MH^+, $C_{13}H_{11}N_3OH^+$; calc. 226.09748).

Chapter 5. Concluding Remarks

This thesis has made use of the common drug heterocycle tetrazole as an anion-binding element in a variety of structural contexts and studied how anion-binding ability is influenced by conformational preferences and electronic effects.

Prior to this research the number of anion-binding functional groups was limited and I attempted to expand this small group by introducing the tetrazole as a potent, highly acidic hydrogen bond donor on a variety of supramolecular scaffolds, and study its interaction with a number of biologically relevant anions. In chapter 1 I outlined the aforementioned group of anion-binding elements and the wide complexity of ways researchers have used them in exotic constructs in order to create better anion binders as well as functional hosts which are capable of anion extraction from aqueous media, anion sensing and transmembrane transport.

I have successfully appended the tetrazole moiety to a calix[4]arene scaffold, attached it directly to the common anion binding agent pyrrole, a feat that resulted in compound **3.2**, one of the most potent bidentate anion receptors which utilize only hydrogen bonds as binding elements known (Chapter 3). I then further elaborated this new pyrrolyl-tetrazole binding motif by affixing to it another common element in the amide. Studies of this new construct led to the conclusion that the amide N-H appeared to be a spectator in anion recognition within this particular structural context and binding strength was enhanced by the electron withdrawing nature of the adjacent carbonyl rather than the extra hydrogen bond donor. Overall, during the course of these studies several important lessons were learned about the tetrazole and its role in anion binding.

5.1 Tetrazoles on calix[4]arene

The first studies I conducted on the tetrazole with respect to anion binding involved affixing it to the common supramolecular scaffold calix[4]arene (chapter 2). The calix[4]arene platform is attractive as on its upper rim, it contains four possible sites available for functionalization and a well defined cavity size which would presumably provide an element of selectivity toward a guest of similar size. As a consequence,

compound **2.9** and **2.10** were synthesized and their affinity toward various anions studied in acetonitrile-d_3.

These studies revealed an unexpected result in that despite four highly acidic, strong hydrogen bond donating tetrazoles were present in the host, anion binding was not especially strong (Chapter 2, Table 2.1). This prompted me to probe the reasons for this strange result. Through DFT calculations and database mining, I discovered that in order for the tetrazoles, directly bonded to the calix[4]arene platform, to engage a guest within the central cavity of the host scaffold they must be in an orthogonal orientation with respect to the phenyl groups to which they were attached. This conformation was found to be the most energetically disfavoured as conjugation between the two groups needed to be broken to achieve it, and in order to reach a more energetically stable state the tetrazole prefers co-planarity when directly bonded to an aromatic species.

This finding accentuates the importance of considering conformational preference with respect to binding elements when designing new hosts for anions and other species. With this in mind, it is conceivable that installation of a spacer between the tetrazole and the parent calix[4]arene would likely enhance binding strength significantly. A methylene group separating the binding element from the scaffold would allow for an extra degree of rotational freedom allowing the tetrazole to more easily engage the guest with little or no energetic penalty.

5.2 Pyrrolyl-tetrazole hybrids

The findings outlined in chapter 2 prompted the idea to construct hybrids where pyrroles are directly bonded to tetrazoles as this motif would satisfy the energetic preference of the latter to maintain co-planarity and thus conjugation with its partner. The scope of diversity in which pyrroles have been employed in anion binding compounds has already been demonstrated in Chapter 1. The macrocycles porphyrins,[32,104,111,159] sapphyrins,[40,160] and calixpyrroles[35,56,161,162] are all powerful and at times functional anion receptors. Another diverse class of pyrrole based anion receptors are amidopyrroles[6,35,146,149] such as **3.4** and **3.5**. As seen in figure 3.1 (Chapter 3), these compounds show less than impressive binding strength with chloride.

Our hypothesis based on the findings in chapter 2 was that replacement of the amide in these types of constructs with a tetrazole would significantly increase binding ability. We then set out to synthesize a simple bidentate pyrrolyl-tetrazole hybrid (**3.2**) in this proof of concept study, along with the analogous bipyrrole **3.6.** **3.2** was found to have affinity for chloride two orders of magnitude greater than **3.4** and **3.5** and one order of magnitude greater than **3.6** and was among the strongest bidentate chloride binders to date. One drawback of tetrazole-containing hosts is that their binding is limited to less basic anions. When complexed with the more basic benzoate anion, the data could not be fit to any conventional binding isotherm and Job plot data could not be fit to any clear binding stoichiometry. We postulated that a proton transfer event between the anion and tetrazole was occurring with addition of excess guest, and bipyrrole **3.6** did not exhibit this behavior (Table 3.1).

To extend this study, we constructed **3.11** containing two tetrazoles appended to a central pyrrole. Binding studies revealed a preference for chloride, with binding strength of ca. 20,000 M^{-1} in contrast to diamidopyrrole **1.15** which showed an affinity of 190 M^{-1}. **1.15** however did show stable binding with benzoate while the aforementioned proton transfer event was observed when benzoate was introduced into a solution of **3.11**.

These studies successfully displayed the potency of pyrroly-tetrazoles and their ability to outperform amidopyrroles when binding less basic anions. The *bis*(tetrazolyl) pyrrole, while a potent anion binder leaves no room for further derivatization. Affixing amides to this new pyrrolyl-tetrazole motif would circumvent this issue and provide a novel class of anion binders.

5.3 The pyrrolyl-tetrazole binding motif affixed with carbonyl compounds

The potency of anion binding, especially chloride, of *bis*(tetrazolyl) pyrrole **3.11** has been demonstrated in chapter 3, however the potential for further synthetic diversification ends with the installation of the second tetrazole. I therefore envisaged that since amidopyrroles are so prevalent in the literature (see refs. 2 and 6) it would be logical to attempt to append this new pyrrolyl-tetrazole binding motif with amides where once the second tetrazole lay. Synthesis was carried out and compounds **4.10** and **4.11**

were constructed. *En route* to these hosts an intermediate ester-functionalized pyrrolyl-tetrazole (**4.8**) was isolated which was used as a control compound.

The initial synthetic plan was somewhat lengthy and as the studies continued I discovered a much more concise and higher yielding route to these hosts allowing for the build up of more material, amounts suitable for ^{1}H NMR binding studies (Schemes 4.2 and 4.3). These were performed in acetonitrile-d_3 and the results were unexpected. Not only was the strength binding with halides similar between both amide-functionalized hosts **4.10** and **4.11** but also with the ester-functionlized host **4.8**. Also, it was observed in the proton NMR traces that the amide N-H proton signals shifted very little compared to those of the pyrroles on each amide-functionalized host. This led us to believe that in the case of spherical guests the amide N-H does not engage the guest with great strength and is for all intents and purposes merely a spectator in the complexation event. In contrast, both amide-functionalized hosts **4.10** and **4.11** showed significantly stronger binding with oxyanions than **4.8** suggesting that the N-H protons in **4.10** and **4.11** do play a role in binding events with various geometries of oxyanions.

5.4 Other contemporary developments in anion recognition

While the principal weak interaction in the hosts employed in this thesis work is the hydrogen bond (HB), and is generally the most widely utilized in anion binding host design, other weak interactions have also been exploited in anion receptor construction. Halogen bonding (XB), first observed in the 19th century had largely been ignored until relatively recently.[156] This phenomenon is quite similar to hydrogen bonding with the exception that instead of the electron poor proton being the binding element for an electron rich donor (ie: chloride), halogen bonding involves an electron poor halogen, a Lewis acid, (ie: iodide, bromide) accepting electron density from an electron rich donor. Rigorous computational studies reveal that less electronegative atoms are more likely to halogen bond as the electrons about the nucleus are less tightly bound and therefore a region of partial positive charge can build up on the periphery when attached to a highly electronegative atom.[157] It is for this reason that systems such as [N···X···N] where X = iodide or bromide, or "softer" anions have been investigated much more thoroughly than where X = chloride or fluoride.[158] For some time the system in which X = fluoride was

thought not to exist.[157] The term "soft" in this case refers to anions with larger, more diffuse electron clouds making them more easily polarizable rather than "hard" anions which are smaller and thus have more tightly held electron orbits and are less polarizable.

In contrast, hydrogen bonds are strongest with "harder" anions, or electron rich neutral species. Protons attached to highly electronegative species often have a strong partial positive charge and form asymmetric complexes of the form [N···H—N] ⇌ [N—H···N] and incorporation of both types of interactions in new constructs, while differing in selectivity, provides the potential for use in a wide variety of applications.[158]

Anion-pi interactions, has also received attention recently. Contrary to the ubiquitous cation-pi interaction, anion-pi interactions are much weaker and harder to access.[159] While in the beginning studies of this interaction were for proof of concept (Chapter 1), this interaction has increasingly been utilized in the design of anion receptors. Matile, Schalley and coworkers recently constructed a series of electron deficient naphthalendiimide (NDI) compounds. They found that some of these effectively transported chloride across egg yolk phosphatidylcholine vesicles, monitored by lucigenin quenching, and the most pi-acidic NDIs, namely those decorated with electron withdrawing nitrile groups were most potent. As mentioned in chapter 1, most transmembrane anion transporters utilize hydrogen bonding as the main weak interaction between host and guest, while in the above example only anion-pi interactions exist. This effectively demonstrates the functionality anion-pi interactions can impart even though in this particular example the interaction was too weak to detect by NMR and ITC techniques.[159]

5.5 Concluding remarks: challenges of working on biological anions as targets

In order for any tetrazole-containing host to be an effective extractant of anionic species from aqueous media, the media must be sufficiently acidic (pH ~4) so as not to deprotonate the binding element. Further, any acid containing an anionic component which the tetrazole-containing host can bind would clearly interfere with the extraction process. As for anything in biological systems, namely transmembrane chloride

transport, the tetrazole would certainly be deprotonated at physiological pH (~7.4) which would clearly impede any sort of anion binding. The potential for any sort of therapeutic chloride transporter seems weak, however this new motif is a potent recognition element and the studies outlined in this thesis may pave the way for further research and development of functional anion receptors.

Bibliography

1. Steed, J. W.; Atwood J. L. *Supramolecular Chemistry*; Wiley, 2013.

2. Bianchi, A.; Bowman-James, K.; García-España, E. *Supramolecular chemistry of anions*; Wiley-VCH, 1997.

3. Gribkoff, V. K.; Champigny, G.; Barbry, P.; Dworetzky, S. I.; Meanwell, N. A.; Lazdunski, M. *J. Biol. Chem.* **1994**, *269*, 10983-10986.

4. Günther, W.; Lüchow, A.; Cluzeaud, F.; Vandewalle, A.; Jentsch, T. J. *Proc. Natl. Acad. Sci.* **1998**, *95*, 8075-8080.

5. Simon, D. B.; Bindra, R. S.; Mansfield, T. A.; Nelson-Williams, C.; Mendonca, E.; Stone, R.; Schurman, S.; Nayir, A.; Alpay, H.; Bakkaloglu, A.; Rodriguez-Soriano, J.; Morales, J. M.; Sanjad, S. A.; Taylor, C. M.; Pilz, D.; Brem, A.; Trachtman, H.; Griswold, W.; Richard, G. A.; John, E.; Lifton, R. P. *Nat. Genet.* **1997**, *17*, 171-178.

6. Correll, D. L. *J. Environ. Qual.* **1998**, *27*, 261-266.

7. Gale, P. A. *Chem. Commun.* **2005**, 3761-3772.

8. Richards, P.; Tucker, W. D.; Srivastava, S. C. *Int. J. Appl. Radiat. Is*. **1982**, *33*, 793-799.

9. Beer, P. D.; Gale, P. A. *Angew. Chem. Int. Ed.* **2001**, *40*, 486-516.

10. Gale, P. A.; Quesada, R. *Coord. Chem. Rev.* **2006**, *250*, 3219-3244.

11. Lavigne, J. J.; Anslyn, E. V. *Angew. Chem. Int. Ed.* **2001**, *40*, 3118-3130.

12. H. Williams, D.; S. Westwell, M. *Chem. Soc. Rev.* **1998**, *27*, 57-64.

13. Volkert, L. G.; Conrad, M. *J. Theor. Biol.* **1998**, *193*, 287-306.

14. Karshikoff, A. *Non-covalent interactions in proteins*; Imperial College Press, 2006.

15. Hobza, P.; Müller-Dethlefs, K.; Chemistry, R. S. O. *Non-covalent Interactions: Theory and Experiment*; Royal Society of Chemistry, 2010.

16. *Jaypee's Review of Med. Biochemistry*; Jaypee Brothers Medical Publishers, 2005.

17. Ringer, A. L.; Technology, G. I. o. *From Small to Big: Understanding Noncovalent Interactions in Chemical Systems from Quantum Mechanical Models*; Georgia Institute of Technology, 2009.

18. Mati, I. K.; Cockroft, S. L. *Chem. Soc. Rev.* **2010**, *39*, 4195-4205.

19. Perrin, C. L.; Nielson, J. B. *Annu. Rev. Phys. Chem.* **1997**, *48*, 511-544.

20. Xu, D.; Tsai, C. J.; Nussinov, R. *Protein Eng.* **1997**, *10*, 999-1012.

21. Wahl, M. C.; Sundaralingam, M. *Trends Biochem. Sci.* **1997**, *22*, 97-102.

22. Resnati, G. *ChemPhysChem* **2002**, *3*, 225-226.

23. Gao, J.; Bosco, D. A.; Powers, E. T.; Kelly, J. W. *Nat. Struct. Mol. Biol.* **2009**, *16*, 684-690.

24. Alkorta, I.; Elguero, J. *Chem. Soc. Rev.* **1998**, *27*, 163-170.

25. Dutzler, R.; Campbell, E. B.; Cadene, M.; Chait, B. T.; MacKinnon, R. *Nature* **2002**, *415*, 287-294.

26. Thiyagarajan, N.; Smith, B. D.; Raines, R. T.; Acharya, K. R. *FEBS J.* **2011**, *278*, 541-549.

27. Chmielewski, M.; Jurczak, J. *Tetrahedron Lett.* **2004**, *45*, 6007-6010.

28. Szumna, A.; Jurczak, J. *Eur. J. Org. Chem.* **2001**, *2001*, 4031-4039.

29. Valiyaveettil, S.; Engbersen, J. F. J.; Verboom, W.; Reinhoudt, D. N. *Angew. Chem. Int. Ed.* **1993**, *32*, 900-901.

30. Hettche, F.; Hoffmann, R. W. *New J. Chem.* **2003**, *27*, 172-177.

31. Davis, A. P.; Perry, J. J.; Williams, R. P. *J. Am. Chem. Soc.* **1997**, *119*, 1793-1794.

32. Dudič, M.; Lhoták, P.; Stibor, I.; Lang, K.; Prošková, P. *Org. Lett.* **2003**, *5*, 149-152.

33. Sasaki, S.; Mizuno, M.; Naemura, K.; Tobe, Y. *J. Org. Chem.* **2000**, *65*, 275-283.

34. Bordwell, F. G. *Acc. Chem. Res.* **1988**, *21*, 456-463.

35. Gale, P. A.; Sessler, J. L.; Kral, V. *Chem. Commun.* **1998**, 1-8.

36. Sato, W.; Miyaji, H.; Sessler, J. L. *Tetrahedron Lett.* **2000**, *41*, 6731-6736.

37. Li, R.; Evans, L. S.; Larsen, D. S.; Gale, P. A.; Brooker, S. *New J. Chem.* **2004**, *28*, 1340-1343.

38. Huggins, M. T.; Butler, T.; Barber, P.; Hunt, J. *Chem. Commun.* **2009**, 5254-5256.

39. Evans, L. S.; Gale, P. A.; Light, M. E.; Quesada, R. *Chem. Commun.* **2006**, 965-967.

40. Shionoya, M.; Furuta, H.; Lynch, V.; Harriman, A.; Sessler, J. L. *J. Am. Chem. Soc.* **1992**, *114*, 5714-5722.

41. Müller, G.; Riede, J.; Schmidtchen, F. P. *Angew. Chem. Int. Ed.* **1988**, *27*, 1516-1518.

42. Wallace, K. J.; Daari, R.; Belcher, W. J.; Abouderbala, L. O.; Boutelle, M. G.; Steed, J. W. *J. Organomet. Chem.* **2003**, *666*, 63-74.

43. Gamez, P.; Mooibroek, T. J.; Teat, S. J.; Reedijk, J. *Acc. Chem. Res.* **2007**, *40*, 435-444.

44. Alkorta, I.; Rozas, I.; Elguero, J. *J. Org. Chem.* **1997**, *62*, 4687-4691.

45. Berryman, O. B.; Hof, F.; Hynes, M. J.; Johnson, D. W. *Chem. Commun.* **2006**, 506-508.

46. Kato, R.; Nishizawa, S.; Hayashita, T.; Teramae, N. *Tetrahedron Lett.* **2001**, *42*, 5053-5056.

47. Miyaji, H.; Sato, W.; Sessler, J. L.; Lynch, V. M. *Tetrahedron Lett.* **2000**, *41*, 1369-1373.

48. Liu, S.; Shi, Z.; Xu, W.; Yang, H.; Xi, N.; Liu, X.; Zhao, Q.; Huang, W. *Dyes Pigm.* **2014**, *103*, 145-153.

49. Lee, D. H.; Lee, H. Y.; Hong, J.-I. *Tetrahedron Lett.* **2002**, *43*, 7273-7276.

50. Cho, E. J.; Moon, J. W.; Ko, S. W.; Lee, J. Y.; Kim, S. K.; Yoon, J.; Nam, K. C. *J. Am. Chem. Soc.* **2003**, *125*, 12376-12377.

51. Kondo, S..; Nagamine, M.; Yano, Y. *Tetrahedron Lett.* **2003**, *44*, 8801-8804.

52. Gunnlaugsson, T.; Kruger, P. E.; Lee, T. C.; Parkesh, R.; Pfeffer, F. M.; Hussey, G. M. *Tetrahedron Lett.* **2003**, *44*, 6575-6578.

53. Gunnlaugsson, T.; Kruger, P. E.; Jensen, P.; Pfeffer, F. M.; Hussey, G. M. *Tetrahedron Lett.* **2003**, *44*, 8909-8913.

54. Jiménez, D.; Martínez-Máñez, R.; Sancenón, F.; Soto, J. *Tetrahedron Lett.* **2002**, *43*, 2823-2825.

55. Miyaji, H.; Sessler, J. L. *Angew. Chem. Int. Ed.* **2001**, *40*, 154-157.

56. Miyaji, H.; Sato, W.; Sessler, J. L. *Angew. Chem. Int. Ed.* **2000**, *39*, 1777-1780.

57. Martínez-Máñez, R.; Sancenón, F. *Chem. Rev.* **2003**, *103*, 4419-4476.

58. Dawson, W. R.; Windsor, M. W. *J. Phys. Chem.* **1968**, *72*, 3251-3260.

59. Miyaji, H.; Anzenbacher Jr, P.; L. Sessler, J.; R. Bleasdale, E.; A. Gale, P. *Chem. Commun.* **1999**, 1723-1724.

60. Zyryanov, G. V.; Palacios, M. A.; Anzenbacher, P. *Angew. Chem. Int. Ed.* **2007**, *46*, 7849-7852.

61. Sorrell, T. N. *Organic Chemistry*; University Science Books, 2006.

62. *Nuclear Wastes:Technologies for Separations and Transmutation*; The National Academies Press, 1996.

63. Eller, L. R.; Stępień, M.; Fowler, C. J.; Lee, J. T.; Sessler, J. L.; Moyer, B. A. *J. Am. Chem. Soc.* **2007**, *129*, 11020-11021.

64. Kunz, W.; Henle, J.; Ninham, B. W. *Curr. Opin. Colloid Interface Sci.* **2004**, *9*, 19-37.

65. Levitskaia, T. G.; Marquez, M.; Sessler, J. L.; Shriver, J. A.; Vercouter, T.; Moyer, B. A. *Chem. Commun.* **2003**, 17, 2248-2249.

66. Judd, L. W.; Davis, A. P. *Chem. Commun.* **2010**, *46*, 2227-2229.

67. Fürstner, A. *Angew. Chem. Int. Ed.* **2003**, *42*, 3582-3603.

68. Sessler, J. L.; Eller, L. R.; Cho, W.-S.; Nicolaou, S.; Aguilar, A.; Lee, J. T.; Lynch, V. M.; Magda, D. J. *Angew. Chem. Int. Ed.* **2005**, *117*, 6143-6146.

69. Patra, S.; Maity, D.; Gunupuru, R.; Agnihotri, P.; Paul, P. *J. Chem. Sci.* **2012**, *124*, 1287-1299.

70. Daze, K. D.; Pinter, T.; Beshara, C. S.; Ibraheem, A.; Minaker, S. A.; Ma, M. C. F.; Courtemanche, R. J. M.; Campbell, R. E.; Hof, F. *Chem. Sci.* **2012**, *3*, 2695-2699.

71. Métay, E.; Duclos, M. C.; Pellet-Rostaing, S.; Lemaire, M.; Schulz, J.; Kannappan, R.; Bucher, C.; Saint-Aman, E.; Chaix, C. *Supramol. Chem.* **2009**, *21*, 68-80.

72. Wermuth, C. G. *The Practice of Medicinal Chemistry*; Elsevier Science, 2011.

73. Brown, N.; Mannhold, R.; Kubinyi, H.; Folkers, G. *Bioisosteres in Medicinal Chemistry*; Wiley, 2012.

74. Herr, R. J. *Bioorg. Med. Chem.* **2002**, *10*, 3379-3393.

75. Patani, G. A.; LaVoie, E. J. *Chem. Rev.* **1996**, *96*, 3147-3176.

76. Olesen, P. H. *Curr. Opin. Drug. Disc.* **2001**, *4*, 471-478.

77. Nattel, S. *Nat. Clin. Pract. Cardiovasc. Med.* **2005**, *2*, 332-333.

78. Skulnick, H. I.; Johnson, P. D.; Aristoff, P. A.; Morris, J. K.; Lovasz, K. D.; Howe, W. J.; Watenpaugh, K. D.; Janakiraman, M. N.; Anderson, D. J.; Reischer, R. J.; Schwartz, T. M.; Banitt, L. S.; Tomich, P. K.; Lynn, J. C.; Horng, M.-M.; Chong, K.-T.; Hinshaw, R. R.; Dolak, L. A.; Seest, E. P.; Schwende, F. J.; Rush, B. D.; Howard, G. M.; Toth, L. N.; Wilkinson, K. R.; Kakuk, T. J.; Johnson, C. W.; Cole, S. L.; Zaya, R. M.; Zipp, G. L.; Possert, P. L.; Dalga, R. J.; Zhong, W.-Z.; Williams, M. G.; Romines, K. R. *J. Med. Chem.* **1997**, *40*, 1149-1164.

79. Reddy, N. S.; Mallireddigari, M. R.; Cosenza, S.; Gumireddy, K.; Bell, S. C.; Reddy, E. P.; Reddy, M. V. R. *Bioorg. Med. Chem. Lett.* **2004**, *14*, 4093-4097.

80. Lobb, K. L.; Hipskind, P. A.; Aikins, J. A.; Alvarez, E.; Cheung, Y.-Y.; Considine, E. L.; De Dios, A.; Durst, G. L.; Ferritto, R.; Grossman, C. S.; Giera, D. D.; Hollister, B. A.; Huang, Z.; Iversen, P. W.; Law, K. L.; Li, T.; Lin, H.-S.; Lopez, B.; Lopez, J. E.; Cabrejas, L. M. M.; McCann, D. J.; Molero, V.; Reilly, J. E.; Richett, M. E.; Shih, C.; Teicher, B.; Wikel, J. H.; White, W. T.; Mader, M. M. *J. Med. Chem.* **2004**, *47*, 5367-5380.

81. Stansfield, I.; Pompei, M.; Conte, I.; Ercolani, C.; Migliaccio, G.; Jairaj, M.; Giuliano, C.; Rowley, M.; Narjes, F. *Bioorg. Med. Chem. Lett.* **2007**, *17*, 5143-5149.

82. Hu, X.; Sun, J.; Wang, H.-G.; Manetsch, R. *J. Am. Chem. Soc.* **2008**, *130*, 13820-13821.

83. Borst, P.; Zelcer, N.; van de Wetering, K. *Cancer Lett.* **2006**, *234*, 51-61.

84. Morehouse, N. F.; Baron, R. R. *Exp. Parasitol.* **1970**, *28*, 25-29.

85. Petros, A. M.; Dinges, J.; Augeri, D. J.; Baumeister, S. A.; Betebenner, D. A.; Bures, M. G.; Elmore, S. W.; Hajduk, P. J.; Joseph, M. K.; Landis, S. K.; Nettesheim, D. G.; Rosenberg, S. H.; Shen, W.; Thomas, S.; Wang, X.; Zanze, I.; Zhang, H.; Fesik, S. W. *J. Med. Chem.* **2005**, *49*, 656-663.

86. McKie, A. H.; Friedland, S.; Hof, F. *Org. Lett.* **2008**, *10*, 4653-4655.

87. Watson, A. T. H., C. H. *Org. Synth.* **1998**, *68*, 234.

88. Casnati, A.; Pirondini, L.; Pelizzi, N.; Ungaro, R. *Supramol. Chem.* **2000**, *12*, 53-65.

89. Hioki, H.; Nakaoka, R.; Maruyama, A.; Kodama, M. *J.Chem. Soc. Perk. T. 1* **2001**, 3265-3268.

90. Demko, Z. P.; Sharpless, K. B. *J. Org. Chem.* **2001**, *66*, 7945-7950.

91. Morzherin, Y.; Rudkevich, D. M.; Verboom, W.; Reinhoudt, D. N. *J. Org. Chem.* **1993**, *58*, 7602-7605.

92. Fish, P. V.; Allan, G. A.; Bailey, S.; Blagg, J.; Butt, R.; Collis, M. G.; Greiling, D.; James, K.; Kendall, J.; McElroy, A.; McCleverty, D.; Reed, C.; Webster, R.; Whitlock, G. A. *J. Med. Chem.* **2007**, *50*, 3442-3456.

93. Bunnett, J. F.; Bassett, J. Y. *J. Org. Chem.* **1962**, *27*, 3714-3715.

94. Cossu, S.; Giacomelli, G.; Conti, S.; Falorni, M. *Tetrahedron* **1994**, *50*, 5083-5090.

95. Massah, A. R.; Adibi, H.; Khodarahmi, R.; Abiri, R.; Majnooni, M. B.; Shahidi, S.; Asadi, B.; Mehrabi, M.; Zolfigol, M. A. *Bioorg. Med. Chem.* **2008**, *16*, 5465-5472.

96. Xiang, J.; Ipek, M.; Suri, V.; Tam, M.; Xing, Y.; Huang, N.; Zhang, Y.; Tobin, J.; Mansour, T. S.; McKew, J. *Bioorg. Med. Chem.* **2007**, *15*, 4396-4405.

97. Bebernitz, G. R.; Beaulieu, V.; Dale, B. A.; Deacon, R.; Duttaroy, A.; Gao, J.; Grondine, M. S.; Gupta, R. C.; Kakmak, M.; Kavana, M.; Kirman, L. C.; Liang, J.; Maniara, W. M.; Munshi, S.; Nadkarni, S. S.; Schuster, H. F.; Stams, T.; St. Denny, I.; Taslimi, P. M.; Vash, B.; Caplan, S. L. *J. Med. Chem.* **2009**, *52*, 6142-6152.

98. Job, P. *Ann. Chim. Appl.* **1928**, *9*, 113-203.

99. Creaven, B. S.; Donlon, D. F.; McGinley, J. *Coord. Chem. Rev.* **2009**, *253*, 893-962.

100. Shchipanov, V. P.; Krashina, K. I.; Skachilova, A. A. *Chem. Heterocycl. Compd.* **1973**, *9*, 1423-1426.

101. Seydel, J. K. *J. Pharm. Sci.* **1968**, *57*, 1455-1478.

102. Hof, F.; Schütz, A.; Fäh, C.; Meyer, S.; Bur, D.; Liu, J.; Goldberg, D. E.; Diederich, F. *Angew. Chem. Int. Ed.* **2006**, *45*, 2138-2141.

103. Senger, S.; Chan, C.; Convery, M. A.; Hubbard, J. A.; Shah, G. P.; Watson, N. S.; Young, R. J. *Bioorg. Med. Chem. Lett.* **2007**, *17*, 2931-2934.

104. Starnes, S. D.; Arungundram, S.; Saunders, C. H. *Tetrahedron Lett.* **2002**, *43*, 7785-7788.

105. Bondy, C. R.; Loeb, S. J. *Coord. Chem. Rev.* **2003**, *240*, 77-99.

106. Rostami, A.; Colin, A.; Li, X. Y.; Chudzinski, M. G.; Lough, A. J.; Taylor, M. S. *J. Org. Chem.* **2010**, *75*, 3983-3992.

107. Rostami, A.; Wei, C. J.; Guérin, G.; Taylor, M. S. *Angew. Chem. Int. Ed.* **2011**, *50*, 2059-2062.

108. Caltagirone, C.; Bates, G. W.; Gale, P. A.; Light, M. E. *Chem. Commun.* **2008**, 61-63.

109. Nie, L.; Li, Z.; Han, J.; Zhang, X.; Yang, R.; Liu, W.-X.; Wu, F.-Y.; Xie, J.-W.; Zhao, Y.-F.; Jiang, Y.-B. *J. Org. Chem.* **2004**, *69*, 6449-6454.

110. Anzenbacher, P.; Jursíková, K.; Lynch, V. M.; Gale, P. A.; Sessler, J. L. *J. Am. Chem. Soc.* **1999**, *121*, 11020-11021.

111. Sessler, J. L.; Camiolo, S.; Gale, P. A. *Coord. Chem. Rev.* **2003**, *240*, 17-55.

112. Camiolo, S.; Gale, P. A.; Hursthouse, M. B.; Light, M. E. *Org. Biomol. Chem.* **2003**, *1*, 741-744.

113. Sessler, J. L.; Cho, D.-G.; Lynch, V. *J. Am. Chem. Soc.* **2006**, *128*, 16518-16519.

114. Bates, G. W.; Gale, P. A.; Light, M. E. *Chem. Commun.* **2007**, 2121-2123.

115. Chmielewski, M. J.; Charon, M.; Jurczak, J. *Org. Lett.* **2004**, *6*, 3501-3504.

116. Fuentes de Arriba, A. L.; Turiel, M. G.; Simon, L.; Sanz, F.; Boyero, J. F.; Muniz, F. M.; Moran, J. R.; Alcazar, V. *Org. Biomol. Chem.* **2011**, *9*, 8321-8327.

117. Rostovtsev, V. V.; Green, L. G.; Fokin, V. V.; Sharpless, K. B. *Angew. Chem. Int. Ed.* **2002**, *41*, 2596-2599.

118. Jones, M. R.; Service, E. L.; Thompson, J. R.; Wang, M. C. P.; Kimsey, I. J.; DeToma, A. S.; Ramamoorthy, A.; Lim, M. H.; Storr, T. *Metallomics* **2012**, *4*, 910-920.

119. Juwarker, H.; Lenhardt, J. M.; Pham, D. M.; Craig, S. L. *Angew. Chem. Int. Ed.* **2008**, *47*, 3740-3743.

120. Hua, Y.; Flood, A. H. *Chem. Soc. Rev.* **2010**, *39*, 1262-1271.

121. Cantillo, D.; Gutmann, B.; Kappe, C. O. *J. Am. Chem. Soc.* **2011**, *133*, 4465-4475.

122. Demko, Z. P.; Sharpless, K. B. *Angew. Chem. Int. Ed.* **2002**, *41*, 2110-2113.

123. Pinter, T.; Jana, S.; Courtemanche, R. J. M.; Hof, F. *J. Org. Chem.* **2011**, *76*, 3733-3741.

124. Courtemanche, R. J. M.; Pinter, T.; Hof, F. *Chem. Commun.* **2011**, *47*, 12688-12690.

125. Lenda, F.; Guenoun, F.; Tazi, B.; Ben larbi, N.; Allouchi, H.; Martinez, J.; Lamaty, F. *Eur. J. Org. Chem.* **2005**, *2005*, 326-333.

126. Dohi, T.; Morimoto, K.; Maruyama, A.; Kita, Y. *Org. Lett.* **2006**, *8*, 2007-2010.

127. Wiberg, K. B.; Laidig, K. E. *J. Am. Chem. Soc.* **1987**, *109*, 5935-5943.

128. Aleman, J.; Parra, A.; Jiang, H.; Jorgensen, K. A. *Chem. Eur. J.* **2011**, *17*, 6890-6899.

129. Curiel, D.; Cowley, A.; Beer, P. D. *Chem. Commun.* **2005**, 236-238.

130. Torii, H.; Nakadai, M.; Ishihara, K.; Saito, S.; Yamamoto, H. *Angew. Chem. Int. Ed.* **2004**, *43*, 1983-1986.

131. Tominey, A.; Andrew, D.; Oliphant, L.; Rosair, G. M.; Dupre, J.; Kraft, A. *Chem. Commun.* **2006**, 2492-2494.

132. Peters, L.; Fröhlich, R.; Boyd, A. S. F.; Kraft, A. *J. Org. Chem.* **2001**, *66*, 3291-3298.

133. Amendola, V.; Fabbrizzi, L.; Mosca, L.; Schmidtchen, F.-P. *Chem. Eur. J.* **2011**, *17*, 5972–5981.

134. Amendola, V.; Boiocchi, M.; Fabbrizzi, L.; Palchetti, A. *Chem. Eur. J.* **2005**, *11*, 120-127.

135. Gale, P. A.; Caltagirone, C.; Bates, G. W.; Light, M. E. *Chem. Commun.* **2008**, 61-63.

136. Gale, P. A.; Evans, L. S.; Light, M. E.; Quesada, R. *Chem. Commun.* **2006**, 965-967.

137. Perez-Casas, C.; Yatsimirsky, A. K. *J. Org. Chem.* **2008**, *73*, 2275-2284.

138. Gale, P. A.; Camiolo, S.; Chapman, C. P.; Light, M. E.; Hursthouse, M. B. *Tetrahedron Lett.* **2001**, *42*, 5095-5097.

139. Knizhnikov, V.; Borisova, N.; Yurashevich, N.; Popova, L.; Chernyad'ev, A.; Zubreichuk, Z.; Reshetova, M. *Russian J. Org. Chem.* **2007**, *43*, 855-860-860.

140. Mazet, C.; Gade, L. H. *Chem. Eur. J.* **2002**, *8*, 4308-4318.

141. Bondi, A. *J. Phys. Chem.* **1964**, *68*, 441-451.

142. Huyskens, P. L.; Luck, W. A. P.; Zeegers-Huyskens, T., *Intermolecular forces: an introduction to modern methods and results*. Springer-Verlag: 1991.

143. Schmidtchen, F. P. *Coord. Chem. Rev.* **2006**, *250*, 2918-2928.

144. Nielsen, K. A.; Cho, W. S.; Lyskawa, J.; Levillain, E.; Lynch, V. M.; Sessler, J. L.; Jeppesen, J. O., *J. Am. Chem. Soc.* **2006,** *128* (7), 2444-2451.

145. Michalska, A.; Maksymiuk, K., On the pH Influence on Electrochemical Properties of Poly(pyrrole) and Poly(N-methylpyrrole). *Electroanalysis* **1998,** *10* (3), 177-180.

146. Pina, J.; Pinheiro, D.; Nascimento, B.; Pineiro, M.; Seixas de Melo, J. S., *Phys. Chem. Chem. Phys.* **2014,** *16* (34), 18319-18326.

147. Lin, C. H.; Yang, D. Y., *Org. Lett.* **2013,** *15* (11), 2802-2805.

148. Gale, P. A.; Lee, C.-H. *Top. Heterocycl. Chem.* **2010**, *24*, 39-73.

149. Maeda, H. *Top. Heterocycl. Chem.* **2010**, *24*, 103-144.

150. Amendola, V.; Fabbrizzi, L.; Mosca, L. *Chem. Soc. Rev.* **2010**, *39*, 3889-3915.

151. Mahnke, D. J.; McDonald, R.; Hof, F. *Chem. Commun.* **2007**, 3738-3740.

152. Tominey, A. F.; Docherty, P. H.; Rosair, G. M.; Quenardelle, R.; Kraft, A. *Org. Lett.* **2006**, *8*, 1279-1282.

153. Kraft, A.; Osterod, F.; Froehlich, R. *J. Org. Chem.* **1999**, *64*, 6425-6433.

154. Gale, P. A.; Camiolo, S.; Tizzard, G. J.; Chapman, C. P.; Light, M. E.; Coles, S. J.; Hursthouse, M. B. *J. Org. Chem.* **2001**, *66*, 7849-7853.

155. Loader, C. E.; Anderson, H. J. *Can. J. Chem.* **1981**, *59*, 2673-2683.

156. Brooks, S. J.; Gale, P. A. In *Macrocyclic Chemistry*; Springer: Netherlands, 2005, p 153-172.

157. Camiolo, S.; Gale, P. A.; Hursthouse, M. B.; Light, M. E. *Tetrahedron Lett.* **2002**, *43*, 6995-6996.

158. Bates, G. W.; Triyanti; Light, M. E.; Albrecht, M.; Gale, P. A. *J. Org. Chem.* **2007**, *72*, 8921-8927.

159. Maeda, H.; Morimoto, T.; Osuka, A.; Furuta, H. *Chem. – Asian J.* **2006**, *1*, 832-844.

160. Sessler, J. L.; Davis, J. M. *Acc. Chem. Res.* **2001**, *34*, 989-997.

161. Levitskaia, T. G.; Marquez, M.; Sessler, J. L.; Shriver, J. A.; Vercouter, T.; Moyer, B. A. *Chem. Commun.* **2003**, 2248-2249.

162. Gale, P. A.; Anzenbacher Jr, P.; Sessler, J. L. *Coord. Chem. Rev.* **2001**, *222*, 57-102.

163. Carlsson, A.-C. C.; Gräfenstein, J.; Budnjo, A.; Laurila, J. L.; Bergquist, J.; Karim, A.; Kleinmaier, R.; Brath, U.; Erdélyi, M. *J. Am. Chem. Soc.* **2012**, *134*, 5706-5715.

164. Politzer, P.; Lane, P.; Concha, M.; Ma, Y.; Murray, J. *J. Mol. Model.* **2007**, *13*, 305-311.

165. Karim, A.; Reitti, M.; Carlsson, A.-C. C.; Grafenstein, J.; Erdelyi, M. *Chem. Sci.* **2014**, *5*, 3226-3233.

166. Dawson, R. E.; Hennig, A.; Weimann, D. P.; Emery, D.; Ravikumar, V.; Montenegro, J.; Takeuchi, T.; Gabutti, S.; Mayor, M.; Mareda, J.; Schalley, C. A.; Matile, S. *Nat. Chem.* **2010**, *2*, 533-538.

Appendix

1H and 13C NMR Spectra

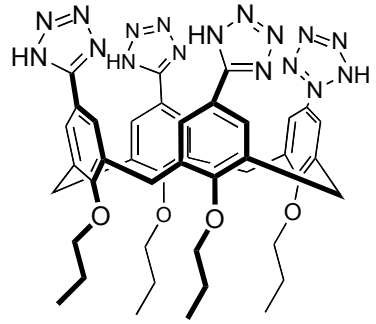

10.5 10.0 9.5 9.0 8.5 8.0 7.5 7.0 6.5 6.0 5.5 5.0 4.5 4.0 3.5 3.0 2.5 2.0 1.5 1.0 0.5 0.0 ppm
7.95
4.16
8.02
4.03
7.90
12.21

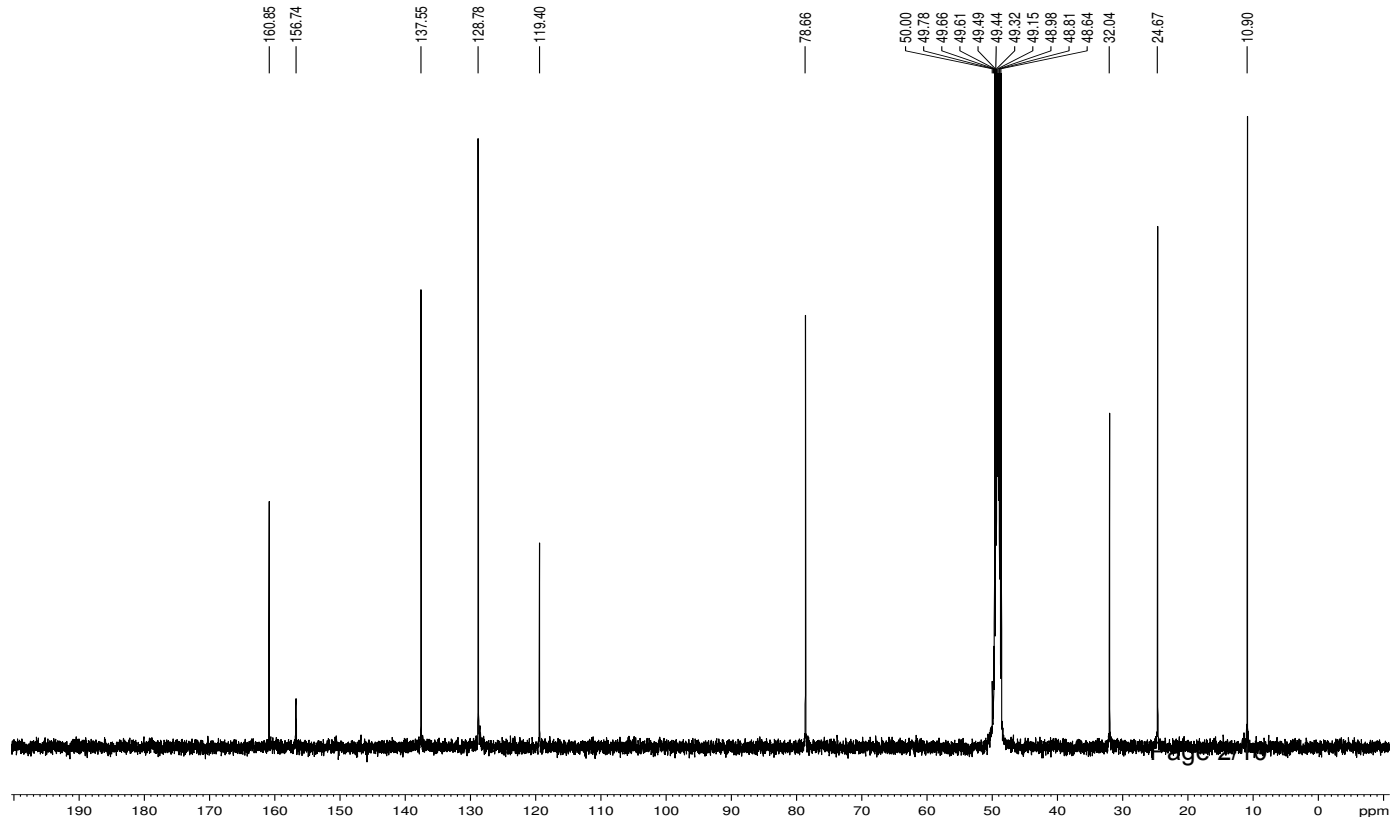
160.85
156.74
137.55
128.78
119.40
78.66
50.00
49.78
49.66
49.61
49.49
49.44
49.32
49.15
48.98
48.81
48.64
32.04
24.67
10.90
190 180 170 160 150 140 130 120 110 100 90 80 70 60 50 40 30 20 10 0 ppm

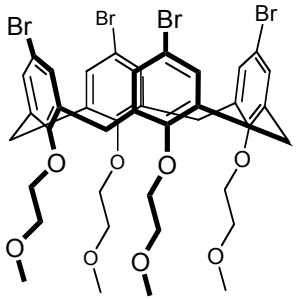
Br
Br
Br
Br
O
O
O
O
O
O
O
O

10.0
9.5
9.0
8.5
8.0
7.5
7.0
6.5
6.0
5.5
5.0
4.5
4.0
3.5
3.0
2.5
2.0
1.5
1.0
0.5
0.0
ppm
1.78
0.18
0.21
3.67
0.29
0.24
7.10
4.25
6.29
1.19
7.39
0.23
7.08
0.10


155.32
136.41
131.06
115.50
77.41
76.99
76.57
73.33
71.67
58.58
30.49

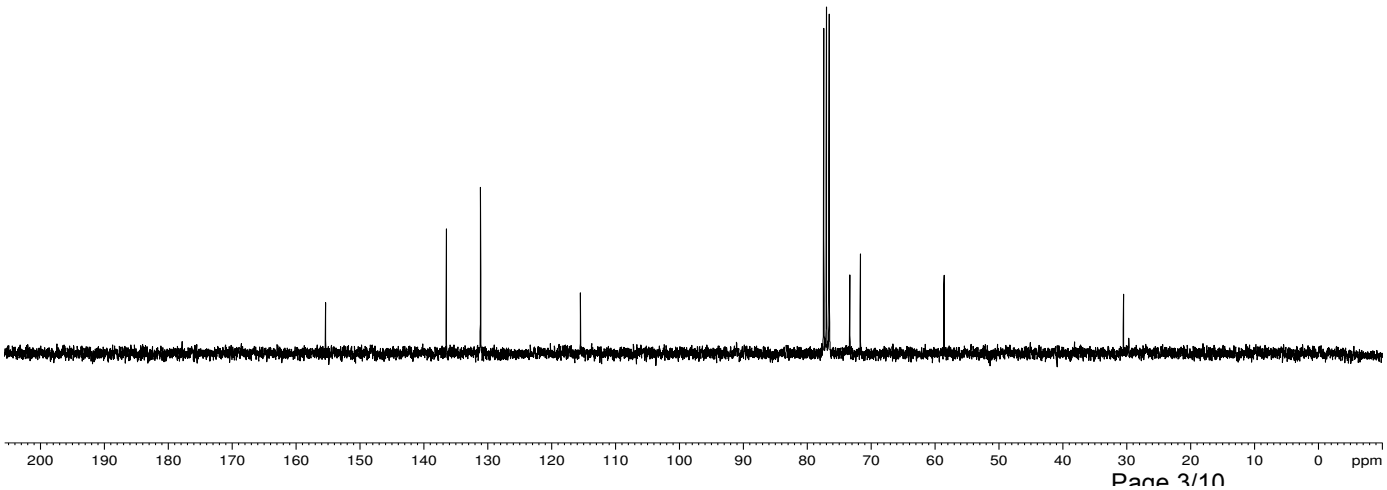
200
190
180
170
160
150
140
130
120
110
100
90
80
70
60
50
40
30
20
10
0
ppm

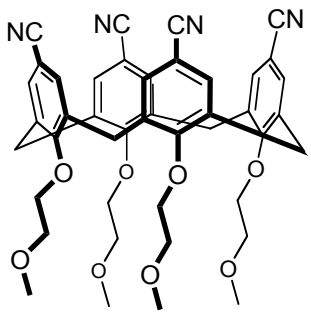
NC
NC
CN
CN
O
O
O
O
O
O
O
O

10.0
9.5
9.0
8.5
8.0
7.5
7.0
6.5
6.0
5.5
5.0
4.5
4.0
3.5
3.0
2.5
2.0
1.5
1.0
0.5
0.0
ppm
7.75
3.99
8.13
8.31
1.93
4.19

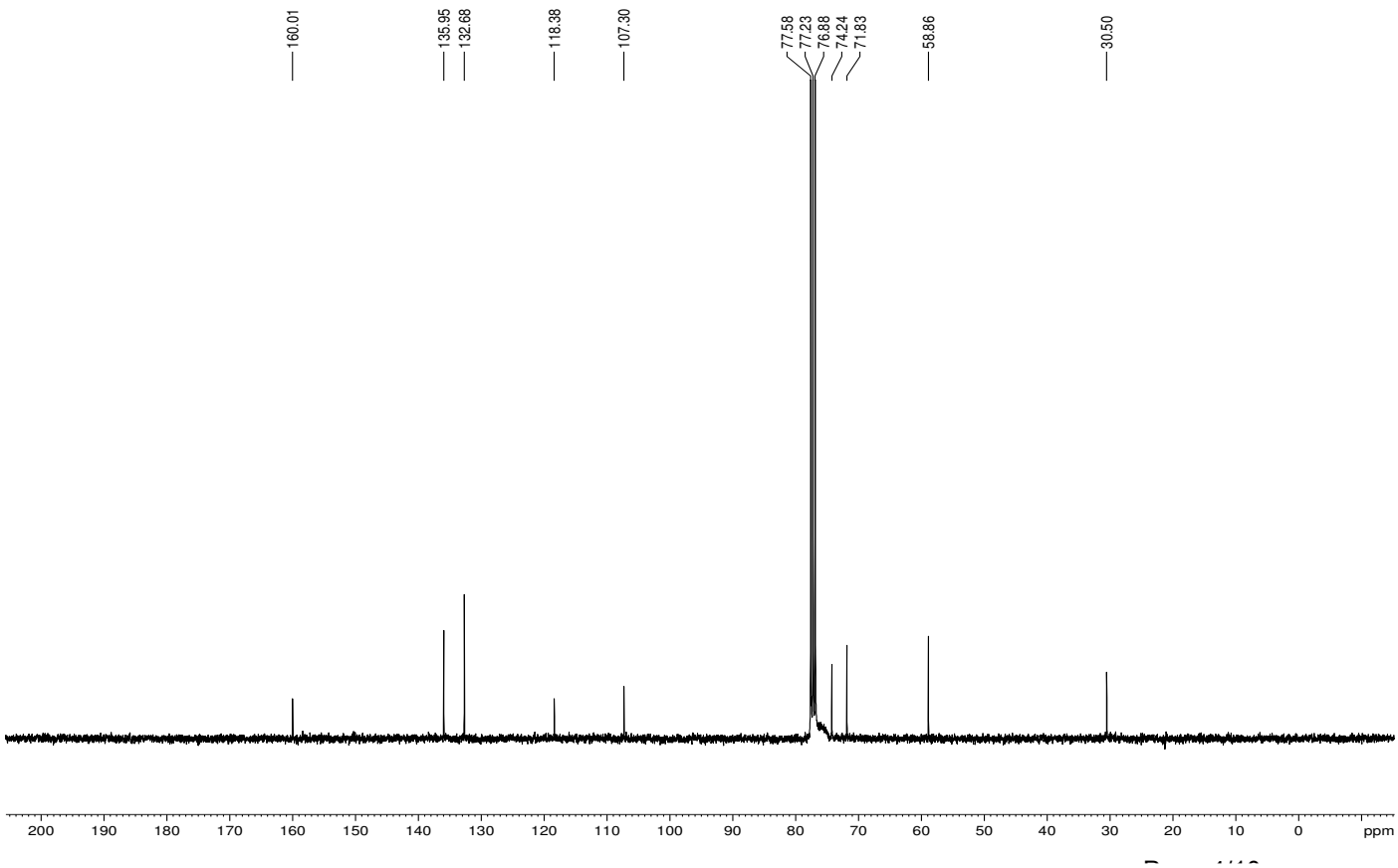
160.01
135.95
132.68
118.38
107.30
77.58
77.23
76.88
74.24
71.83
58.86
30.50
200
190
180
170
160
150
140
130
120
110
100
90
80
70
60
50
40
30
20
10
0
ppm

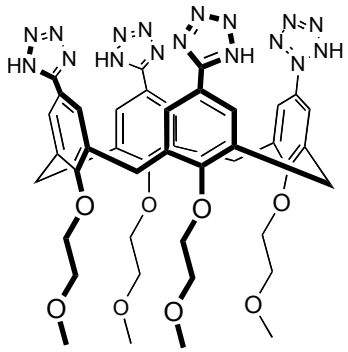

10.0
9.5
9.0
8.5
8.0
7.5
7.0
6.5
6.0
5.5
5.0
4.5
4.0
3.5
3.0
2.5
2.0
1.5
1.0
0.5
0.0
−0.5
−1.0
ppm
7.80
4.08
7.80
7.89
4.09
1.79

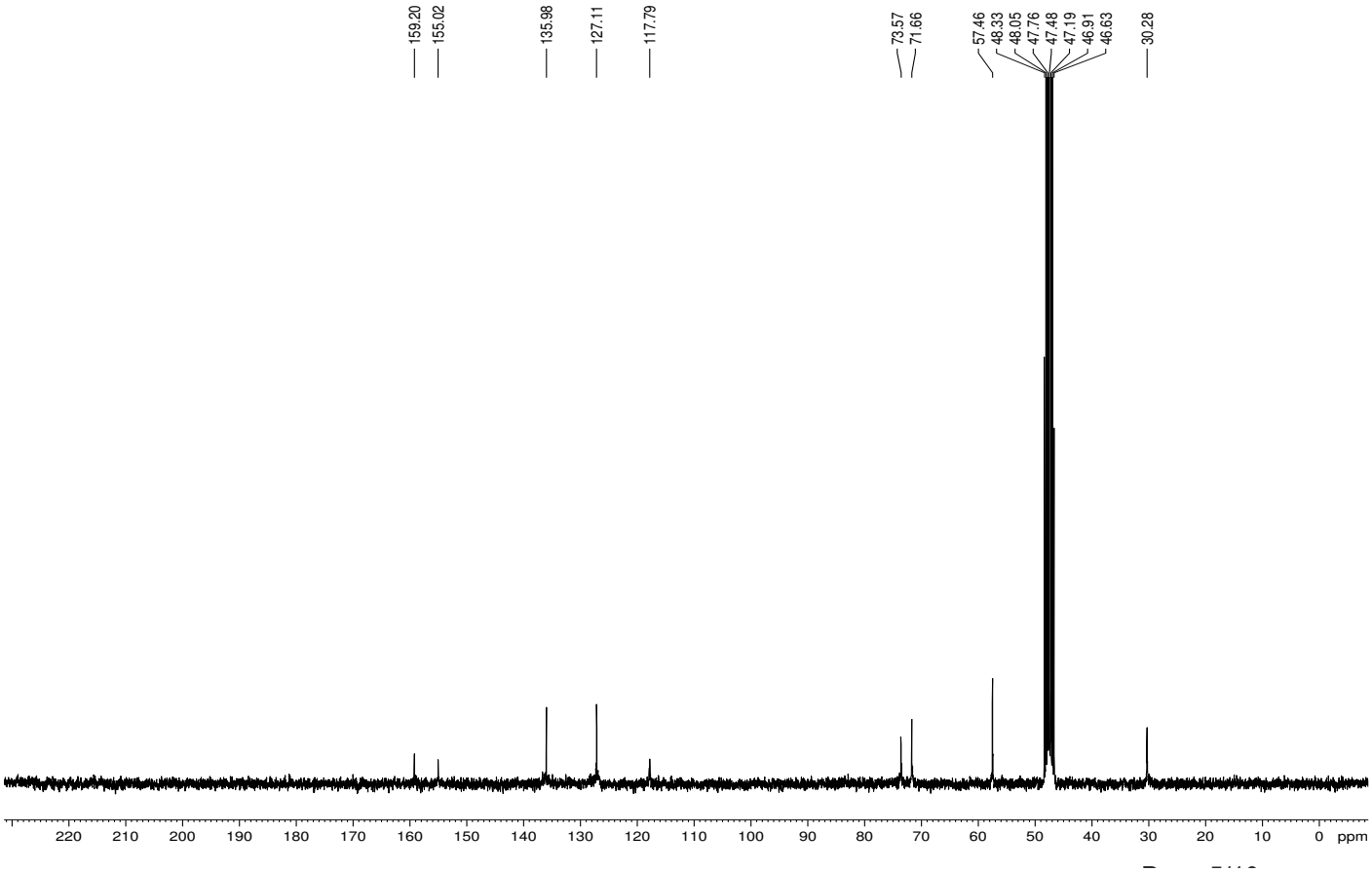
159.20
155.02
135.98
127.11
117.79
73.57
71.66
57.46
48.33
48.05
47.76
47.48
47.19
46.91
46.63
30.28
220
210
200
190
180
170
160
150
140
130
120
110
100
90
80
70
60
50
40
30
20
10
0
ppm

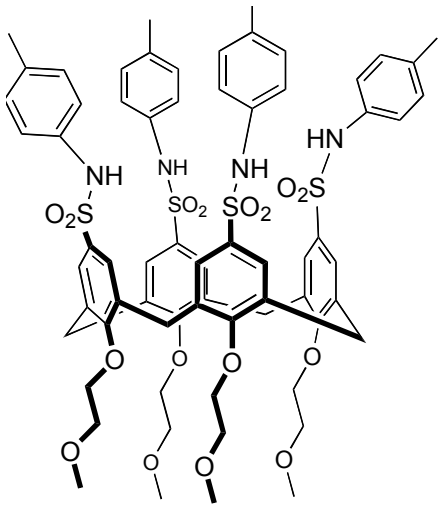
NH
NH
NH
HN
O_2S
SO_2
SO_2
O_2S
O
O
O
O
O
O
O
O

9.5
9.0
8.5
8.0
7.5
7.0
6.5
6.0
5.5
5.0
4.5
4.0
3.5
3.0
2.5
2.0
1.5
1.0
0.5
ppm
5.95
0.97
1.73
1.96
2.80
0.90
2.91

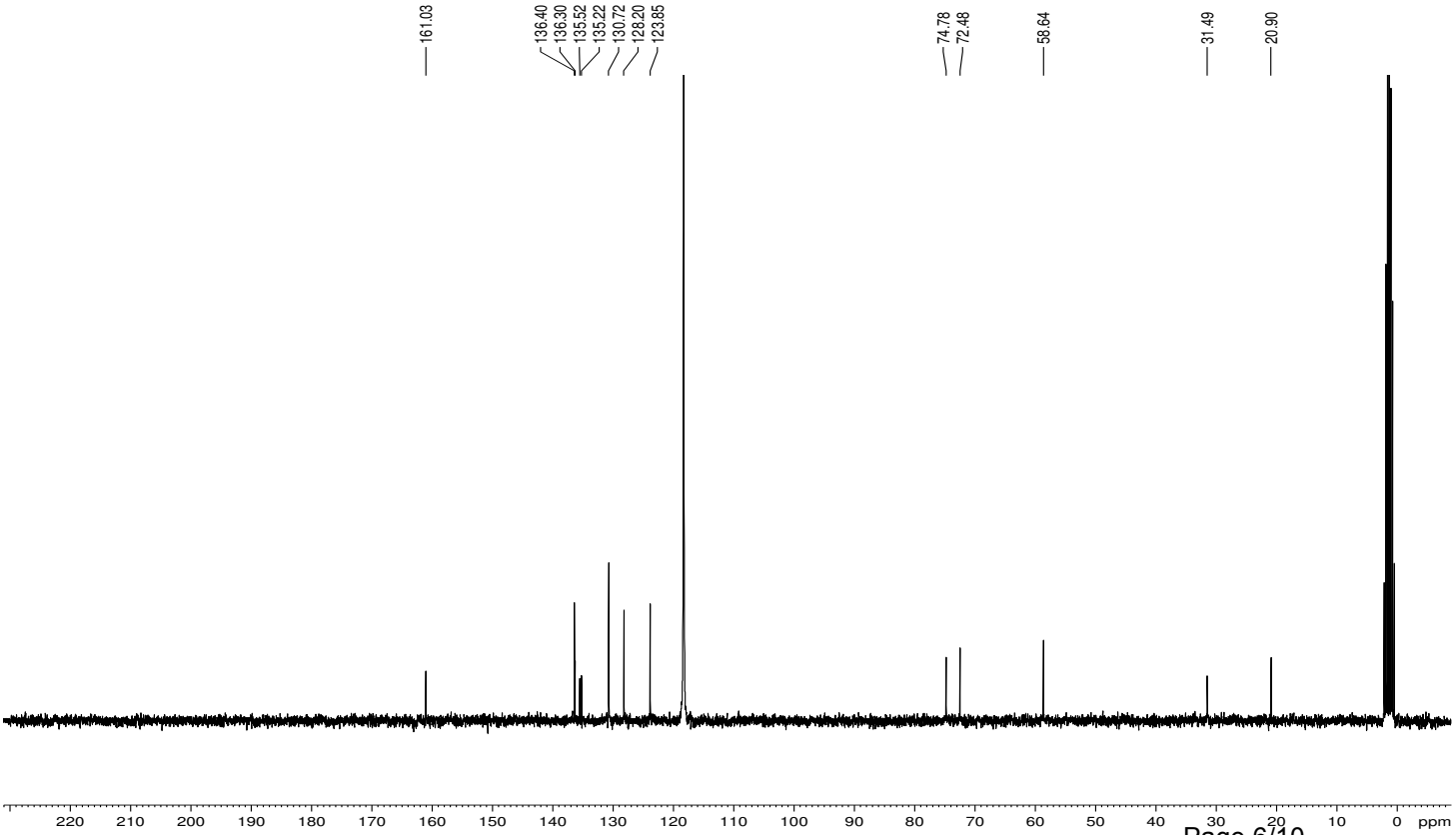
161.03
136.40
136.30
135.52
135.22
130.72
128.20
123.85
74.78
72.48
58.64
31.49
20.90
220
210
200
190
180
170
160
150
140
130
120
110
100
90
80
70
60
50
40
30
20
10
0
ppm

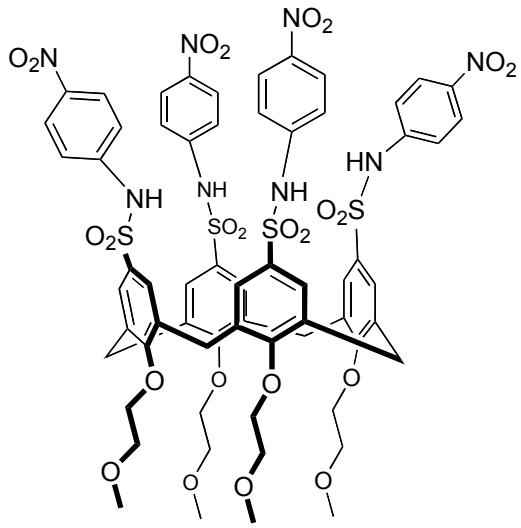
NO2
NO2
NO2
NO2
O2N
HN
NH
NH
NH
O2S
SO2
SO2
O2S
O
O
O
O
O
O
O
O

13
12
11
10
9
8
7
6
5
4
3
2
1
0
−1
ppm
0.86
2.00
3.86
1.02
1.82
2.04
1.06
2.82

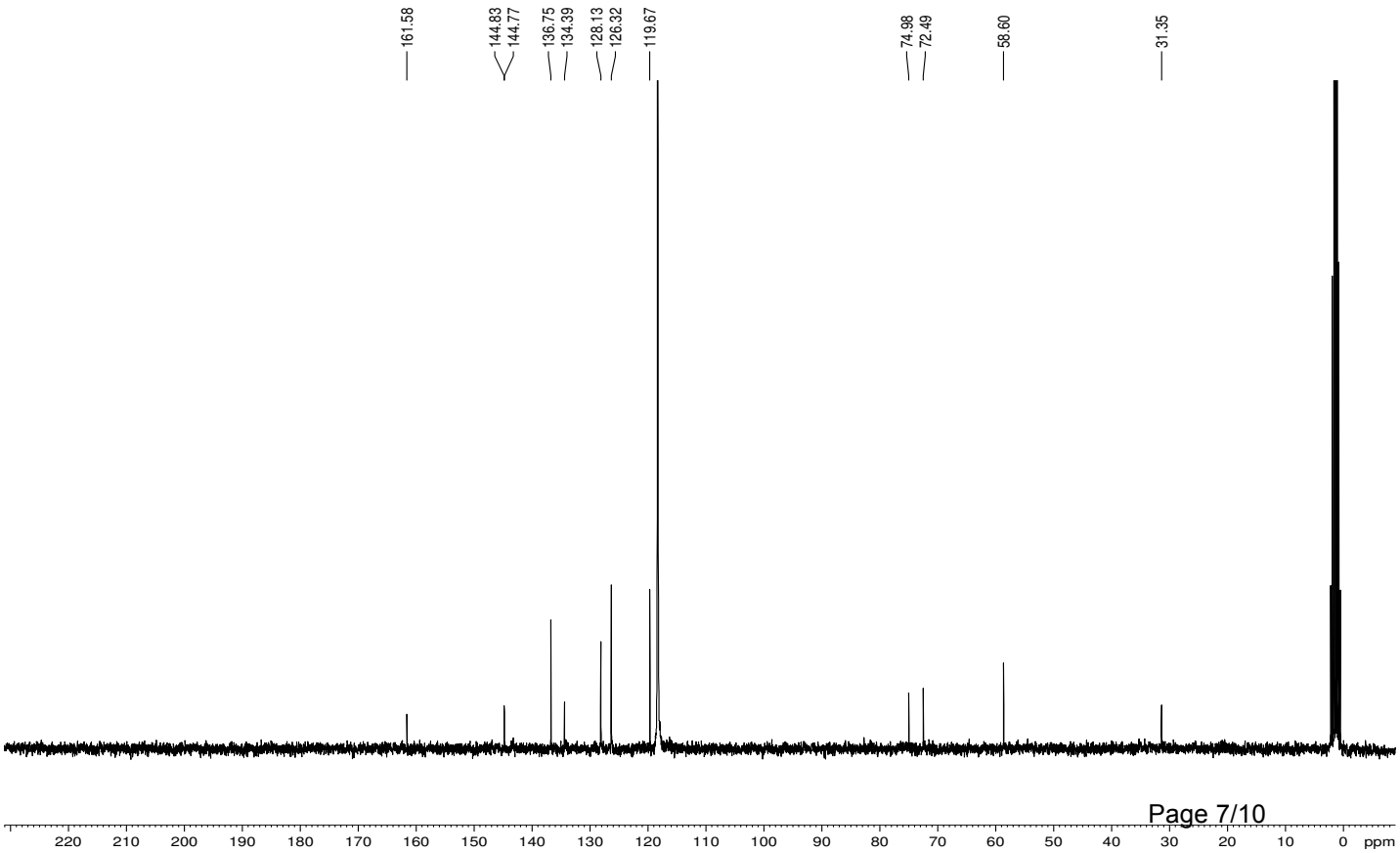
161.58
144.83
144.77
136.75
134.39
128.13
126.32
119.67
74.98
72.49
58.60
31.35
220
210
200
190
180
170
160
150
140
130
120
110
100
90
80
70
60
50
40
30
20
10
0
ppm

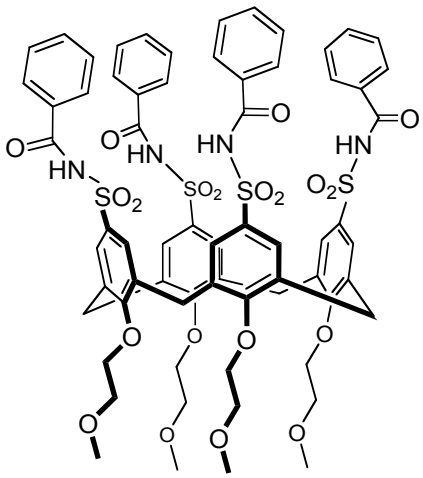
O
HN
SO2
O
HN
SO2
O
HN
SO2
O
HN
O2S
O
O
O
O
O
O
O
O

11.5 11.0 10.5 10.0 9.5 9.0 8.5 8.0 7.5 7.0 6.5 6.0 5.5 5.0 4.5 4.0 3.5 3.0 2.5 2.0 1.5 1.0 0.5 0.0 ppm
0.74
1.88
1.02
1.71
2.00
1.02
1.82
1.97
1.03
2.94

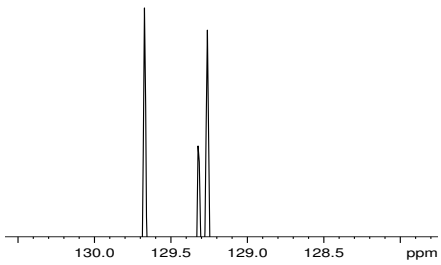
130.0 129.5 129.0 128.5 ppm

190 180 170 160 150 140 130 120 110 100 90 80 70 60 50 40 30 20 10 ppm

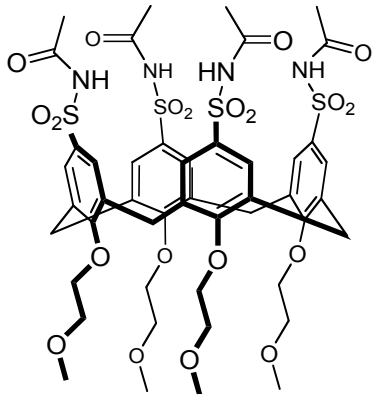

13
12
11
10
9
8
7
6
5
4
3
2
1
0
−1
ppm
0.88
2.00
1.05
2.04
2.09
1.06
3.13
2.96

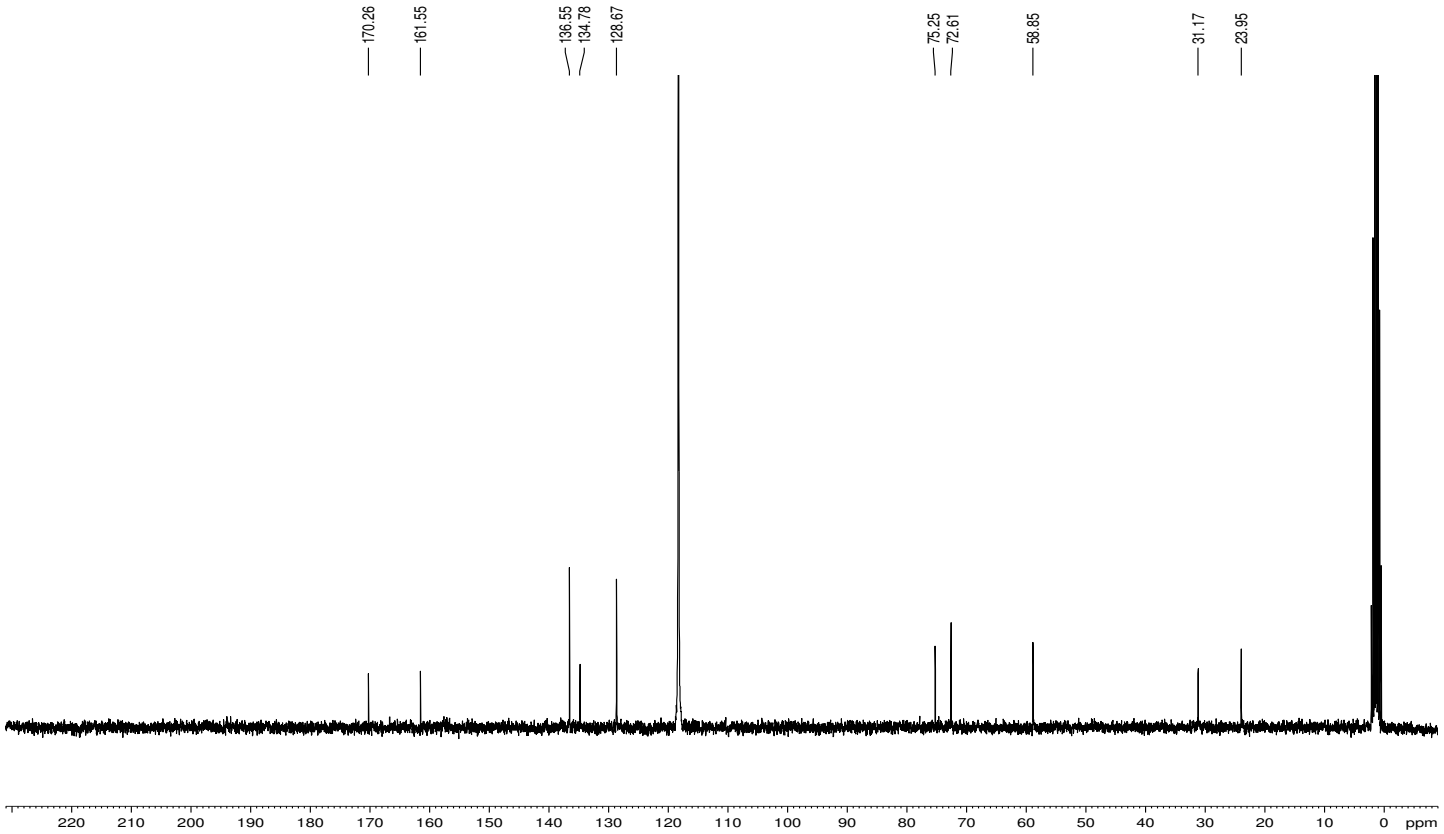
170.26
161.55
136.55
134.78
128.67
75.25
72.61
58.85
31.17
23.95
220
210
200
190
180
170
160
150
140
130
120
110
100
90
80
70
60
50
40
30
20
10
0
ppm

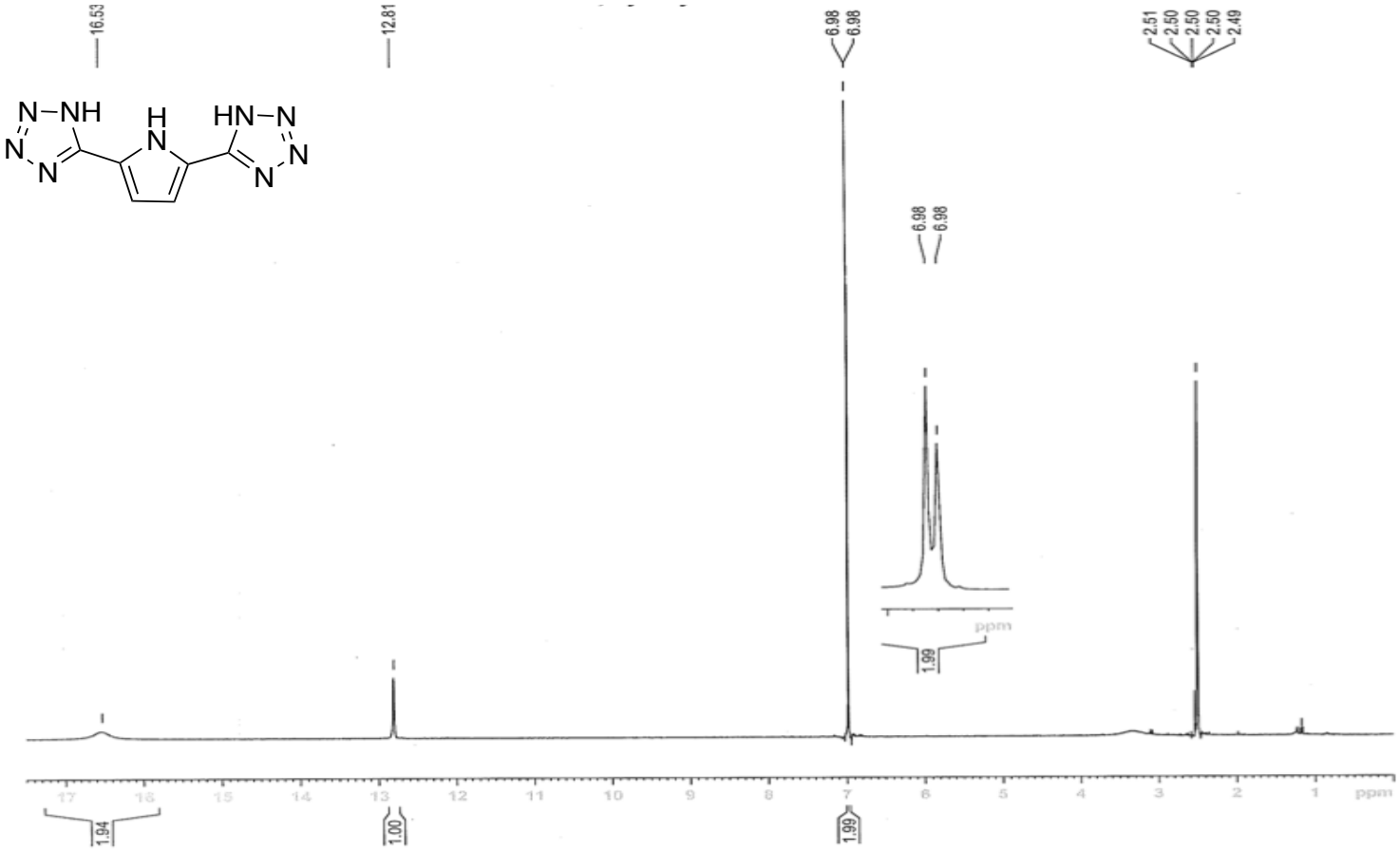
16.53
12.81
6.98
6.98
2.51
2.50
2.50
2.50
2.49
6.98
6.98
ppm
1.99
1.94
1.00
1.99
ppm

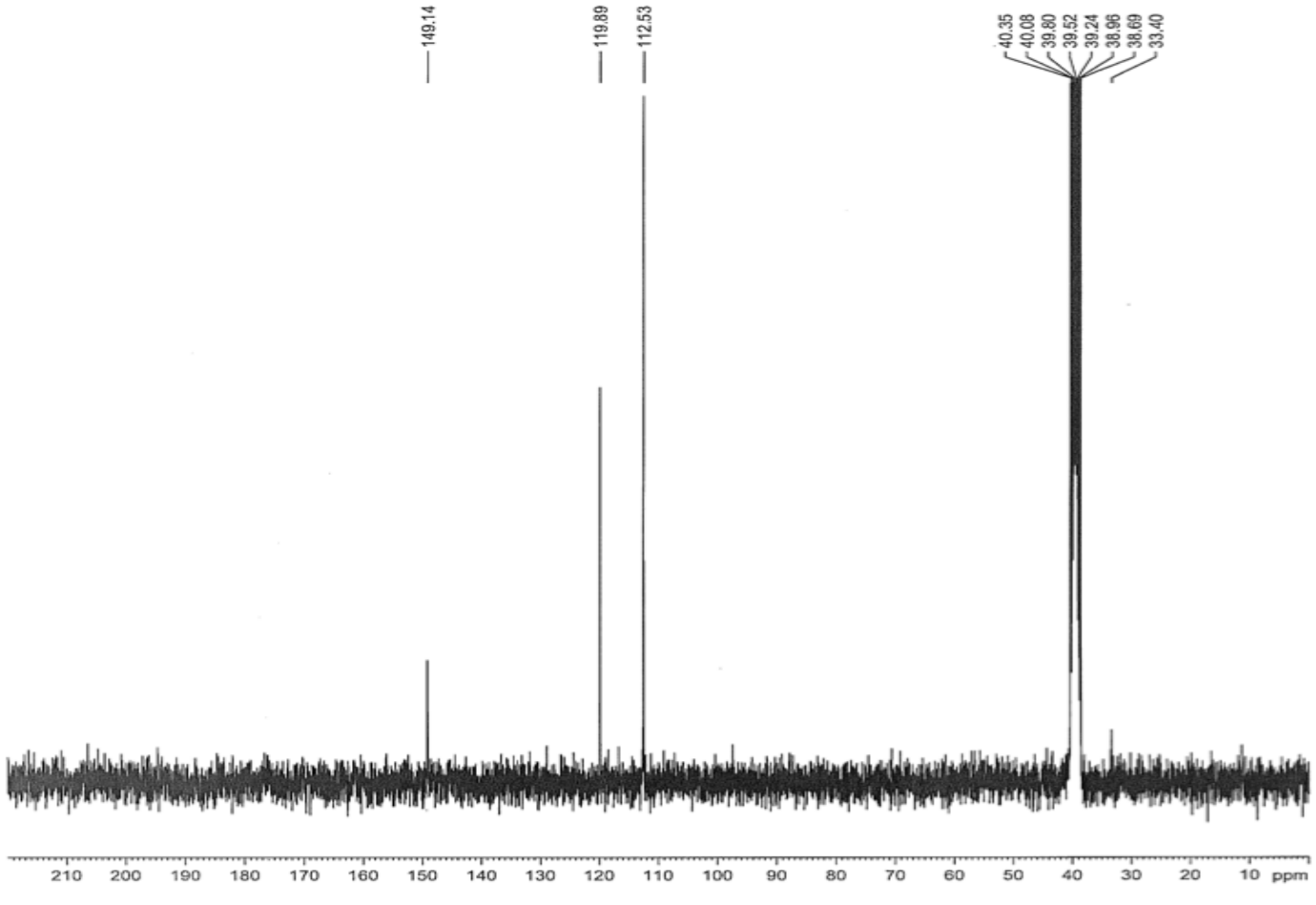
149.14
119.89
112.53
40.35
40.08
39.80
39.52
39.24
38.96
38.69
33.40
ppm

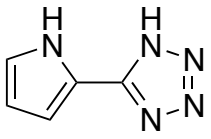

12.68
12.64
12.59
10.22
2.59
1.94
1.27
12.64
10.21
16 15 14 13 12 11 10 ppm
0.75
1.14

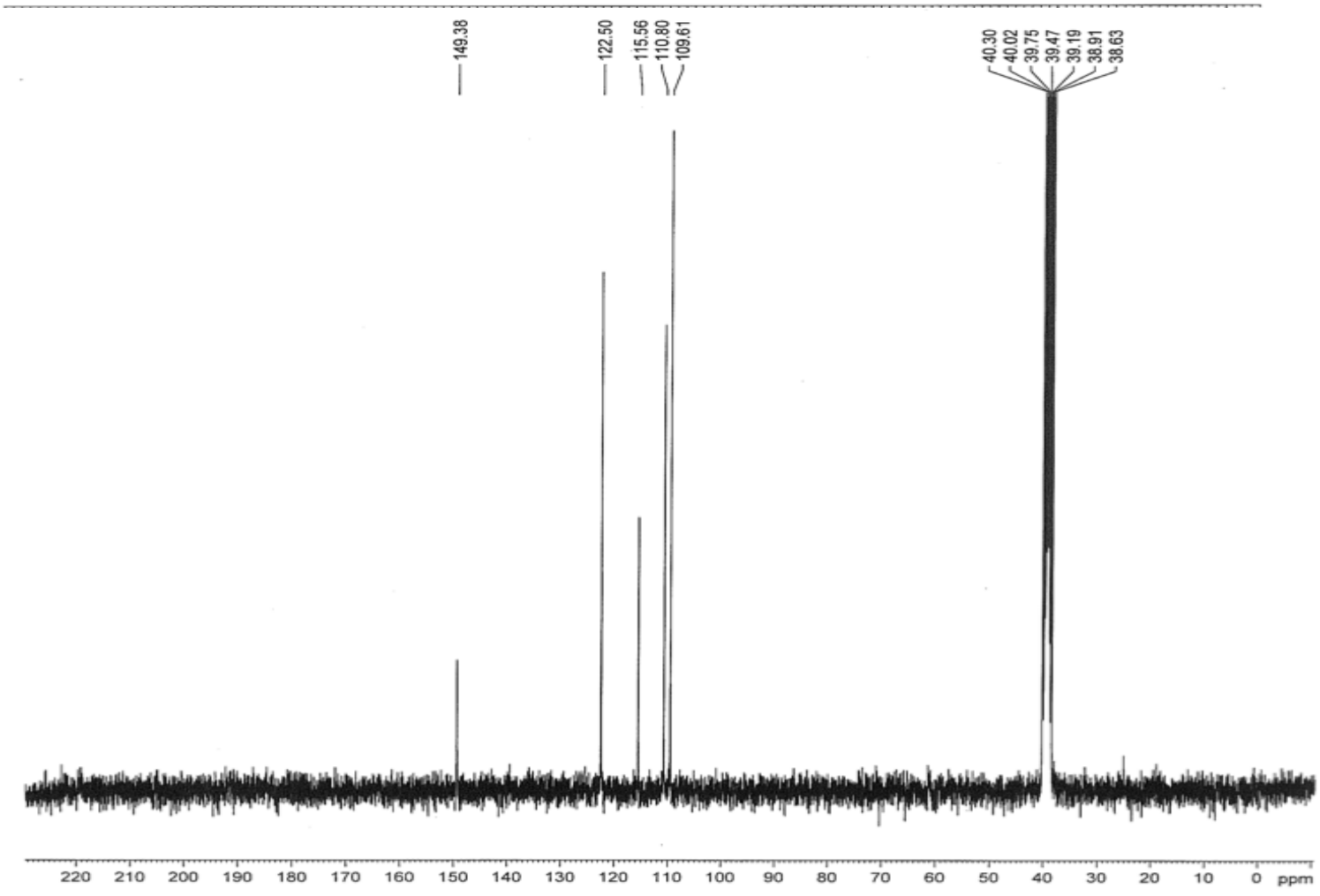
149.38
122.50
115.56
110.80
109.61
40.30
40.02
39.75
39.47
39.19
38.91
38.63
220 210 200 190 180 170 160 150 140 130 120 110 100 90 80 70 60 50 40 30 20 10 0 ppm

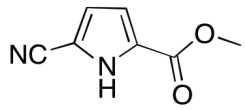
NC
N
H
O
O

13
12
11
10
9
8
7
6
5
4
3
2
1
0
−1
ppm
1.01
1.00
0.97
3.00

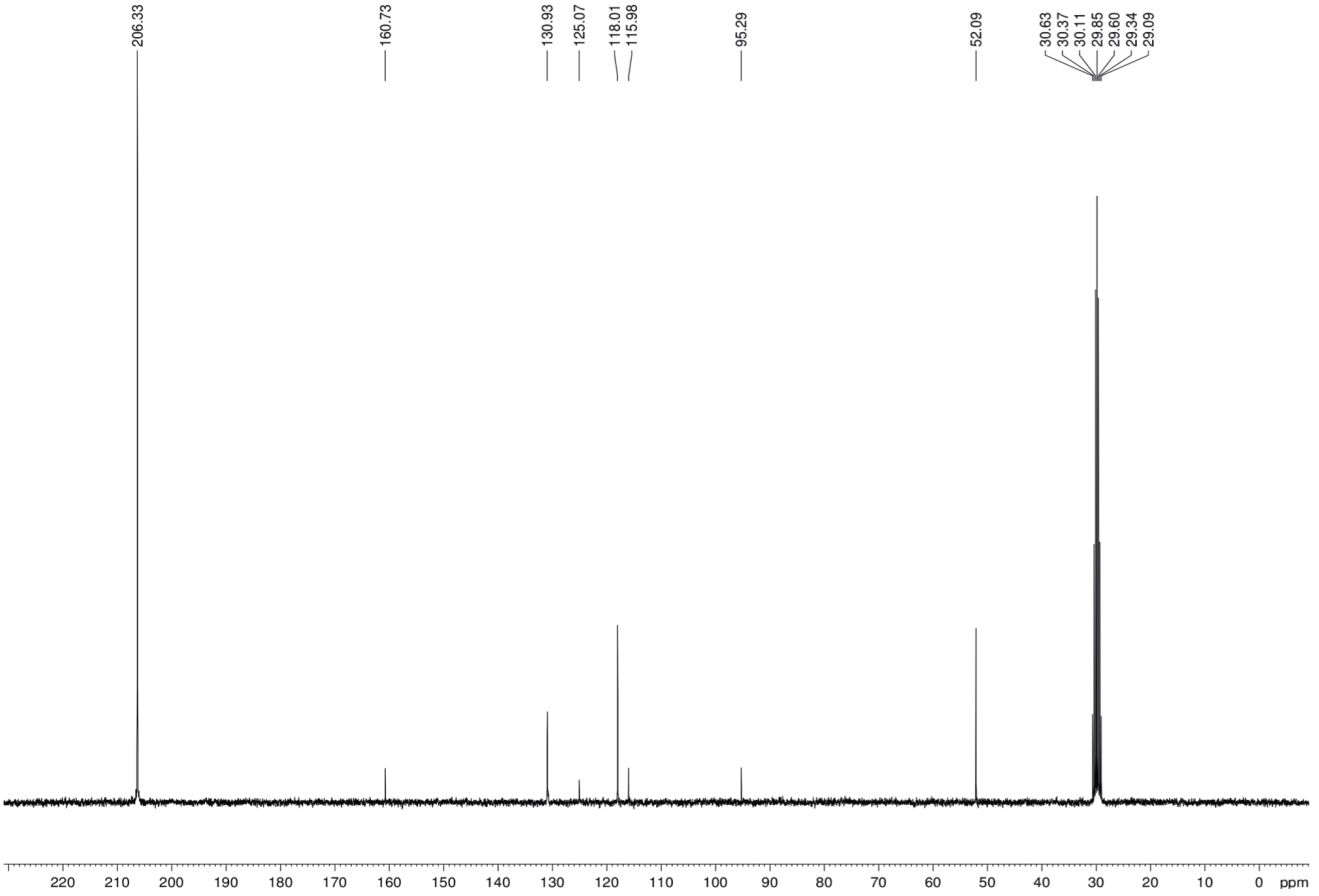
206.33
160.73
130.93
125.07
118.01
115.98
95.29
52.09
30.63
30.37
30.11
29.85
29.60
29.34
29.09
220
210
200
190
180
170
160
150
140
130
120
110
100
90
80
70
60
50
40
30
20
10
0
ppm

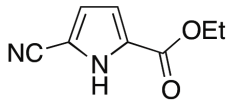
NC
N
H
O
OEt
O

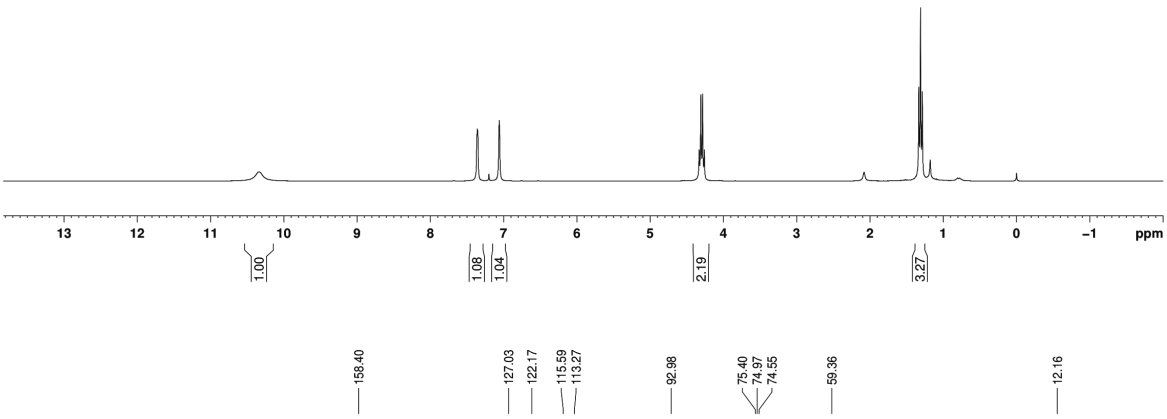
13
12
11
10
9
8
7
6
5
4
3
2
1
0
−1
ppm
1.00
1.08
1.04
2.19
3.27
158.40
127.03
122.17
115.59
113.27
92.98
75.40
74.97
74.55
59.36
12.16

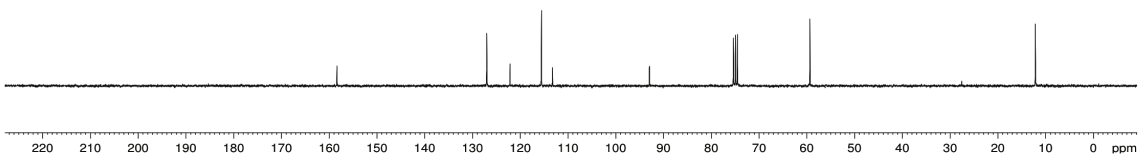
220
210
200
190
180
170
160
150
140
130
120
110
100
90
80
70
60
50
40
30
20
10
0
ppm

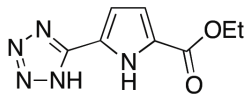
N
N
N–NH
N
H
OEt
O

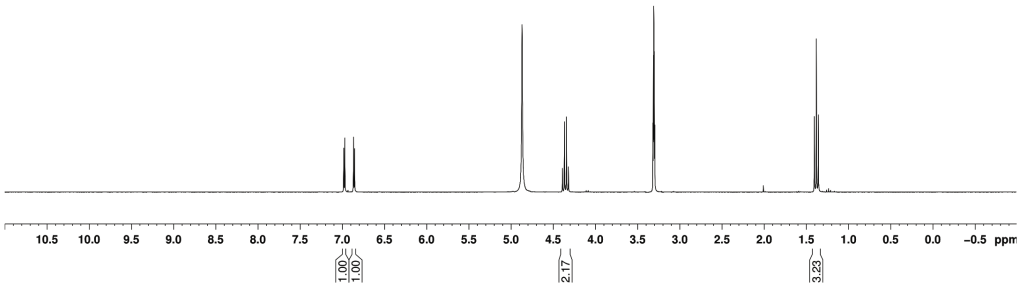
10.5 10.0 9.5 9.0 8.5 8.0 7.5 7.0 6.5 6.0 5.5 5.0 4.5 4.0 3.5 3.0 2.5 2.0 1.5 1.0 0.5 0.0 −0.5 ppm
1.00
1.00
2.17
3.23

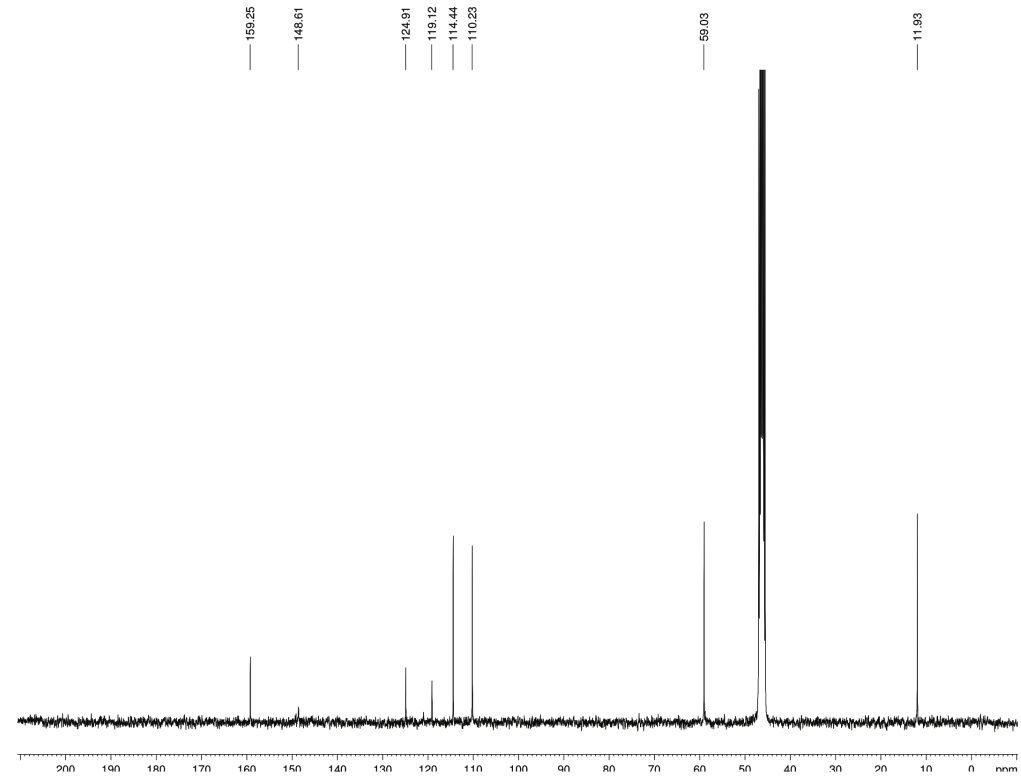
159.25
148.61
124.91
119.12
114.44
110.23
59.03
11.93
200 190 180 170 160 150 140 130 120 110 100 90 80 70 60 50 40 30 20 10 0 ppm

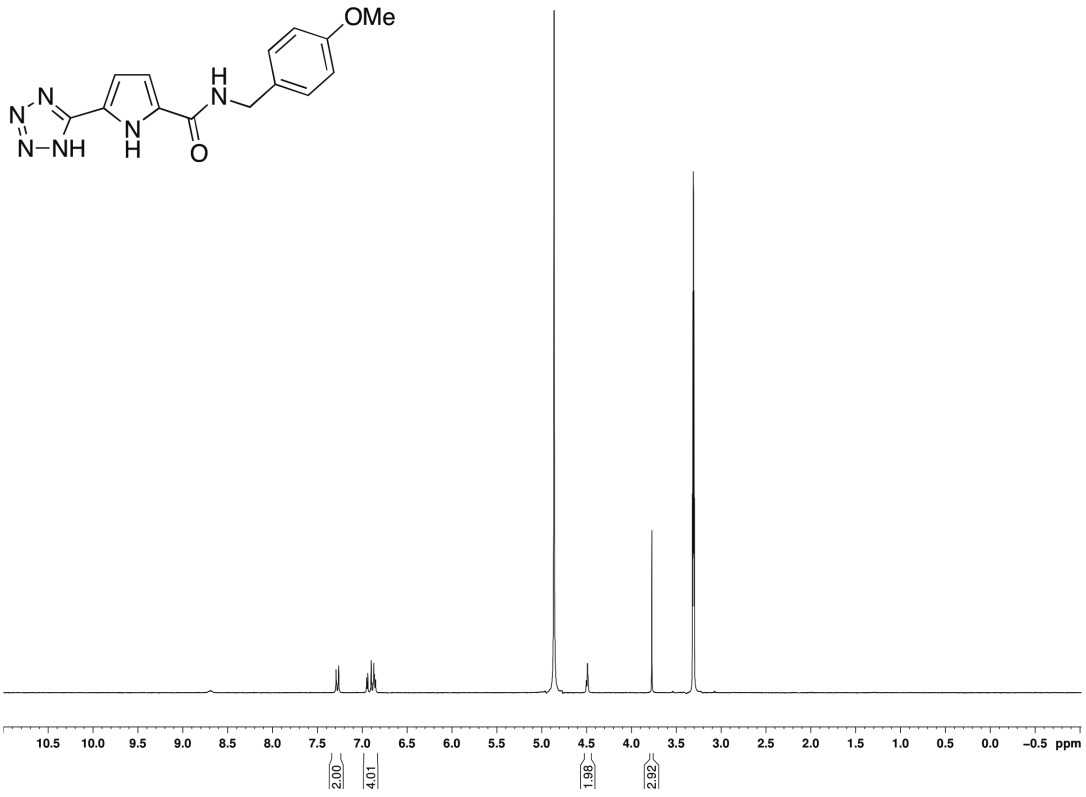
OMe
H
N
N
N
N–NH
N
H
O
10.5 10.0 9.5 9.0 8.5 8.0 7.5 7.0 6.5 6.0 5.5 5.0 4.5 4.0 3.5 3.0 2.5 2.0 1.5 1.0 0.5 0.0 –0.5 ppm
2.00
4.01
1.98
2.92

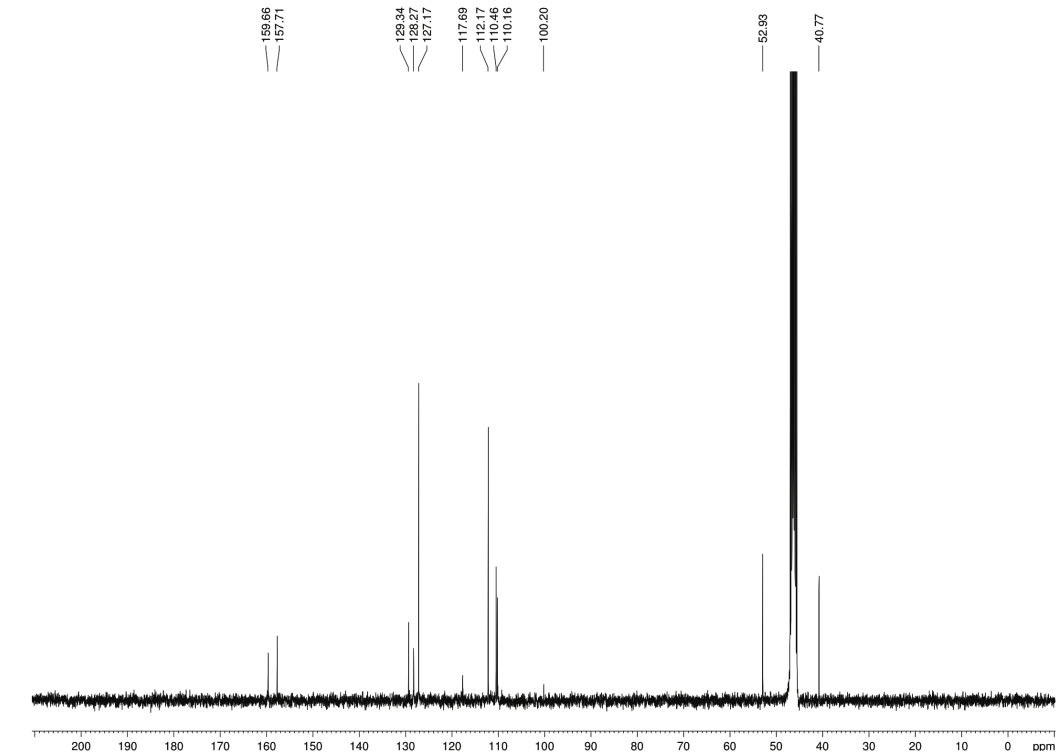
159.66
157.71
129.34
128.27
127.17
117.69
112.17
110.46
110.16
100.20
52.93
40.77
200 190 180 170 160 150 140 130 120 110 100 90 80 70 60 50 40 30 20 10 0 ppm

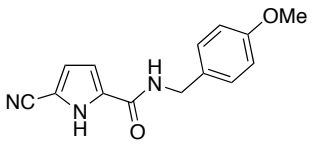
OMe
H
N
NC
N
H
O

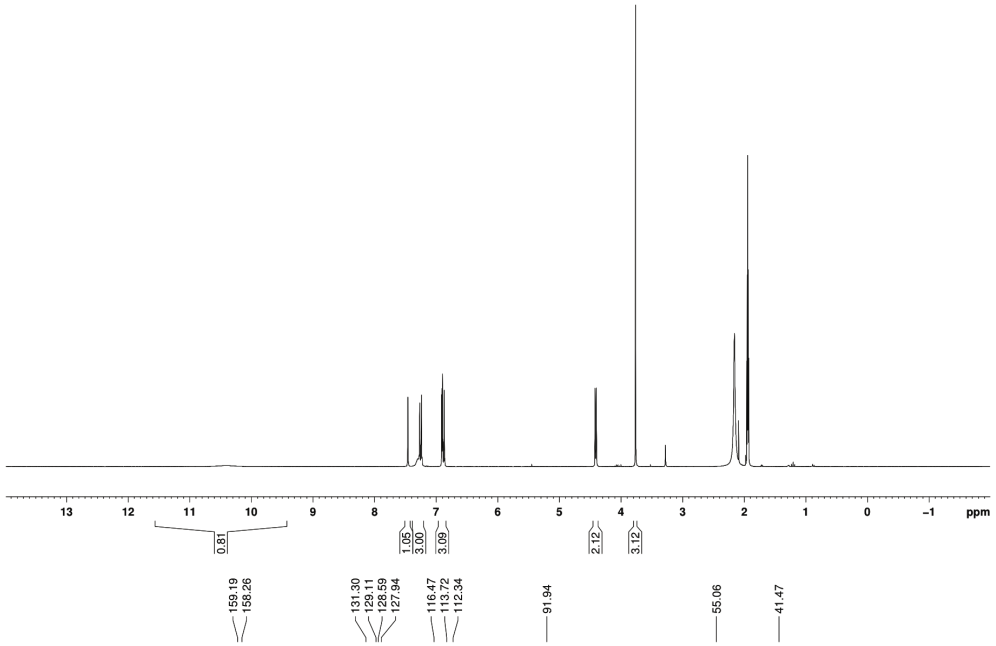
13
12
11
10
9
8
7
6
5
4
3
2
1
0
−1
ppm
0.81
1.05
3.00
3.09
2.12
3.12
159.19
158.26
131.30
129.11
128.59
127.94
116.47
113.72
112.34
91.94
55.06
41.47

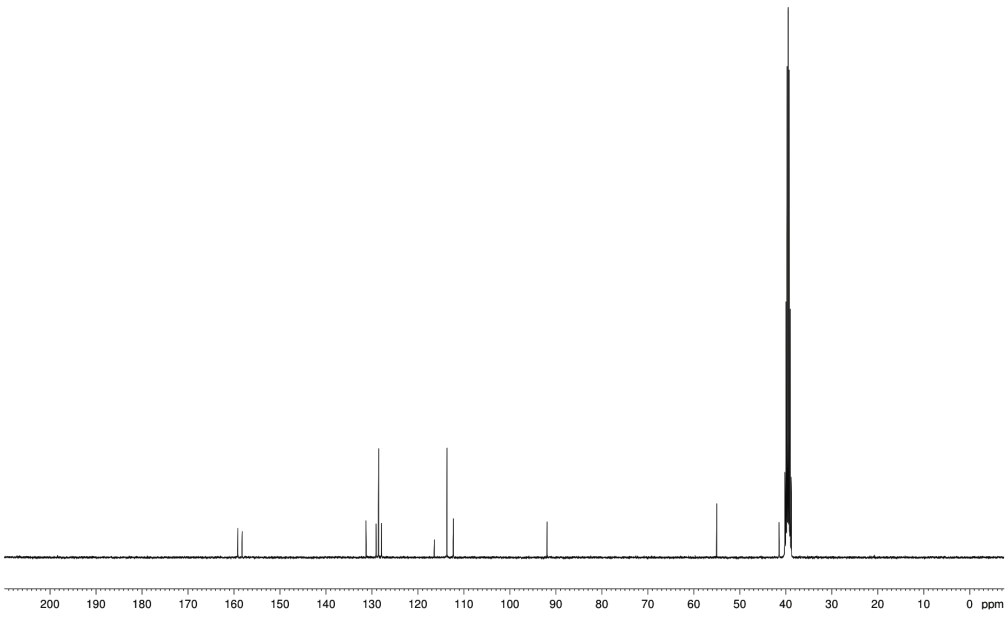
200
190
180
170
160
150
140
130
120
110
100
90
80
70
60
50
40
30
20
10
0
ppm

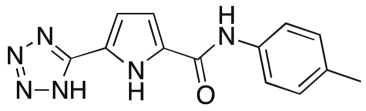
N
N
N–NH
N
H
O
H
N

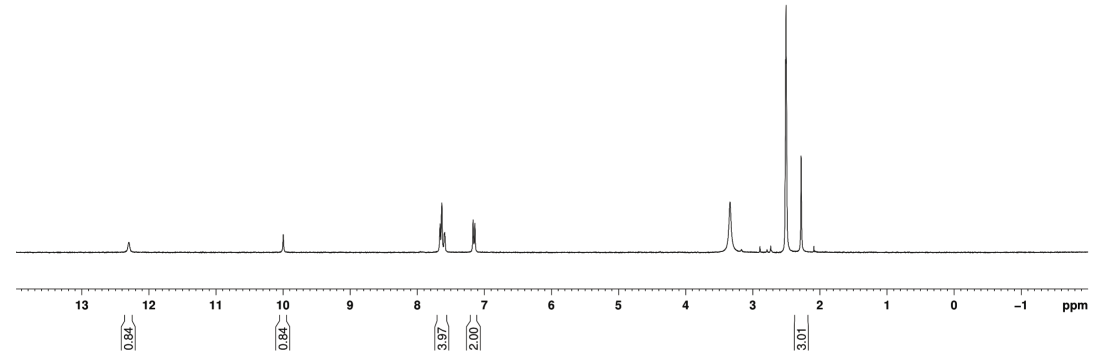
13
12
11
10
9
8
7
6
5
4
3
2
1
0
–1
ppm
0.84
0.84
3.97
2.00
3.01

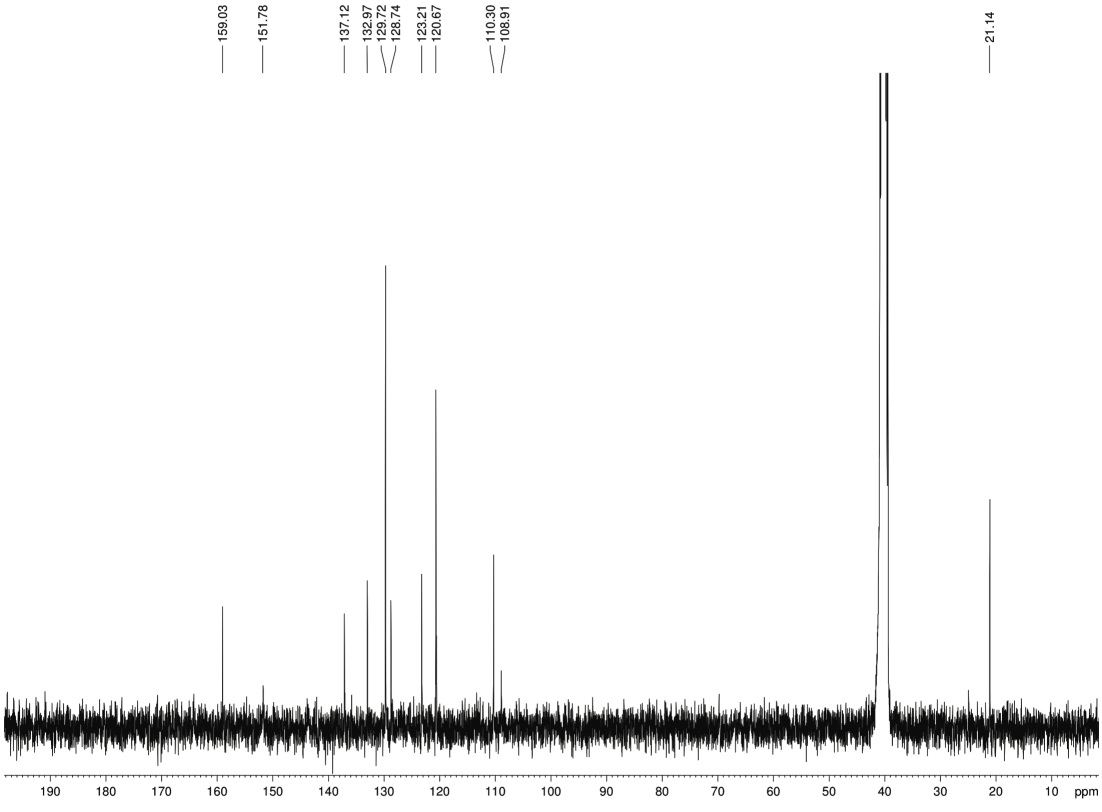
159.03
151.78
137.12
132.97
129.72
128.74
123.21
120.67
110.30
108.91
21.14
190
180
170
160
150
140
130
120
110
100
90
80
70
60
50
40
30
20
10
ppm

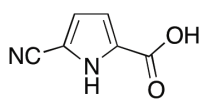
NC
N
H
OH
O

13
12
11
10
9
8
7
6
5
4
3
2
1
0
−1
ppm
0.79
7.49
0.92
7.61
3.00

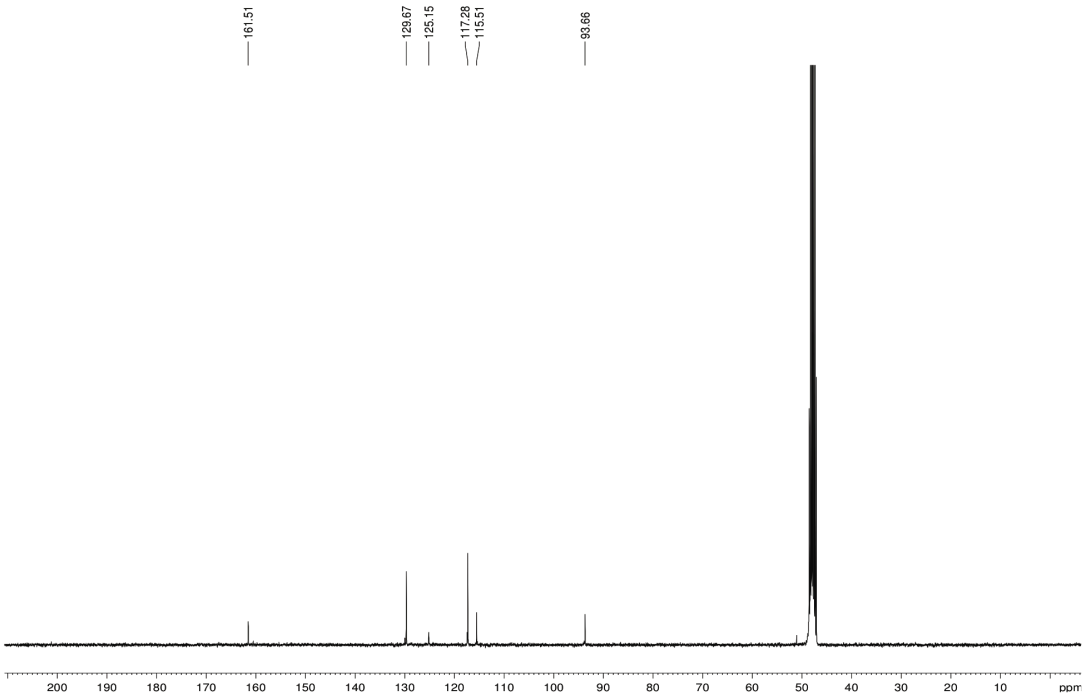
161.51
129.67
125.15
117.28
115.51
93.66
200
190
180
170
160
150
140
130
120
110
100
90
80
70
60
50
40
30
20
10
ppm